FOG

Freiberg Online Geoscience

FOG is an electronic journal registered under **ISSN 1434-7512**

2021, VOL 59

Judy Adamek

Investigation of neotectonic and structural characteristics of the subaerial and submarine system of Panarea Island, Italy

102 pages, 39 figures, 6 tables, 82 references

Abstract

The island of Panarea is located in the southern Tyrrhenian Sea and is part of the Aeolian Archipelago. A shallow water hydrothermal system belonging to the Panarea volcanic system is characterized by a continuous discharge of mixed hydrothermal fluids. These waters and gases are emanated through tectonically induced fractures. The focus of this thesis is set on an inventory of tectonic structures found across the subaerial and submarine portions of the system of Panarea. These structures along with the mixed hydrothermal fluids form a variety of sedimentary structures and impact the ecological setting of this region.

Subaerial field work concentrated on geological mapping and collecting structural data (strike/dip direction). Besides the geological mapping, the submarine field work focused on the investigation of various discharge features connected to tectonic structures as well as secondary indicators for structures lying below a cover of recent sediments. In addition, polished thin sections were prepared in order to apply optical microscopy. Geological measurements were plotted in equal-area projections and rose diagrams for visualization purposes and an integrated structural geological interpretation. Furthermore, a geological map was developed.

The subaerial portions of Panarea Island are characterized by dacitic and andesitic dominated lava domes and flows as well as tuffitic strata. Plug domes and dykes are partially included. Major tectonic structures indicate a NE-SW or NW-SE orientation with high dipping angles (> 70 °). These findings confirm former mapping results presented in common literature (e. g. CALANCHI ET AL., 199; LUCCHI ET AL., 2013). In the north-eastern parts of Panarea, preserved degassing structures were found showing a N-S orientation.

Major portions of the submarine investigation area are covered with recent sediment or densely overgrown with biota. Volcanic hard rocks are characterized by dacitic-andesitic compositions showing strong hydrothermal alterations. In some areas, tuffites and conglomerates are common. Former degassing pathways are filled with dykites (STANULLA, 2021). The number of fluid escape structures is much higher than in the subaerial regions of the system. As secondary indicators, such as fluid discharges, bacterial mats, mineral precipitations, as well as discharge features like cones and tubes, outline fractures underneath the sediment cover their strike direction could be determined. Submarine structures prevail a variety of strike directions, mainly 000-180 °, 030-210 °, 060-240 °, 090-270 °, and 150-330 °. None of the orientations dominates clearly over the other. The findings partially contradict to information given in common literature (e. g. ESPOSITO ET AL., 2006).

The neotectonic inventory of the Panarea system hints on a complex network of influencing components and interacting processes (subrosion/erosion/precipitation) leading to the formation and sometimes also preservation of the mainly extensional structures. Structures follow the general orientation set by recent tectonic processes. It can be assumed that the structures mainly form in a submarine environment. A defined relation between the kind of structure, its size and flow-rate of emanated fluids could not be recognized. Due to the existence of dykites, relative age relations of fractures and degassing structures can be stated in some areas.

Acknowledgements

First of all, I want to thank my supervisors Prof. Dr. Lothar Ratschbacher and Prof. Dr. Broder Merkel for their support during the realization of this thesis. Furthermore, thanks for all the helpful and guiding discussions as well as the feedback regarding the working progress and outcome.

I am also thankful for all the help and support that was shown to me by Dr. Thomas Pohl and the team of the Scientific Diving Center at the Technische Universität Bergakademie Freiberg throughout the whole time of field work and completion of this thesis. My deepest thank goes to those without whom field work would not have been as successful as turned out, especially Jacqueline Engel, Lutz Schüler, Johannes Röttenbacher, Viktoria Kürzinger, and Marina Kleinschroth.

Furthermore, a huge thank is addressed to the whole GeoWiD team for keeping my back free and encouraging me. Most of all, I want to name Richard Stanulla. Besides all other commitments that required his attention, he always had an open ear for all my concerns as well as considerations, who was always there when advice and critics was needed and who encouraged me in my actions with all his patience. Thank you for a number of inspiring conversations and other perspectives as well as proofreading. I am pleased for your suggestions concerning typesetting. I enjoyed developing all kinds of schemes, figures, and models for both our theses. But most of all thank you for enduring all my moods nonetheless when things did not work out the way planned.

My deepest gratitude goes to my family who let me go my own way, even with all the off-road paths and turns, and supported me despite all doubts. I thank you for giving me a place to go whenever I needed to settle down and set focus again. And of course, thanks for all the financial aid throughout traveling times.

This whole work would not have been possible without funding for the field work on Panarea Island and for travel expenses. I was granted by *Förderkreis Freiberger Geowissenschaften* (ffg) and *Freunde und Förderer der TU Bergakademie Freiberg* (vff) several times as well as the German Academic Exchange Service (DAAD).

Last but not least, I want to thank Karin Heinzig for proofreading.

List of abbreviations

Aerial locations

BOT	Bottaro islet
DAT	Dattilo islet
PAN	Panarea Island

Submarine locations

A26	Area 26
BN	Bottaro North
BW	Bottaro West
CA	Cave
FF	Fumarolic Field
HL	Hot Lake
LC	La Calcara
P21	Point 21

Geographical information

SAF	Sisifo-Alicudi fault
TLF	Tindari-Letojanni fault

Physical values and indices

°C	Degrees Celsius
l	Litres
Pa	Pascal
p	Pressure
T	Temperature
°	Degree (angle)
m asl	Meters above sea level
m bsl	Meters below sea level
HKCA	High-K calc-alkaline series

Names

INGV	Instituto Nazinale Gefisica e Vulcanologia/National institute for Geophysics and Volcanology, Catania
FSVG	Flow meter for submarine volcanic gas emissions
SDC	Scientific Diving Center

Others

cf.	Confer
yr	Year

Contents

1. Introduction and aims

1.1 State of research

Aeolian Arc

The Aeolian Arc is located in the southern Tyrrhenian Sea in southern Italy. It is a 200 km long active volcanic arc consisting of several stratovolcanoes which form the seven major islands of the archipelago. In addition, several islets and seamounts belong to the arc as well (Figure *1*). The islands Alicudi, Filicudi, Salina, Lipari, Vulcano, Stromboli, and Panarea form the exposed part of the Arc. The arc itself separates the Pleistocene Marsili basin in the north from the continental slope which is located north of Sicily to the west as well as from the uplifting crust of the Calabrian Arc to the east (CALANCHI ET AL., 1995; FABRIS ET AL., 2010; LUCCHI ET AL., 2013a). The islands and seamounts encircle the Masili basin and the Marsili seamount that is located northwest of the islands in a ring-like structure. The rapidly expanding Marsili basin, a back-arc basin, is characterized by thin lithosphere (TRUA ET AL., 2004). The Aeolian Arc has developed due to the subduction of the African Plate underneath the Eurasian Plate which lead to calc-alkaline to minor shoshonitic volcanism that initiated during the Pleistocene (ESPOSITO ET AL., 2006; LUCCHI ET AL., 2013). Starting in Tortian times, the subduction led to the opening of the Tyrrhenian Sea back-arc basin to which the Aeolian Archipelago belongs (GAMBERI ET AL., 1997).

The Aeolian Arc consists of three sectors, each of which show distinct structural, magmatic and volcanic features (ROSSI ET AL., 1987; MANETTI ET AL., 1989; GABBIANELLI ET AL., 1990; NERI ET AL., 1991 AND 1996; MAZZUOLI ET AL., 1995; LANZAFAME & BOUSQUET, 1997; VENTURA, 1995; VENTURA ET AL., 1999; TIBALDI, 2001; BONACCORSO, 2002).

The western sector comprises the islands Alicudi and Filicudi as well as several minor features, such as the Alicudi North Seamount and the Filicudi North Seamount. This sector is already extinct. Consequently, it does not show any volcanic activity. It is located along a WNW-ESE right lateral fault system in an overall compressional regime due to the convergence of the Eurasian and African continents (ACOCELLA ET AL., 2009; PECCERILLO ET AL., 2013). The magma in the western sector is characterized by calc-alkaline composition. Mostly mafic to intermediate rocks are found in this sector. The uprising of the magma was controlled by the Sisifo-Alicudi fault (SAF) system (DE ASTIS ET AL., 2003). Between 1.3 Ma and approximately 3 ka, volcanism in the western sector developed (BECCALUVA ET AL., 1982; BECCALUVA ET AL., 1985; SANTO & CLARK, 1994).

The islands Salina, Lipari, and Vulcano belong to the central sector that shows a NNW-SSE trend. It developed along a dextral strike-slip fault. This fault is named Tindari-Letojanni fault (TLF) and runs from Salina to the mainland of Sicily (BARBERI ET AL., 1994; ESPOSITO ET AL., 2006; PECERILLO, 2017). The main NNW-SSE regional fault system furthermore influences the morpho-structural setting of this sector (ROMAGNLIO ET AL., 2013). According to BECCALUVA ET AL. (1985), volcanism in the central sector started at about 0.4 Ma. Besides a number of gas vents on Vulcano island, shallow earthquakes indicate that the area is still active (GAMBERI ET AL., 1997). Furthermore, hot springs and gas vents can be found at different spots on Salina and Lipari. The earthquakes are concentrated along a NE-SW alignment (VENTURA, 2013). The rock

composition of the central sector is variable. Besides mafic to silicic calc-alkaline also shoshonitic and potassic-alkaline rocks are characteristic.
The eastern sector of the Aeolian Arc is formed by the islands Stromboli and Panarea. In addition, the Alicone seamount and submerged NE-SW oriented Stromboli Canyon east of the islands belong to this sector (VOLPI ET AL., 1997; GAMBERI AND MARANI, 2004). At around 0.8 Ma, volcanism started which is still ongoing. While volcanism at Stromboli is characterized by recurrent eruptions, Panarea shows gas venting and a shallow seismicity (SOLOVIEV ET AL., 1990). The eastern sector is part of an about 45 km long volcanic belt that is located along NE-SW striking faults showing a predominantly extensional structures. These faults run from northern Calabria to the northeast of Sicily (VENTURA, 2013). Extension rates can reach up to 3 mm/a. The structures may contribute to the rise of hydrothermal fluids in the western arc (ESPOSITO ET AL., 2006; PECERILLO, 2017). The emplacing of magma occurs along NE-SW oriented dyke-like structures. Rocks in this sector show mafic to silicic calc-alkaline composition and shoshonitic to potassic-alkaline affinities. Seismic activity in the western sector can be observed both at mantle and at crustal levels. The earthquake hypocentres outline a steep and narrow Wadati-Benioff zone reaching up to 350 km depth that dips to the NNW (NERI ET AL., 2009; VENTURA, 2013).
The Tindari-Letojanni-fault seems to divide the western and central sectors of the Aeolian Islands from the eastern sector. This affects a number of different aspects, such as the magma evolution, magma uprise, mantle sources, and subducted material (PECCERILLO ET AL., 2013).

Panarea Island and subaerial portions

The island of Panarea is located about 50 km north of Sicily in the eastern sector of the Aeolian island group. It represents the emergent summit of a predominantly submerged stratovolcano that rises about 1600 m from the seafloor and is roughly 20 km in diameter (ANZIDEI ET AL., 2005; FAVALLI ET AL., 2005).
As there are different classifications on the frequency of the eruptions of volcanoes, the following classification will be applied in this thesis. Besides being active, volcanoes can also be dormant or extinct. An active volcano has had at least one eruption within the last 10 kyr. It can be currently erupting, as can be observed at Stromboli volcano. A dormant volcano is expected to be eruptive in the future again but is not active at the moment. In contrast, an extinct volcano is neither active nor is it likely to erupt again in the next 10 kyr. Consequently, the Panarea volcano can be considered an active volcano, since there has been at least one eruption within the last 10 kyr and it still shows hydrothermal activity of different intensity both onshore and in the submarine portions (PECCERILLO, 2017).
Besides several lava domes, also lava flows, volcanic plugs, and pyroclastic deposits with mafic to felsic composition are common features on Panarea Island (CALANCHI ET AL., 1999; LUCCHI ET AL., 2013b). Furthermore, a number of dykes and extension fractures can be observed on the shore and throughout the mainland of Panarea. Dacites and andesites are most common on Panarea Island. Rarely, shoshonites or rocks with shoshonitic affinities can be found (Romano,

1973; CALANCHI ET AL., 2002; LUCCHI ET AL., 2013b). In general, the lavas of Panarea are characterized by a porphyritic texture with zoned plagioclase as the dominant phenocryst phase and a hypo- to holohyaline groundmass and a high content of phenocrysts. Clino- and orthopyroxenes are abundant members of the phenocryst phases in the mafic rocks whereas olivine is scarce and mostly appears as a xenocryst (CIMARELLI ET AL., 2008; DOHERTY ET AL., 2015). Xenoliths, originating from metamorphic and igneous rocks, reaching up to 20 % of the total rock volume, are enclosed into a large number of Panarea's pyroclastic rocks and lavas (GABANELLI ET AL., 1990; CALANCHI ET AL., 2002).

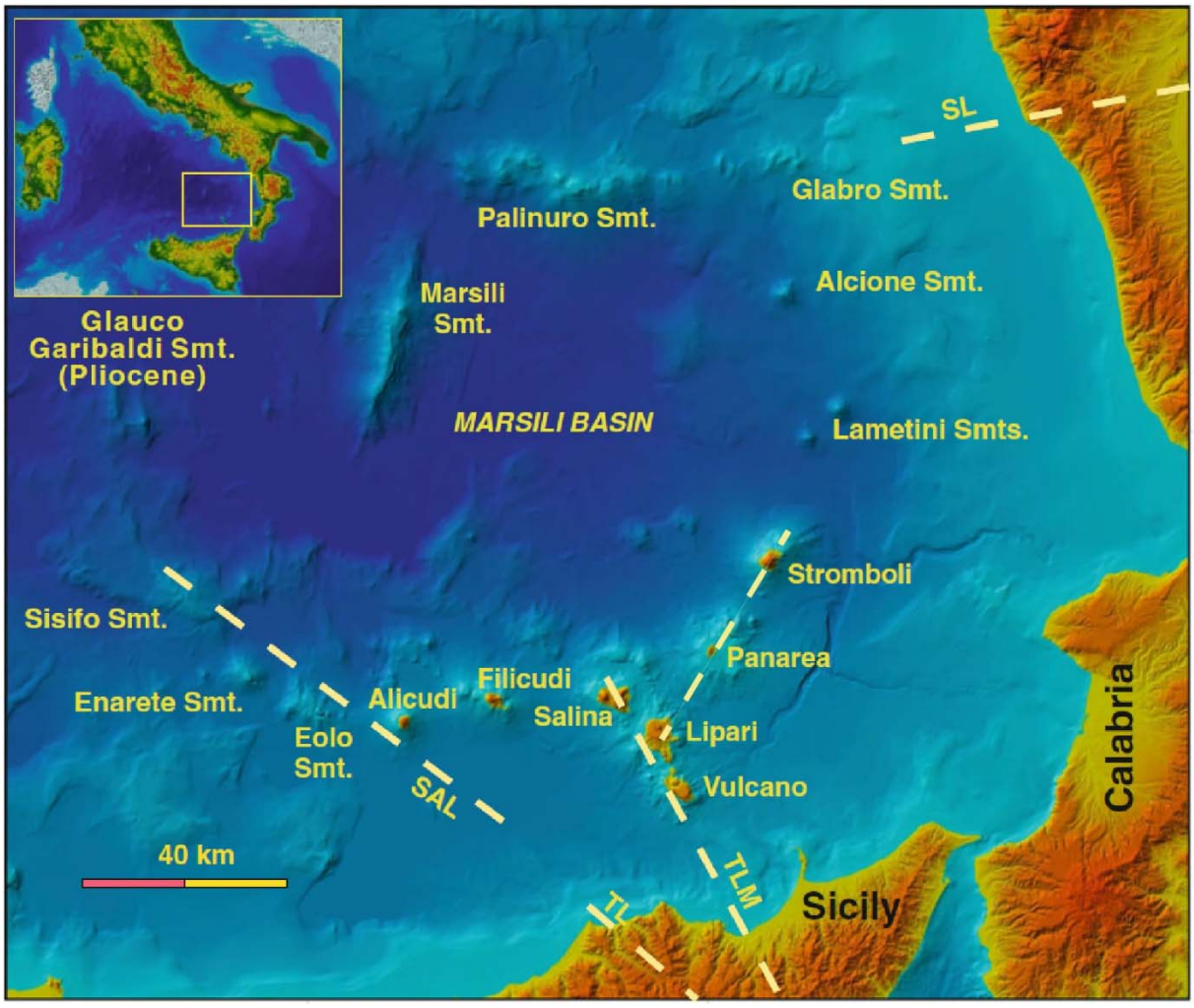

Figure 1: Geographical overview of the Southern Tyrrhenian Sea and the Aeolian Islands. SAL – Sisifo-Alicudi line, TLM – Tindari-Letojanni-Malta line, TL – Taormina line, SL – Sangineto line (after Peccerillo, 2017). Blue colours resemble submarine areas (light shades indicate shallow regions < 100 m; dark shades indicate deep regions > 3000 m). Greenish/brownish colours mark land masses (green shades indicate flat regions < 50 m; brown shades indicate high regions > 500 m).

Geochemical data of the Panarea volcanites show increased values of P_2O_5, TiO_2 and alkalies (LUCCHI ET AL., 2013b). In silicic rocks, a negative Eu anomalie can be found which is comparable

to the REE behavious of Salina's volcanic rocks (CALANCHI ET AL., 2002). A decrease of Sr^{87}/Sr^{86} ratios can be observed from shoshonitic to calcalkaline rocks. Compared with the composition of the other Aeolian Islands, Pb-isotopes are less variable. In contrast, Nd and Sr ratios show a higher variability. These values lie between the ones of the central Aeolian Islands and the ones of Stromboli Island of the eastern sector (DOHERTY ET AL., 2015).

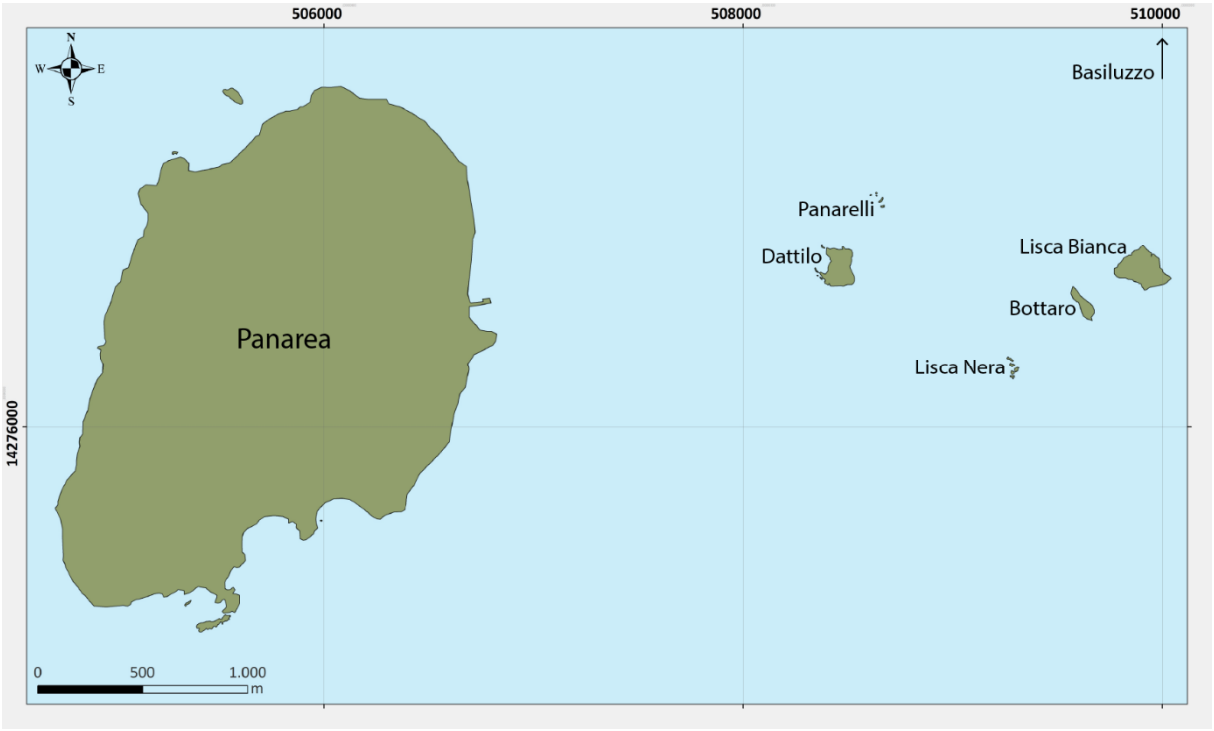

Figure 2: Geographical overview of the Panarea volcanic complex. The island of Panarea is located east of the islets of Panarelli, Lisca Bianca, Bottaro, Lisca Nera and Dattilo which form a ring-like structure. The largest islet off Panarea's shore, Basiluzzo, is located north of the other islets. The highest peak of the complex is located at Punta del Corvo (421 m asl) at Panarea Island.

Panarea lavas evolved under the strong influence of fractional recrystallization (LUCCHI ET AL., 2013b; DOHERTY ET AL., 2015). Based on geobarometry, the recrystallization of lavas at Panarea Island started at a depth of about 22 km, respectively 830 MPa and continued to a depth of 0.8 km (30 MPa) (DOHERTY ET AL., 2015). The depth of approximately 22 km corresponds to the location of the Moho in the area of the eastern Aeolian Arc. The variable depths of crystallization indicate the existence of more than a single magma source underneath Panarea Island. CALANCHI ET AL. (2002) suggest a heterogeneous mantle source below Panarea where parts of the magma resemble the magmas from the western Aeolian Arc while the other part of the Panarea lavas results from a mixture of the Stromboli mantle and the western arc mantle. Hence, Panarea can be considered an intermediate between the islands of the central and the eastern Aeolian islands both concerning geographical aspects and geochemical aspects likewise.

The subaerial portions of the Panarea volcanic complex grew within a relatively short time between 150-100 kyr while the islet of Basiluzzo started to develop about 54 kyr ago, after a 50 kyr long period of quiescence (CALANCHI ET AL., 1999; CAPACCIONI ET AL., 2007). Within this period, several eruptive epochs and phases of crystallization led to the placement of several lava domes which resulted in the today's complex morphology of Panarea Island (GUGLIANDOLO ET AL., 2006; LUCCHI ET AL., 2007; TASSI ET AL., 2014). The volcanic products of each epoch resemble each other in terms of petrochemical features, eruptive style as well as the location of the eruption centre. Table 1 sums up the 7 successive eruptive stages and characteristics of each period. In between each stage, subaerial and marine reworking took place. Paleo shores formed that resulted from the sea-level fluctuations as well as the crustal uplift (LUCCHI ET AL., 2013). The paleo shores are characterized by terraced marine deposits that are made of coarse and poorly sorted conglomerates along with rounded pebbles and sands. On Panarea Island, five successive shorelines can be identified between 115 and 5 m above sea level using sequence stratigraphy which is combined with cross-cutting relations to the other Aeolian islands (KELLER, 1967; ROMANO, 1973; LUCCHI ET AL. 2017). After LUCCHI ET AL. (2006) the crust uplifted up to 1.56 mm/a, considering also sea level variations. These processes interacted during the main quiescent stages.

Besides the main island of Panarea, several smaller islets in the east belong to the Panarea volcanic complex. These islets, remains of lava domes, are named Basiluzzo, Bottaro, Lisca Bianca, Lisca Nera and Dattilo (Figure 2). Along with Panarea Island, they are considered the subaerial remnants of the stratovolcano. They encircle a shallow, 1 km large depression by forming a rounded structure that resembles a crater. Between 150 and 14 kyr the islets east of the main island developed (ESPOSITO ET AL., 2006). According to DOHERTY ET AL. (2015), the islets' lavas starting depth of crystallization is about 16 km. Since Panarea lavas crystallized at a slightly lower level, a polybaric distribution of the crystallization depth is suggested which can be referred to the different sources of magma.

Table 1: Eruptive stages and characteristics of Panarea Island after Calanchi et al. (1999) and Lucchi et al. (2007).

Eruptive stage	Time [ka]	Location	Characteristics
1	± 155-127	Northern and western portion, most of main Panarea	Effusive, lava domes aligned on NW-SE and NE-SW trends
2			
3			Placement of the islets east of Panarea
4	± 124-118	Central and southern portion	Lava flows and domes, emplacement of minor pyroclastic products
5	± 118-105	East of Panarea, near islets	Explosive pyroclastic activity
6	± 54 ± 8.7	Basiluzzo and Drauto	Eruptive, development of Basiluzzo
7	± 42-13	Punta Torrione	Eruptive, pyroclastic layers deposited

The islets are mainly made of andesitic to dacitic lavas that show a HKCA affinity. Compared to the Panarea lavas, the abundance of potassium increases at the islets (DOHERTY ET AL., 2015). The rocks of the islets of Panarelli and Bottaro are characterized by basaltic to andesitic composition. Furthermore, the rocks embed metamorphic and igneous xenoliths. In contrast, Lisca Bianca and Dattilo are made of dacitic-andesitic lava flows and domes, respectively (CALANCHI ET AL., 2002). Basiluzzo, a lava dome, which is located farther north from the crater, is considered the youngest portion of the Panarea volcanic complex. In contrast to the other islets, it represents a lava dome of mainly rhyolitic composition, enriched with xenoliths of volcanic and metamorphic nature (CALANCHI ET AL., 2002; LUCCHI ET AL., 2013).
The Panarea volcanic complex is characterized by degassing processes throughout several fumarolic areas which can be observed offshore as well as on the main island. The lava units on Panarea Island and the eastern islets are characterized by hydrothermal alterations of variable degree which result in strongly modified mechanical properties of the rocks (ESPOSITO ET AL., 2010; CAS ET AL., 2011). According to ACOCELLA ET AL. (2009), the onshore hydrothermal vents are aligned along NE-SW oriented fractures.

Submarine area

The main investigation area is located about 2.5 km east of Panarea Island where the minor islets Dattilo, Panarealli, Lisca Bianca, Bottaro, and Lisca Nera are located. The islets encircle a shallow depression which is up to 30 m deep and has a spatial extent of about 2.3 km^2. The submarine shelf of the Panarea volcanic system that is encircled by the islets is assumed to be a result of recurrent phases of erosion and deposition. These processes have taken place since sea-level fluctuations during the Late-Quaternary (LUCCHI ET AL., 2013). While depths within the encircled area of the islets are rather shallow, outside of this shelf, especially in the north-western and south-eastern regions, the seafloor goes down to depths of over 100 m (e.g. ANZIDEI ET AL., 2005; STANULLA ET AL., 2017).
Since historical times exhalative activities have been known in the investigation area (GABANELLI ET AL., 1990; ITALIANO AND NUCCIO, 1991; CALANCHI ET AL., 1995). Between the islets east of Panarea, recent discharge of hydrothermal fluids as well as gas-venting can be observed (GABBIANELLI ET AL., 1990; CALANCHI ET AL., 1995; ESPOSITO ET AL., 2006). Close to Panarea Island, around La Calcara bay, minor exhalative activity can be found as well. In 2015, another vent field, called *Smoking Lands*, of a large spatial extent close to Basiluzzo islet about 70 m bsl was found and described by ESPOSITO ET AL. (2018). Water and gas chemistry have been investigated for several decades, especially using scuba diving techniques. The discharge behavior was of interest as well. Data is presented by ITALIANO AND NUCCHIO (1991), CARACAUSI ET AL., (2005), GUGLIANDOLO ET AL. (2006), CAPACCIONI ET AL. (2007), BAUER ET AL. (2009), ITALIANO (2009), MAUGERI ET AL (2009), SIELAND (2009), STEINBRÜCKNER (2009), ANDALORO ET AL. (2010), HAMEL (2010), HEINICKE ET AL. (2010), PETERS ET AL. (2010), PONEPAL ET AL. (2010), MERKEL ET AL. (2011), PETERS ET AL. (2011), SCHIPEK AND MERKEL (2011), TASSI ET AL. (2014) and MEINARDIUS (2016).

Accompanied by an increased earthquake activity a major gas outburst on the western shore of Bottaro islet was observed in November 2002 leading to the formation of a crater with a diameter of approximately 15-20 m (ESPOSITO ET AL., 2006; TASSI ET AL., 2009). It is considered a rapid input of fluids related to magmatism. However, fluid exhalation declined significantly about six months later. As a consequence, the chemical composition of the hydrothermal fluids returned to the typical composition measured in the area prior to the outburst (CAPACCIONI ET AL., 2007; ALIANI ET AL., 2010; TASSI ET AL., 2014). Fluids, mainly gases, are dominated by CO_2 (94.0-99.5 Vol.%). Furthermore, H_2S (0.5-6.0 Vol.%) and trace gases, such as SO_2, HCl, HF, He, H_2, CO as well as light unsaturated carbons, are included in the emitted mixed hydrothermal gas. Hydrothermal water is also contained in the fluid mixture. Based on a specific gas flow-rate, gas emissions in the submarine part of Panarea Island have been divided into five classes (A – E from weak to strong, Table 2) according to SIELAND ET AL. (2009) and STEINBRÜCKNER (2009).

Table 2: Classification of hydrothermal fluid exhalations according to STEINBRÜCKNER (2009). The majority of fluid vents are classified class A or B, whereas only few emanation points of class E have been spotted yet.

Class	**A**	**B**	**C**	**D**	**E**
Flow-rate [l/min]	< 2.1	2.1 – 3.6	3.6 – 7.2	7.2 – 40	> 40

As a result of the continuous discharge of hydrothermal fluids, degassing structures have been formed. In the investigated area, both active and inactive structures can be observed. Data on hydrothermal fluid discharges is given by DEKOV ET AL. (2013), PRAUTSCH ET AL. (2013), HILDEBRANDT (2013), STANULLA ET AL. (2016a), STANULLA ET AL. (2017), KÜRZINGER (2019). According to ESPOSITO ET AL. (2006), the hydrothermal discharges are primarily aligned along NE-SE, NW-SE, and N-S trends.

Within the investigation area, porphyric basaltic to andesitic lavas are mainly covered with a layer of Holocene volcanoclastic sediments (CAPPACCIONI ET AL., 2007). The sediments resulted from the erosion of the surrounding lava domes (islets) and their deposition during the last Glacial Maximum (CAS ET AL., 2011; LUCCHI ET AL., 2013b). The loose or partly consolidated sediment covers primary volcanic features.

Digital terrain models (DTM) were generated of Panarea Island and the eastern submarine area, respectively, to model ground deformations of the volcanic system of Panarea (ANZIDEI ET AL., 2005; ESPOSITO ET AL., 2010). In order to do so, bathymetric, LIDAR and photogrammetric methods were combined (ANZIDEI 2000; FABRIS ET AL., 2010).

1.2 Aim of the thesis/objectives

The Aoelian Arc is an area of known neotectonic activity that has been investigated for several decades. Since the majority of this area is covered by sea water, the submarine portions have not been investigated in person concerning neotectonics but only by applying bathymetric methods and modelling the submarine ground to depict structures of a decametre scale or larger. For Panarea Island and its surrounding area only few data is available.

Therefore, this thesis aims to address two topics concerning the neotectonic system of the Panarea volcano. The first part focuses on an inventory of the neotectonic structures that can be found in the system of Panarea, both in subaerial and submarine areas. This includes the determination of the geometry and kinematic nature of the structures, their size and spatial extension. Furthermore, the subaerial and submarine structures are to be compared with each other. The second part aims to determine a relative age from the spatial arrangement of various neotectonic structures.

Given these aims, the author poses the following hypotheses:

- The submarine and subaerial neotectonic inventory of the Panarea system resemble each other in their appearance and extension.
- Although Panarea is located in the north-eastern sector of the Aeolian arc not only north-east oriented extensional structures can be found but also compressional and transversal structures of different orientation. Most structures prevail an extensional character.
- The neotectonic structures of the Panarea system indicate that the stress field of the volcanic system has undergone a westward rotation.

2. Description of the investigation area

2.1 Subaerial sites

The emergent area of Panarea Island measures about 3.4 km^2 which makes it the smallest island of the Aeolian Islands. The highest peak of the island, Punta del Corvo, is 421 m high (Figure 3). Some of the outcrops are described in detail below. The coordinates of these outcrops are listed in

Table *3*. An overview of the documented outcrops, except for the islet of Bottaro, is shown in Figure 4. Due to the steep flanks leading into the Mediterranean Sea in the north and west of Panarea Island, some prominent places can only be described based on remote sensing.

Table 3: List of the coordinates of some significant outcrops on Panarea Island and Bottaro islet. Coordinates are listed in UTM WGS84, Zone 33S after rectifying the daily shift (cf. 3.2.2). The outcrops are marked in Figure 3. Bottaro islet is shown in Figure 5.

Investigation site	**UTM coordinates 33S WGS 84**	
	E	**N**
Bottaro islet	509620	14276559
Capo Milazzese	505586	14275133
Entrance of natural reservation	505914	14277473
La Calcara Bay	506551	14277361
Punta del Tribunale and Castello	505520	14275930
Prehistoric village near Calcara	506562	14277272
Western flank near Costa del Capraio	505100	14276242

2.1.1 Bottaro islet

Belonging to the subaerial part of the Panarea volcano, Bottaro islet is one of the small land portions east of Panarea Island, encircling the submarine crater (cf. Figure 10 A). The islet is located southwest of Lisca Bianca islet. The submarine investigation sites Bottaro North and Bottaro West are named after the islet due to their vicinity to each other. Bottaro islet has an elongated shape. The islet measures about 185 m in its NNW-SSE orientated long axis and 60 m in its short axis. On its northern edge, the islet rises several decametres from the sea. Going south, the islet shows a moderate slope so that the southern edge runs gently into the sea without forming cliffs.

2.1.2 Capo Milazzese

Capo Milazzese (Figure 4 A) is a peninsula located directly on the shore in the southeast of Panarea Island where a Middle Bronze age village was excavated (ALBERTI, 2013; ORLANDO ET AL.

2018). A narrow neck of land connects the peninsula with the rest of the island to the north reaching up to 45 m asl. The other sides are running into the sea, leaving behind steep slopes.

Figure 3: Overview of Panarea Island. Mapping of Panarea was conducted during the field work in 2018. Characteristic spots introduced in this thesis are marked in the map (red dots). The underwater investigation site La Calcara which is located outside the "crater" east of Panarea is marked in the north-east of the island. The highest peak of Panarea, Punta del Corvo (421 m asl), is situated in the north-west of the island. Peaks are marked with stars. Some smaller islets, such as Scoglio la Nave, are located close to the main island of Panarea. The sea (blue) in the vicinity of Panarea Island is rather shallow. The vilaages Drauto, San Pietro and Ditella are located along the eastern shore of Panarea Island.

The western side of Capo Milazzese is characterized by a small beach of well-rounded gravel and boulders. The beach is surrounded by igneous rocks. Several dykes can be spotted in the vicinity of the beach, both onshore as well as in rocks that rise from the sea nearby.
Capo Milazzese's eastern side runs steeply into the sea. Columnar joints rise from the sea and continue towards the islet Cala Junco. The islet of Cala Junco can be reached by foot through the water when the sea is quiet. While most of the islet is composed of the columnar joints, also dykes can be located on the islet at some spots rising between the joints.

2.1.3 Entrance of natural reservation

The approximately 30 m broad outcrop is located about 160 m asl, close to the entrance of the natural reservation at the northern shoreline of Panarea Island. Overgrown by few Mediterranean plants and grass in the upper regions, the outcrop is characterized by steep slopes of volcanic rocks emerging from the sea (Figure 4 B). Due to the steepness along the northern coastal line, only a minor part of the outcrop can be investigated in detail while major

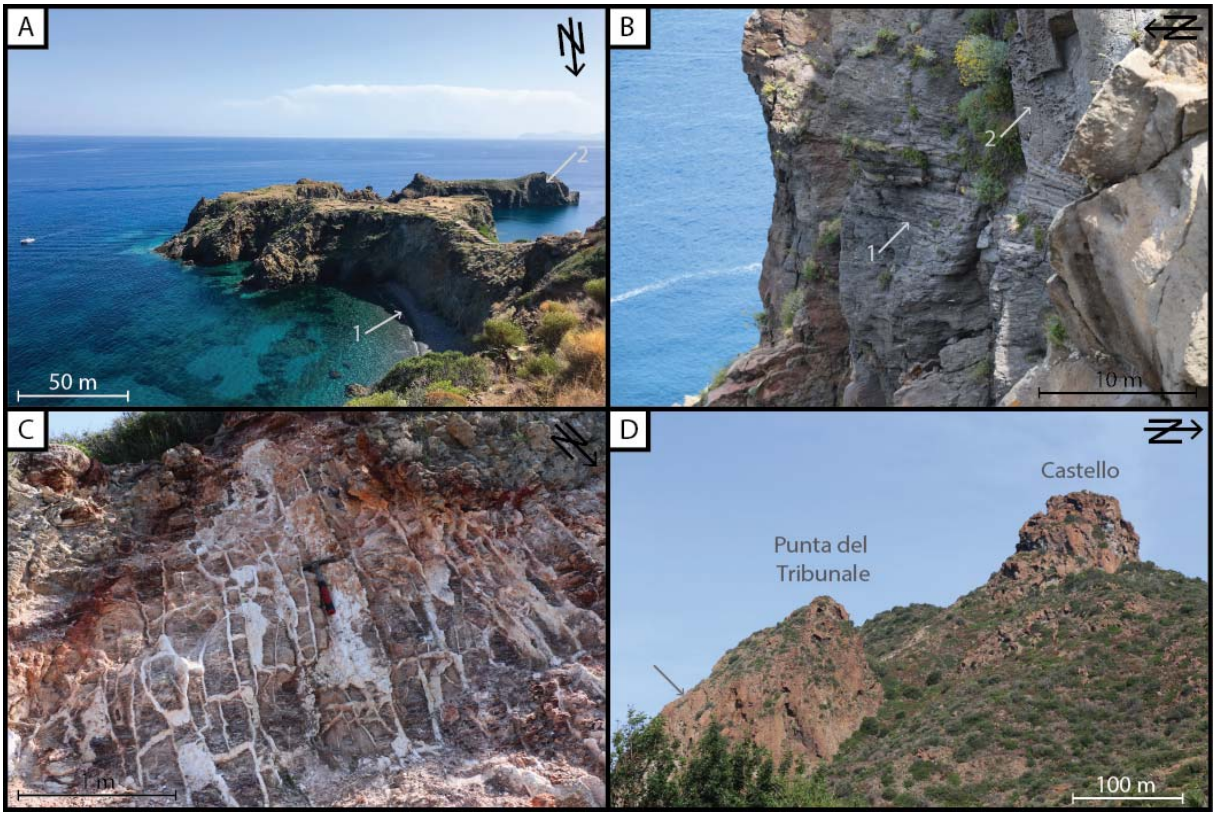

Figure 4: Overview of some investigated outcrops at Panarea Island. A – Capo Milazzese at the south-eastern edge of Panarea. Recent sea shore deposits can be found in the bay left and right of the peninsula from which steep slopes (arrow 1) run to the prehistoric village at the top of Capo Milazzese (ALBERTI, 2013; ORLANDO ET AL. 2018). Several smaller islets rise from the sea in the vicinity, mainly formed of columnar lava flows (arrow 2). B – Steep slope at the entrance of the natural reservation in the North of Panarea Island (ca. 160 m asl). Different eruption stages can be observed: one of the eruptive stages produced a layered rock where light and dark coloured layers alternate (arrow 1), the hanging rocks are porous and vesicular volcanites. C - The volcanic rock near the prehistoric village at La Calcara is cut vertically and horizontally by a whitish rock. In some parts, the

white material is soft and resembles chalky material while other parts of it are hard and splintery showing a vesicular texture. D - The volcanic plug domes Punta del Tribunale (168 m asl) and Castello (257 m asl) in the southeast of Panarea Island. At certain wind directions a sulphurous scent can be recognized. Additionally, a light yellow cover is distributed across the wall of the south-western side of the plug dome (arrow).

Parts, distant structures in dm-scale or larger, can only be described based on remote sensing. Close to the shore, remnants of colluvial deposits can be found covering recent well-rounded sea-shore deposits. The cliffs appear sharply edged and massive. Several dykes running in various directions can be located in the vicinity as well as on the islet Scoglio la Nave nearby from the top of the outcrop.

2.1.4 La Calcara Bay

As indicated by the name, this spot is directly located at the bay of La Calcara in the northeast of Panarea Island. The bay is bordered by high cliffs made of dacitic to andesitic rocks coming from the landside whereas it runs shallowly into the sea on its north-eastern and eastern flank. The outcrop runs about 50 m from the slope to the sea in its short axis whereas it extends over about 200 m in its long axis. The spot is characterized by well-rounded surf conglomerates. In the centre of the bay, sulphur fumaroles are scattered from which hydrothermal gases are emitted. However, no chemical characteristics or temperature data was documented by the SDC. Going to the extensions of the bay, columnar joints rise from the sea, especially in the southern part of the bay.

2.1.5 Prehistoric village near Calcara

A prehistoric settlement of Late Neolithic to Early Bronze age (DAWSON, 2015) is located in the northeast of Panarea near the bay of Calcara at an altitude of about 45 m asl. The outcrop is separated into two parts. While one part is located close to the cliffs running towards La Calcara bay, the other part can be found further landwards. Both parts are connected by a small path that diverges from the trail to the Calcara bay. The outcrop extends over some tens of metres and is about 4 m high. The part close to the cliffs is dominated by a wall of altered volcanites which are cut by a soft, whitish to greyish material (Figure 4 C). The second part is characterized by a tuff wall where a paleo hydrothermal discharge structure can be observed.

2.1.6 Punta del Tribunale and Castello

East of the village Drauto, in southern Panarea two massive volcanic structures rise. These volcanic plug domes are named Punta del Tribunale and Castello and are 168 m and 257 m high, respectively (Figure 4 D). Both of the domes are surrounded by volcanic ashes and bombs. Due to the dense vegetation growing around these bodies, only boulders in their vicinity could be examined. Depending on the wind direction, a sulphurous scent can be recognized.

2.1.7 Western flank near Costa del Capraio

The western coast of Panarea is characterized by steep, subvertical cliffs that can be observed from a small trail near Costa del Capraio. This flank can be seen when walking on the trail to Punta del Corvo from the south, but it cannot be reached by foot. Hence, all mapping and the associated descriptions are based on distant observations. The western flank of Panarea is several 100 m longs and about 400 m high, rising from the sea. The upper parts of the cliffs are overgrown with various plants while the lower portions are mostly covered by gravel and boulders since a major part of the cliffs have collapsed. This block of colluvial deposits runs into the sea.

2.2 Submarine investigation sites

The submarine investigation sites visited during the field trips to Panarea Island will be described in the following chapters. In Table 4 the coordinates of these spots are listed. Figure 5 gives an overview of the different investigation sites east of Panarea Island. La Calcara is not marked in this figure due to its proximity to the Panarea shore near La Calcara bay. Hence, the location of La Calcara is marked in the map of Panarea Island (cf. Chapter 2.1, Figure 3).
Most of the diving spots are marked with buoys which are used to find the spot when navigating to them with the boat. In addition, divers use the buoys' lines to descend and ascend in the vicinity of the boat which typically drops anchor near the buoys or directly in the lines of the buoys.

Table 4: List of coordinates of each submarine investigation site of the submarine investigation area. Coordinates are listed in UTM WGS84, Zone 33S after rectifying the daily shift (cf. 3.2.2).

Investigation site	**UTM coordinates 33S WGS 84**	
	E	**N**
Area 26 (A26)	509111	14276753
Black Point (BP)	509111	14276498
Bottaro North (BN)	509578	14276690
Bottaro West (BW)	509573	14276555
Cave (CAV)	509376	14276740
Fumarolic Field (FF)	509542	14276825
Hot Lake (HL)	509545	14276859
La Calcara (LC)	506616	14277411
Point 21 (P21)	509247	14276621

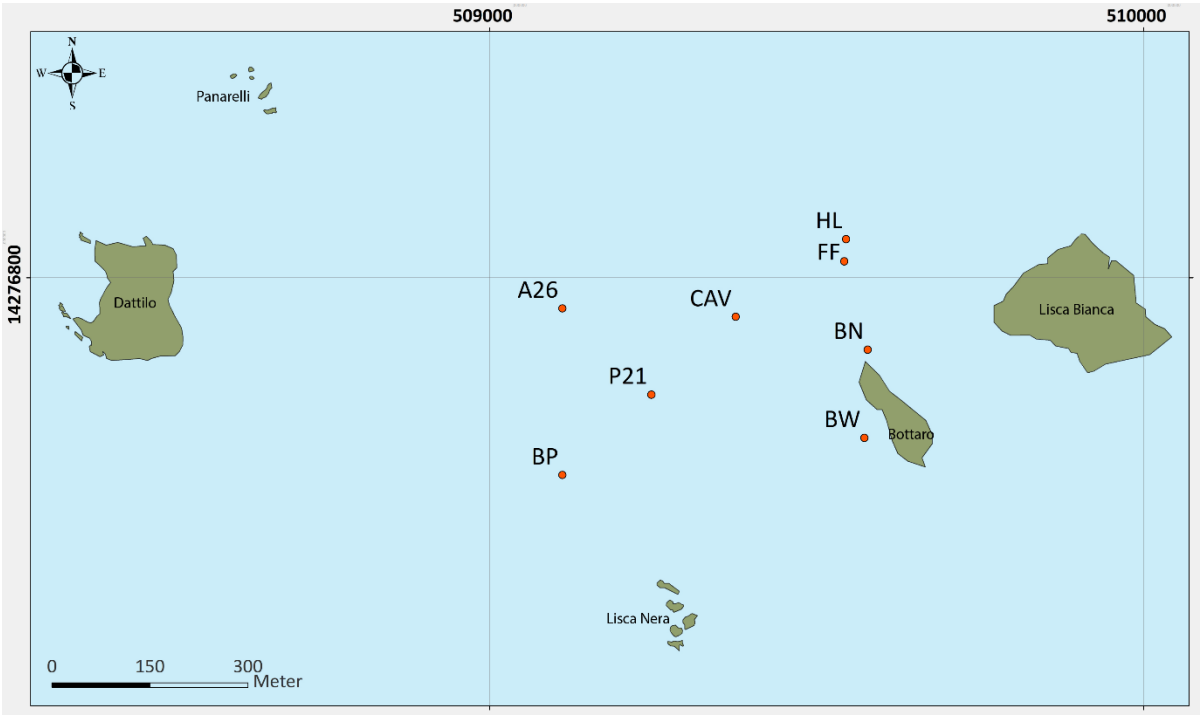

Figure 5: Submarine investigation sites (red) east of Panarea Island. The shallow submarine area (light blue) is surrounded by the islets of Dattilo, Panarelli, Lisca Bianca, Bottaro and Lisca Nera (green). All the spots were visited for various investigations during the field trips to Panarea in September 2017 and 2018. La Calcara is not marked in the map but was visited several times.

2.2.1 Area 26

Area 26 (A26) is located about 600 m east of Dattilo and 100 m northeast of Point 21. The location lies in the central part of the crater. It is characterized by widespread sediment plains at a water depth of 26 m which makes this spot the deepest one within the investigation area. The plain expands more than 50 m in its N-S axis and in its E-W axis, respectively. In the southern and eastern section of Area 26 large Posidonia fields can be found (Figure 6 A). In addition, several smaller Posidonia fields are located in the north-western area of this location. Due to its lateral extent, several sub locations have been defined for points of interests in addition to the two ascending buoys which are situated in the north and in the south of Area 26. These sub locations are named after prominent structures. Close to the northern buoy (Buoy 2), *Mouth* is located as one of the sub locations. *3-Bowls*, *Lineament*, *Hot Bowl* as well as *Brodor* are sub locations situated close to Buoy 1 (cf. Figure 12, Appendix 4) in the south, while *"Lava" tongue* is found in the central parts of Area 26.

2.2.2 Black Point

Black Point (BP) is the southernmost underwater investigation site. It is located near Lisca Nera, about 600 m west of Bottaro and marked by a large buoy by the INGV on the sea surface which contains a submarine monitoring module (MAUGERI ET AL., 2010). This investigation site is made of two submarine craters of which the inner one lies at a depth of about 23.5 m. The

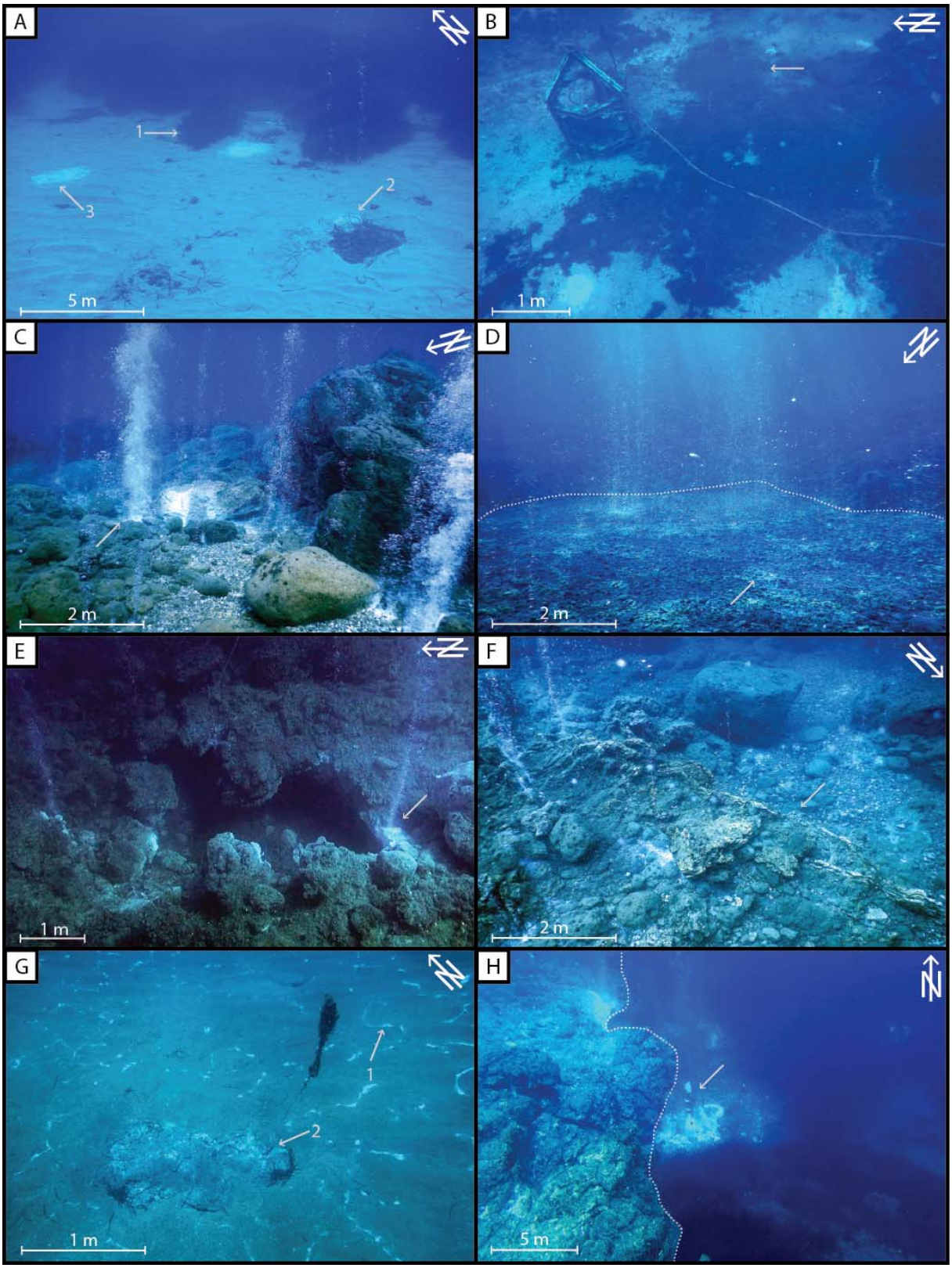

Figure 6: Overview of some investigated sites near Panarea Island. A - Sandy plains surrounded by Posidonia fields (arrow 1) at Area 26. Some small hydrothermal fluid vents occur throughout the area (arrow 2). In some cases, these outlets are indicated by whitish bacterial mats, as can be seen at the 3-Bowls structure in the southeast of Area 26 (arrow 3). B – A measuring station by the INGV is installed next to the shallow water smoker Black Point (arrow). The smoker is located in the inner crater of the location Black Point which is covered with light sediment. Biota cover the outskirts of the crater as well as its rims (lower right hand corner). C – Gravel field

between large boulders at Bottaro North. Numerous strong hydrothermal vents (e.g. arrow) are located between the boulders, often accompanied by mineral precipitations or bacterial mats. Behind the boulders the slope rises towards the islet of Bottaro. D - Diffuse hydrothermal fluid vents in the southern crater at Bottaro West (outlined by dotted line). The crater is filled with gravel underneath which conglomerates occur. Whitish bacterial mats settle on the gravel (arrow). E - Overview of Cave. The depression is filled with Posidonia leaves covering the sediment on the ground. Around the depression, large boulders can be found as well as some hydrothermal fluid vents. The southern portion of Cave represents a grotto (arrow) in which the discharge of hydrothermal fluids can be observed and the walls are covered with thick bacterial mats. F - Silicified rocks (arrow) in the south of the gravel field at Fumarolic Field. G - Wide sediment field at La Calcara, partly covered with whitish bacterial mats (arrow 1). At some spots, such as *Mordor* (arrow 2), hydrothermal fluid discharges can be found only a few centimetres underneath the sediment cover. H - Plateau (left hand side) traversed by cracks and fissures next to the scarp wall at Point 21. On the bottom of the scarp wall the FSVG (arrow) is located which is used by the SDC Freiberg to measure gas flow-rates. The construction is positioned at the two strongest hydrothermal fluid vents that could be found throughout the investigated sites of the SDC. (Photography: A, G – R. Stanulla; B, D – L. Schüler; C – M. Kleinschroth; E, H – S. Kluge; F - SDC)

seafloor of the craters is covered with sediment. The flanks surrounding the crater rise about 1 m leading to the outer crater and are mostly overgrown by Posidonia. Some small hydrothermal gas vents are distributed across the inner crater and its vicinity. Along the northern rim of the crater hydrothermal water discharges can be observed due to a scintillation of the sea water that can be recognized from a distance of a few metres when diving close to the sea bottom. The outer crater rim lies at a depth of about 20.5 m. Posidonia fields cover major parts of the outer crater. The sediment fields are often covered with whitish bacterial mats which is why these mats are commonly good indicators for hydrothermal fluid outlets.

The location is named after a grey smoker which is a grey-black sinter body, named Black Point, in the south-eastern section of the inner crater (Figure 6 B). The body measures about 2.7 m in length, 1.0 m in width and is about 0.5 m high. It consists of fine-layered mineral crusts on top of the original porous conglomeratic rock (BECKE, 2009). In the north-eastern part of the body hydrothermal waters discharge out of a vent. Only small amounts of hydrothermal gas are contained. Small particles in the emanated water give it a greyish colour. The Fluid temperatures at Black Point can each up to 130 °C (CALIRO ET AL., 2004; BECKE, 2009). Along with the hydrothermal discharges ore precipitations can be observed.

2.2.3 Bottaro North

Bottaro North (BN) is located at the north-west shore of Bottaro islet, close to the narrow channel between the islets of Lisca Bianca and Bottaro. Fumarolic Field is located about 200 m north of this site. With a maximum depth of 9 m below sea level it is a very shallow submarine site. To the south, the ground rises towards the steep shore of Bottaro islet (Figure 6 C). Bottaro North is characterized by a central gravel field that is surrounded by boulders which can reach several meters in diameter. Numerous class A to E vents can be found on the gravel field as well as between the boulders (STEINBRÜCKNER, 2009). At some places, the

hydrothermal fluid vents are covered with whitish bacteria mats. In the vicinity of the vents water temperatures range between 27.9 and 56 °C (SIELAND, 2009). Due to the shallowness of this site gas bubbling is visible at the sea surface. In addition, a smell of hydrogen sulphur is recognizable on the northern shore of Bottaro islet as well as on the water at moderate wind speed.

2.2.4 Bottaro West

About 30 m west of Bottaro islet the investigation site Bottaro West (BW) is located around 12 to 14 m below sea level. The structure of this site was formed during the 2002 gas burst event (ESPOSITO ET AL., 2006). Bottaro West's central part represents a submarine crater. As the crater was refilled with sediment and rock debris its original size that extended about 40 m in diameter initially has decreased (ESPOSITO ET AL., 2006). The crater is enclosed by an outer margin that can be found between 7 and 9 m below sea level. To the east the slope rises due to the proximity to Bottaro islet. Several hydrothermal discharges are located in the southern part of the crater (Figure 6 D). Outside of the crater, large Posidonia fields cover the sea floor.

2.2.5 Cave

Cave (CAV) is located about 200 m northeast of Point 21. It is up to 23 m deep. This site represents a partly collapsed cave whose roof is missing now (Figure 6 E). The scale of this structure is comparable to Hot Lake (cf. 2.2.7). Around this depression there are Posidonia fields of a large expansion. This investigation site is named after a small grotto in the southeast of the depression. It is characterized by intense hydrothermal fluid discharge as the dense bacterial mats covering the inside walls of this grotto show. Due to these mats the grotto is not accessible with the applied scuba techniques because the exhalation air would disturb the divers' visibility. However, discharges, yet more moderate, can also be observed at other spots in the vicinity of Cave's depression. In the western part of Cave many silicified structures can be observed at the overhang of the depression.

2.2.6 Fumarolic Field

Fumarolic Field (FF) is located south of Hot Lake. This site represents a flat sediment field that measures about 30 m in its E-W axis and 20 m in its N-S axis. The plane is located about 15-17 m below sea level and dips slightly towards the south-east. Some Posidonia fields can be found on the northern slopes whereas the other slopes are covered with some boulders. Numerous class A to C vents can be found at Fumarolic Field. Besides the gas-dominated discharges water outflows can be observed. At Fumarolic Field, temperatures between 39.7 and 59.1 °C were measured (HAMEL, 2010). South-east of the sediment field silicified structures can be observed (Figure 6 F).

2.2.7 Hot Lake

Hot Lake (HL) is a depression north of Fumarolic Field, 18 m below sea level. It is located about 250 m north of Bottaro islet and approximately 300 m west of Lisca Bianca. In the north-eastern section of Hot Lake, the depression extends farther to the east. Both the sediment and the Posidonia filling the inside of the depression are covered with white bacterial mats at some spots. The basin is enclosed by walls that are up to 2 m high whereas the walls in the northern section are smaller than in the southern section. In the southern part of Hot Lake, the walls are overhanging forming cave-like structures that are covered with thick layers of white bacteria.

Rare hydrothermal fluid discharges were observed in the northern and the western part of Hot Lake, at the rims of the depression. This location was named Hot Lake due to the hot hydrothermal fluids that discharged dispersedly from within the depression. However, during the mapping campaigns in 2017 and 2018 no fluid discharges could be observed at this site as discharges have cooled down continuously (personal communication SDC). During former campaigns, maximum temperatures of about 96 °C were measured at this location (HAMEL, 2010). Discharges at Hot Lake are water-dominated. Gas-dominated discharges are scarce at this spot. The surrounding of Hot Lake is characterized by large fields of Posidonia as well as boulders of various size.

2.2.8 La Calcara

La Calcara (LC) is the closest underwater site to Panarea Island. It is located at the shore, east of La Calcara bay, about 900 m north of the mole on Panarea Island. Out of all submarine spots having discussed in this thesis, La Calcara is the only one not being located within the crater. The area dips slightly to the east which is why it becomes deeper going north-eastward. Because this spot is characterized by a large extent (> 100 m in its length axis and > 50 m in its minor axis), several sub locations were established besides the two ascending buoys in the north and in the south of La Calcara (cf. Figure 31, Appendix 4). These sub locations are called *Black Rock*, *New Rock*, *n.n.-Area*, *Mordor*, *Fixpoint 9*, *The Wall* and *Octopus Rock*. The deepest point of La Calcara is 23 m below sea level where Octopus Rock can be found. The area between *The Wall* and *Octopus Rock* is widely covered with sand plains throughout which several large boulders can be found. The sediment covers clays which seem to be distributed extensively underneath the plains (PRAUTSCH ET AL., 2013). Several Posidonia fields of variable sizes lie between the fix points. Temperatures at La Calcara can reach up to 130 °C a few centimetres below the ground, as for example at *Mordor* (STANULLA, 2021; Figure 6 G). This temperature represents the boiling point of seawater at this depth. Below the sea-bottom, numerous small gas-dominated vents can be found across this site which form secondary structures in the sediment such as cones and tubes. However, water-dominated discharges can also be found, as for example at the sub location *Mordor* (STANULLA ET AL., 2017).

2.2.9 Point 21

Point 21 is a submarine location in the centre of the crater. It is located about 400 m west of Bottaro and 300 m north of Lisca Nera. The deepest point is located 21 m below sea level. The most prominent structure is a *Scarp wall*. The three strongest vents (gas-dominated, class E after STEINBRÜCKNER (2009) of the entire submarine investigation area can be found at the bottom of the southern part of the scarp (Figure 6 H). Hydrothermal fluids are also emitted from the wall (ORDOSCH, 2016). Few class D vents are located east of the *Scrap wall*. Furthermore, several small vents occur close the large vents.

To the west the *Scarp wall* goes over to the *Plateau* at a water depth of about 17 m. It is traversed by numerous cracks and fissures along which small gas-dominated fluid discharges are aligned. These fluids are acidic due to the high amount of hydrothermal gases in the fluid mixture. In the vicinity of some of the vents whitish bacterial mats cover the rock surface. The surroundings of the plateau and the scarp are mostly overgrown by Posidonia. However, small gravel fields occur between the biota. To the south, hard rocks crop out at some spots where fissures along with hydrothermal fluid discharges can be observed.

3. Methods

The aim of the thesis is to gain more information about the structural and tectonic context of Panarea Island and its submarine surroundings. As Panarea Island represents only a small emergent part of the actual volcano, a large portion of the field work was focused on the submarine part of Panarea. Additionally, a mapping campaign took place on the island of Panarea itself. During the field work, rock samples were taken both under water and onshore. Where possible, structural data was sampled. Thin sections were made of some of the samples which were used to identify both the mineral composition and to search for tectonic structures on a smaller scale. Furthermore, the information was put into a map to gain information on large-scale structures on and around Panarea Island. In order to provide a full documentation, especially of the submarine field work, a photo documentation was developed.

3.1 Field work

3.1.1 Subaerial field work

Mapping

For the mapping of the subaerial parts of the investigation area a topographic map as a basis for the geological mapping was used. As a start, outcrops were looked for along the streets and paths marked in the map to get an overview of the diverse lithologies on the island. The outcrops were numbered and the characteristics to each outcrop including details to the rocks, GPS coordinates, as well as inclination and dip directions of geological structures wherever they could be measured with a geological compass, were recorded. For measuring GPS coordinates, a Garmin GPSmap 276c device was used. The geological compass by FPM delivers an accuracy of ± 1 ° for the strike direction and ± 5 ° for the dip direction. Additionally, the outcrops were marked on the map. Depending on the lithology of the rock, the outcrop's background was colourized. If strike and dip directions were measured the average of these values was added to the map.

Working on the map, there has to be distinguished between the locations where the lithology can clearly be distinguished and those where one had to interpolate. Some areas could not be reached due to steep slopes or too much vegetation. In order to investigate these locations as good as possible remote sensing with the help of binoculars was used to describe and compare the rocks with the ones that could be observed elsewhere on the island.

Rock sampling

Rock samples were taken using hammer and chisel. Besides oriented samples whose strike and dip direction were measured and marked on the rock before removing, samples of volcanic rocks were taken. All samples were documented by photograph and described geologically.

Documentation

Visual documentation on Panarea island was conducted using a Canon EOS 70D camera system which was combined with different objective lenses. The images were created using RAW format. White balance could be adjusted manually on the camera.
The Software Adobe Creative Suite CS 6 was applied for image editing.

3.1.2 Submarine field work

Working under water

In order to conduct scientific work at submerged locations methods of Scientific Diving were used. However, diving itself is only an assisting tool that can be used to carry out investigations. The application of scientific methods was tried to be adapted from the standardized methods of subaerial environments as good as possible.
While working under water, semi-dry suits, cold water regulator technics and 15 l, 200 bar scuba tanks as well as diving computers were used as standard equipment for the participating divers. Decompression stops were calculated by the divers' computer. Furthermore, all divers were instructed in various safety regulations based on the work instruction for scientific diving by the Scientific Diving Center of TU Bergakademie Freiberg as well as the methods they were to apply during their work under water. For each dive protocols were prepared including the documentation of general diving procedures as well as the documentation of the data collected.

Mapping

Maps of the various submarine investigation sites within the investigation area already existed prior to the 2017 and 2018 field trips to Panarea. However, the density of information of the maps were variable which is why a major part of the field trip consisted of mapping campaigns with the aim to complement the existing maps and to add further information, particularly focusing on geological data.
Maps as well as sketches were drawn directly on site. For mapping, the GPS coordinates of the fix points at each location were measured using a Garmin GPSMAP 64 device. The fix points (e.g. ascending buoys) were used as a starting point from which the distances to prominent locations were measured. In addition, the directions from the fix point to the different submarine locations were measured using a compass as well as the water depth using a dive computer. Giving this, the locations' coordinates could be calculated. Sketches for the locations were drafted which give detailed information on their dimensions, the kind and flow-rate of mixed hydrothermal fluid discharges, their lithologies as well as their strike and dip direction.
Since some of the structures were covered with recent sediment, a mobile airlift pump was used to excavate them (STANULLA ET AL., 2016b). The airlift can be operated with compressed air from additional scuba tanks. Using a suction hose, the sediment becomes sucked due to

an under pressure that develops in the mixing chamber when air is injected. Consequently, the sediment is led through the riser pipe and exits it at the end of the pipe 3 m above the mixing chamber (Figure 7).
Common geological compasses do not work under water. Hence, a clinometer was built in order to measure strike and dip directions of geological structures.

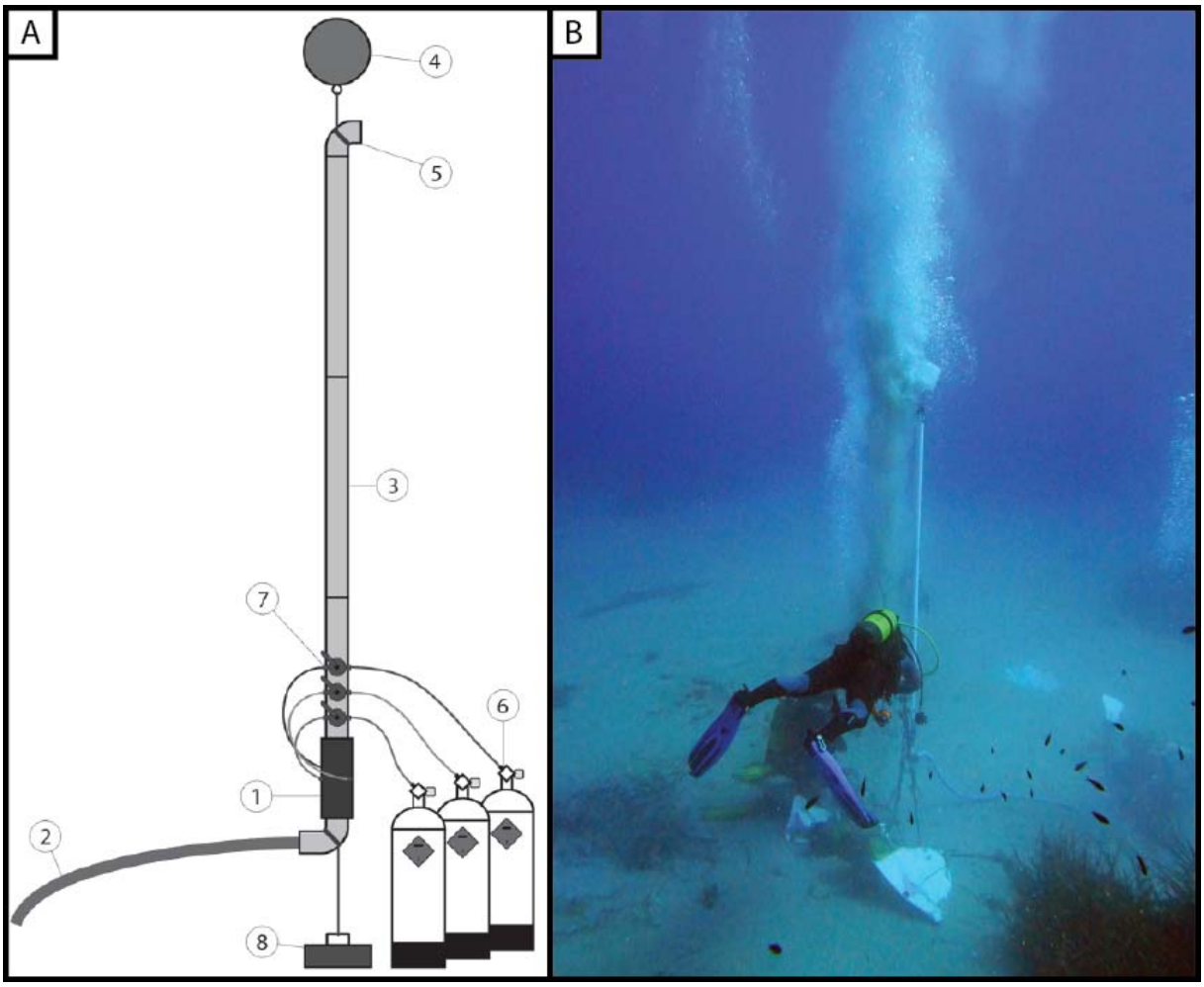

Figure 7: A – Technical model of an airlift pump with its major elements: mixing chamber for gas injection (1), suction hose (2), riser pipe (3), buoy (4), ejector (5), air reservoir (6), control panel (7), and counterweight (8) (STANULLA ET AL., 2016b). B – Mobile airlift pump in use at 3 Bowls, Area 26 in order to excavate the sediment filled bowl structures.

Rock sampling

Common sampling techniques using hammer and chisel proved to be well applicable for hard rock samples under water. In preparation of taking samples, PVC sampling bags were prepared prior to each dive. This includes opening the sampling bags to allow water to flow in during the dive (to adjust to the surrounding pressure) as well as labeling each sampling bag.
After measuring strike and dip direction of the sampled hard rock and photographing the sample as well as its surroundings, the sample could be taken. It was then put into one of the

labeled sampling bags which is then placed into a transport net in order to bring all sampling material to the surface. Prior to the transport to Freiberg, all samples were geologically described and documented photographically.

Documentation

Several camera systems were used for the visual documentation. For the main part, pictures were taken of geological structures as well as greater parts of the various locations. However, a video documentation was also done in order to get an overview of large structures or to record sequences in order to observe hydrothermal fluid discharges in more details. For image editing, the software Adobe Creative Suite CS 6 was applied.

Most pictures were taken with a waterproof camera system Nikon Coolpix W300. This 16 MP camera system uses a MP4 format for video files and creates images in JPEG format. White balance is done automatically by the camera and cannot be adjusted.

Some images were taken with a Sony DSC-RX 100 MII compact-camera system along with a waterproofed polycarbonate UW-housing and special LED video lamps with a colour temperature of 3200 K. White-balance was adjusted manually on the camera. The images were created using the RAW format. An AVCHD format was used with rates of 50 half images per second for video files.

Further images were taken with a compact camera system Sony Alpha 6000 in an Ikelite polycarbonate UW-housing. Images were taken using RAW format. For this 24 MP camera system, an AVCHD-format was used which has rates of 50 half images per second. White balance could be adjusted manually on the camera.

Sometimes, the above-mentioned camera systems were also used to record videos. However, the main video documentation was carried out with a Sony HDR-PJ780 VE camera type. The camera was protected from water by an BS kinetics UW housing.

Furthermore, a Blackmagic URSA Mini 4.6K EF cinema camera was used for video documentation. This type was combined with various objective lenses. A Nauticam waterproof UW-housing was used in combination with external LED video lamps which could be installed either on the housing or on separate tripods.

The postproduction of the videos was mainly conducted using the software Avid Media Composer 5.5. The pictures were summarized in a database using the software Microsoft Access (Version 2016). The database is used to order the pictures concerning the locations and the sub locations as well as to add information about the geological characteristics and structures.

3.2 Laboratory methods

3.2.1 Sample preparation and microscopy

After the field work ten oriented thin sections were prepared. Due to the high fragility of the sample material most of the samples had to be stabilized using epoxy resin (Araldite 2020).

For some samples, this had to be applied multiple times to ensure that the resin reaches the core of the sample as well. Then, the samples were cut into pieces to choose the area for the thins section.

The sections were prepared by the laboratory of the Technische Universität Bergakademie Freiberg, based in Institute for Geology and lead by Dr. Michael Magnus. The polished thin sections have a thickness of 30 µm and a size of 28 x 48 mm. Table 5 shows the samples of which thin sections were prepared, the location where these samples were taken and the purpose for preparing the section. Each sample was prepared orthogonally to the strike direction which was marked on the sample before removing from its origin.

Optical microscopy was carried out using different types of Zeiss polarization microscopes and binoculars. Due to the hydrothermal alteration of the rock samples, most minerals' optical properties do not coincide with the general properties of these minerals. In addition, the minerals' size does not allow further characterization concerning the crystal habitus often. Shapes of minerals appear to be altered due to hydrothermal alterations. Therefore, in most cases, mineral identification based on these properties was not possible (Figure 8).

Table 5: List of prepared polished thin sections.

Sample	Location	Purpose
PAN_HL_20170908_GEO_24	HL	Search for microscopic tectonic features along a crack in the wall of the tuff body, mineral identification
PAN_P21_20170909_GEO_27	P21	Search for microscopic tectonic features along or near cracks in the plateau's rocks, mineral identification
PAN_P21_20170909_GEO_28	P21	
PAN_A26_20170913_GEO_45	A26	Search for tectonic features in the wall of a degassing structure
PAN_P21_20170913_GEO_46	P21	Search for microscopic tectonic features along or near cracks in the scarp wall, mineral identification
PAN_BOT_20170913_GEO_51_1	BOT	Silicified structure, further specification and search for tectonic structures, mineral identification
PAN_BOT_20170913_GEO_51_2	BOT	
PAN_BOT_20170913_GEO_51_3	BOT	
PAN_BOT_20170913_GEO_51_4	BOT	
PAN_BOT_20170913_GEO_51_5	BOT	

3.2.2 Geological map

In order to display the results of the field work maps have been compiled of various regions and with different contexts. Map production used the software ArcGIS 10.4 by ESRI.

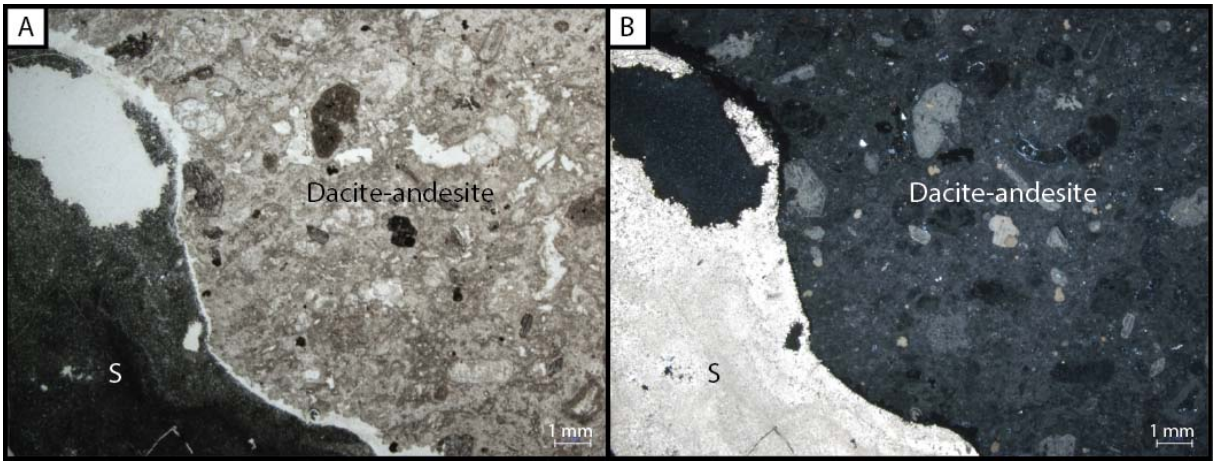

Figure 8: Thin section of a strongly altered dacite-andesite from Point 21. A crust of native sulphur is found on the outer margins of the rock (S). Underneath, single crystals of the dacite-andesite can be recognized, such as Feldspar and Biotite. However, they show signs of severe alteration. Due to this alteration, optical characterization of the rock is difficult. *A* –II-Pol., 2,5x. B – X-Pol., 2,5x.

To ensure the right location of the outcrops and investigation sites, the GPS coordinates were measured. However, a daily shift was recognized when plotting the values of the subaerial outcrops into the base map. For the submarine investigation points, this problem was known, yet the reason has not been found out until the field work for this thesis was carried out (compare KÜRZINGER, 2019; STANULLA, 2021).

Supposedly, a topographic map (scale 1:5 000) should be the base map for further mapping results when producing a geologic map at a scale of 1:10 000. Since open source maps do not display the topography at this scale, the use of a topographic base map was not given. Hence, an orthophoto taken on 2019-07-07 of the investigation area was exported from Google Earth (version 7.3.2.5776) and georeferenced. This orthophoto was georeferenced by a number of points that could be identified exactly. For this, the coordinates given by Google Maps were used.

After the orthophoto was inserted correctly into the GIS program, clearly identifiable outcrops were chosen whose location could be stated in the photo. When plotting this point, the daily shift could be measured and afterwards all sample points of this day were corrected by the shift difference. The daily shift varied between 10-120 m in all directions. This was done individually for those days when field work was carried out on Panarea Island (subaerial portions excluding Bottaro islet).

As for the submarine investigation points, a shift was recognized as well. However, it could not be stated how the shift behaved. Hence, investigation points, such as Area 26, and Black Point, were referenced based on the orthophoto. Since Black Point has been marked by a large buoy by the INGV this spot was clearly distinguishable as well as the large sandy plains of Area 26. The points, for which this could not be stated by the orthophoto, were plotted based on the estimated distances to the surrounding islets and to the submarine investigation sites whose coordinates were known exactly in the orthophoto. Accordingly, it cannot be ruled out

that the underwater locations may be dislocated slightly. Yet, the dislocation is not larger than a few decametres. The overall array of the investigation points is correct.
After the outcrops of Panarea Island were stated correctly, the geological map was digitalized based on the field sketch. For this, the various lithologies were assigned to a colour. Since there were areas of the island that could not be reached by foot, each lithology is also displayed by a paler hue of its colour to distinguish these areas in the map. While clearly distinguishable borders of lithologies are marked with solid lines, supposed borders are marked with dashed black lines.
The map does not include the anthropogenic portions on the eastern side of Panarea Island. Both the colluvial and aeolian sediments that can be found on the island are not specified any further because they are not of interest concerning the aim of this thesis.
The same procedure was done for Bottaro islet. The geology of the other islets east of Panarea was interpolated based on remote sensing (distance mapping and description) and rubblestones and boulders that were found when dives took place in the vicinity of the islets.
Since the submarine investigation sites are covered by water, the geologic map does not show these spots' geologic specifications on the large scale. Yet, the maps of each submarine investigation sites were georeferenced as well and can be seen when zooming into the large base map. The subaerial colours do not correspond to the colours of the subaerial sketches because there were much less lithologies to distinguish in the submarine portions.
Structural information was inserted in a separate map with red lines both solid and dashed based on whether their course was clearly identifiable or interpolated.
All maps are attached in the appendix. The following maps can be found there:

- geological map (overview) including Panarea Island as well as submarine investigation sites east of the main island at scale 1:10000;
- geological map of subaerial investigation sites along with the underwater investigation site La Calcara (scale 1:5500), more detailed than overview, including lithologies, structures;
- geological maps of submarine investigation site along with the islet of Bottaro (scale 1:5000), more detailed than overview, including lithologies, structures, geological measurements.

The maps of the submarine investigation sites are attached in Appendix 4. In addition, the GIS file is attached to this thesis as digital appendix (Appendix 5).

3.2.3 Structural data

Structural data was digitalized using the software Stereo32, version 1.0.3 provided by the Ruhr-University of Bochum. In order to display the structural data of the submarine investigation sites and the subaerial outcrops, two different plots were chosen. The first plot shows an equal area projection of the lower hemisphere displaying the inclination and dipping angle. This plot is especially of interest for the locations where both strike and dip direction could be measured. The second plot displays a rose diagram which is of special interest for

the submarine locations where only strike directions (perpendicular to inclination angle) could be measured, for example by discharge points along lines on a sediment field. For these plots, dip directions were not taken into account.

3.2.4 Photo documentation

A photo documentation has been developed using a Microsoft Access database. In the database, the pictures taken during the field work are assigned to a unique ID number. More than 1200 datasets have been generated. Besides the pictures, each dataset also shows information concerning the height or depth, location, lithology, and geological features that are displayed in the photograph. Furthermore, a comment field was added to each dataset allowing to add more precise information, such as strike and dip direction or detailed information to the structures or the lithologies. After adding all information and data, the most descriptive and most characteristic datasets were chosen to generate the photo documentation. The documentation is subdivided into the nine submarine locations and two aerial locations which are also listed at the foot of each page.

The height is listed in metres above sea level (m asl), whereas water depth is listed in metres below sea level (m bsl). Both, height and depth, are rounded to an integer. An extra field was added for some locations to locate specific spots or structures more precisely when the location expands to several tens of metres or even hundreds of metres. If the picture shows more than just one lithology, a second field was added for another information. The photo documentation can be found in the digital Appendix 6. The abbreviation *HFE* mentioned in the photo documentation stands for *hydrothermal fluid exhalation*.

4. Results

The following presented results are split up into aerial and subaerial portions. As the focus of this thesis was set on structural data, rock description and characterization is mainly based on the findings during the field sessions on Panarea Island. The submarine field work was realized with other members of the SDC who wrote a thesis for themselves. Hence, some of the data resulting from the team work has already been published. References concerning further information, especially concerning chemical data or secondary structures, are added in the following chapters. Further information for the aerial portions was derived from literature.

4.1 Subaerial investigation sites

Geological mapping

The following findings of geological mapping are displayed in the geological map attached to this thesis (Appendix 3). Structural data is added as well.

The island of Panarea is mainly composed of volcanic rocks. The south-eastern portions of the island, between Punta Falcone and Punta Torrione, are mainly composed of dacitic lava flows. The rocks of this lithology appear intensively altered, some portions are washed out. The rocks are vesicular and slightly porous. Fresh rock surfaces prevail a light grey coloured matrix in which unoriented light coloured, polygonal minerals (?quartz, plagioclase) along with elongated dark minerals (?pyroxenes, ambhiboles) can be spotted. These minerals can be up to several millimetres large. According to GABIANELLI ET AL. (1990), the K/Ar age of this lithology is 132,5 ± 8,0 kyr. Sporadically up to decimetre large xenoliths along with tuffitic inclusions are prevailed. Along the shore, the dacitic rocks are weathered. At some spots, fine to medium-grained sand has formed as a weathering product.

Tuff portions crop out in between the dacites as well as in the southern and central parts of Panarea. In addition, large portions of tuff is also found in the north-east of the island. Large portions of the tuff are washed out. Hence, the surfaces of these compact and vesicular rocks are smooth. Weathered surfaces show a reddish colouring. The massive tuff of brown colouring mostly prevails a dark matrix. The matrix embeds polygonal, whitish minerals (?quartz) in addition to elongated minerals of dark colour (?pyroxene). The minerals generally do not show a preferential orientation. The light coloured ones are much bigger than the dark ones. Volcanic glasses are contained as well. Furthermore, decimetre large xenoliths as well as volcanic ashes are embedded in this lithology at some locations. In the northern portions of the island the tuffs often prevail cross-beddings.

The southern portions of Panarea along with the islets Punta Milazzese and islets in the bay of Cala Junco consist of andesitic lava flows. In addition, this lithology crops out in the vicinity of Punta Falcone. The vesicular rocks show a dark greyish, almost black colour while weathered surfaces tend to turn into a reddish to brown colour. Polygonal, whitish to yellow inclusions dominate over dark brown to black coloured, elongated ones. The fabric is unoriented. According to CALANCHI ET AL. (1999) the HK-CA andesites include up to 20 % of metamorphic and volcanic xenoliths. The rocks tend to be sharp-edged and splintery and have

a massive and compact appearance. Typical for this lithology are numerous spots where columnar joints have formed cooling fans (Figure 9 A). In between single joints a whitish, clayish material can often be found which is similar to the alunitic veins described by CAS ET AL. (2011).

In the south of Panarea, two volcanic plug domes are located which can clearly be distinct from the surrounding lithologies (cf. Figure 4D). The plugs' rocks show a dark grey matrix with even fracture planes. Whitish and light-coloured inclusions as well as dark-coloured ones of elongated shape are included in the matrix. Various xenoliths, both of volcanic and metamorphic composition, are embedded into the massive rocks. After CALANCHI ET AL. (1999), these dacitic rocks have a $^{40}Ar/^{39}Ar$ age of 127,0 ± 1,5 kyr. The southern walls of the plug domes show various spots of hydrothermal alterations where sulphur and other sulphurous minerals crystallize. To the south of Castello and Punta del Tribunale slope debris can be observed which fall towards the bay of Caletta dei Zimmari.

Large portions of Panarea Island, from the south-western cliffs of Costa del Capraio to the north-eastern Punta Cardosi, are covered with lava flows of dacitic-andesitic composition which include gabbroic aggregates. According to LUCCHI ET AL. (2013b), the composition ranges between high-K dacites to CA andesites. The $^{40}Ar/^{39}Ar$ age was dated to 155 ± 12 kyr (DOLFI ET AL., 2007). The highly weathered volcanic rocks show different stages of hydrothermal alteration as well as erosion. The light coloured, microcrystalline gabbroid inclusions can reach up to 2 dm in size. Pumiceous clasts and tuffs can also be contained in the vesicular rock. The rocks' matrix is of alternating light to darker grey colour. Up to 1 cm long pyroxene minerals are dominating inclusions. Some parts of the steep cliffs show banded lava flows (cf. Fig 4 B). The rock composition seems to alter between individual bands according the rocks' colour and extent porous appearance.

The prehistoric village in the north of the island and its surroundings, near La Calcara bay, displays a complex region on Panarea Island. Besides the dacitic to andesitic host rock, further lithofacies crop out. Yet, these facies are too small of scale to be displayed in the map. The part close to the cliffs is dominated by a wall showing intensively hydrothermally altered dacites to andesites showing reddish colours due to weathering. At some portions, decimetre large basaltic rock portions crop out in the steep slopes which run to this location from the sea. At an elevation of approximately 45 m asl, the rock body is cut through by whitish to greyish material both horizontally and vertically (Figure 9 C). In some parts this light-coloured material resembles clay minerals, being soft and chalk-like, while in other parts this this material is hard, brittle, porous, and splintery. About 30 m west of the cliffs the outcropping rocks are characterized by a tuff wall showing an overall reddish to brownish colour. A transition between two tuff strata can be observed. Along the border of this transition, a paleo discharge structure of about 10 m lengths has developed (Figure 9 D, E). Its width varies between only a few centimetres and up to 50 cm. Along the shore of La Calcara bay several spots can be found where native sulphur or sulphur-bearing minerals, such as pyrite, mineralized.

Panarea Island's (north-)western coastal cliffs, between Punta Muzza and Punta Scrita, are mainly composed of andesitic to gabbroic lava flows. As LUCCHI ET AL. (2013b) state, high-K andesites are characteristic for this lithology. The rocks prevail a dark coloured matrix. Finely crystalline gabbroic inclusions with a light grey matrix can be up to several decimetres in size. Sporadically, the andesites are overlain by massive, highly altered pyroclastic breccias. As this area is mainly characterized by steep slopes running into the sea it was not possible to inspect this lithology further.

The northern sector of Panarea Island, between Punta del Corvo and Punta Falcone, is characterized by lava flows and domes of HK-CA andesites to dacites which have a K/Ar age ranging between 132.5 ± 8.0 kyr and 127.0 ± 12 kyr (CALANCHI ET AL., 2002). The surfaces of the rocks are weathered and partly also washed out, assumedly by wind action, and show a reddish-brown colouring, while fresh surfaces prevail with a mainly dark greyish matrix with elongated dark minerals, such as pyroxenes and amphiboles, along with polygonal light coloured inclusions, as quartz and plagioclase. Gabbroic aggregates as well as volcanic and metamorphic inclusions reaching up to several centimetres in size are embedded.

Along the northern shore of Panarea as well as on the islet of Scoglio la Nave dykes of several decametres thickness run through the surrounding volcanic rocks. Most of the dykes rise almost upright. As none of the dykes could be reached, a more detailed description is not possible. Close to these dykes, hydrothermal alterations of the rock can be spotted at some places.

Along the eastern sector of the island andesitic lavas can be found from the surrounding of Punta Falcone towards the village of Ditella. As CALANCHI ET AL. (2002) state, this lithology is mainly composed of HK-CA andesites and have an average age of 132.5 ± 8.0 kyr. The vesicular and porous volcanites prevail dark grey surfaces with few signs of alteration. Sporadically the rocks show banded lava flows of alternating colours (light/dark). The light grey matrix is finely crystalline and contains unoriented inclusions. Dark, elongated inclusions (?amphibole/pyroxene) are larger than the polygonal light-coloured inclusions (?quartz/plagioclase). Yet, none of the inclusions are larger than a few millimetres. Besides gabbroic inclusions of centimetre-scale, polygonal xenoliths are embedded.

Poorly sorted recent sediments cover the island of Panarea at different locations, such as the surroundings of Punta del Corvo. Their grain size ranges from silty sand to fine gravel, yet sand components are dominating. Clasts are well rounded. Besides single minerals, as for example quartz, the sediments also contain volcanic products, such as pumice or volcanic glasses. Larger clasts prevail different volcanic compositions. At several spots along the shore of Panarea Island beaches can be found which resemble each other in their appearance. These spots are covered with recent, well-rounded sea-shore deposits of variable size (cm to m).

Volcanic rocks of andesitic composition along with sporadic basaltic inclusions and flow structures are characteristic for the islet of Bottaro (Figure 10 A). The mainly banded, andesitic lava flows prevail a dark matrix in which a high amount of light coloured inclusions, such as quartz and plagioclase, of mm-scale in combination with few dark, elongated inclusions.

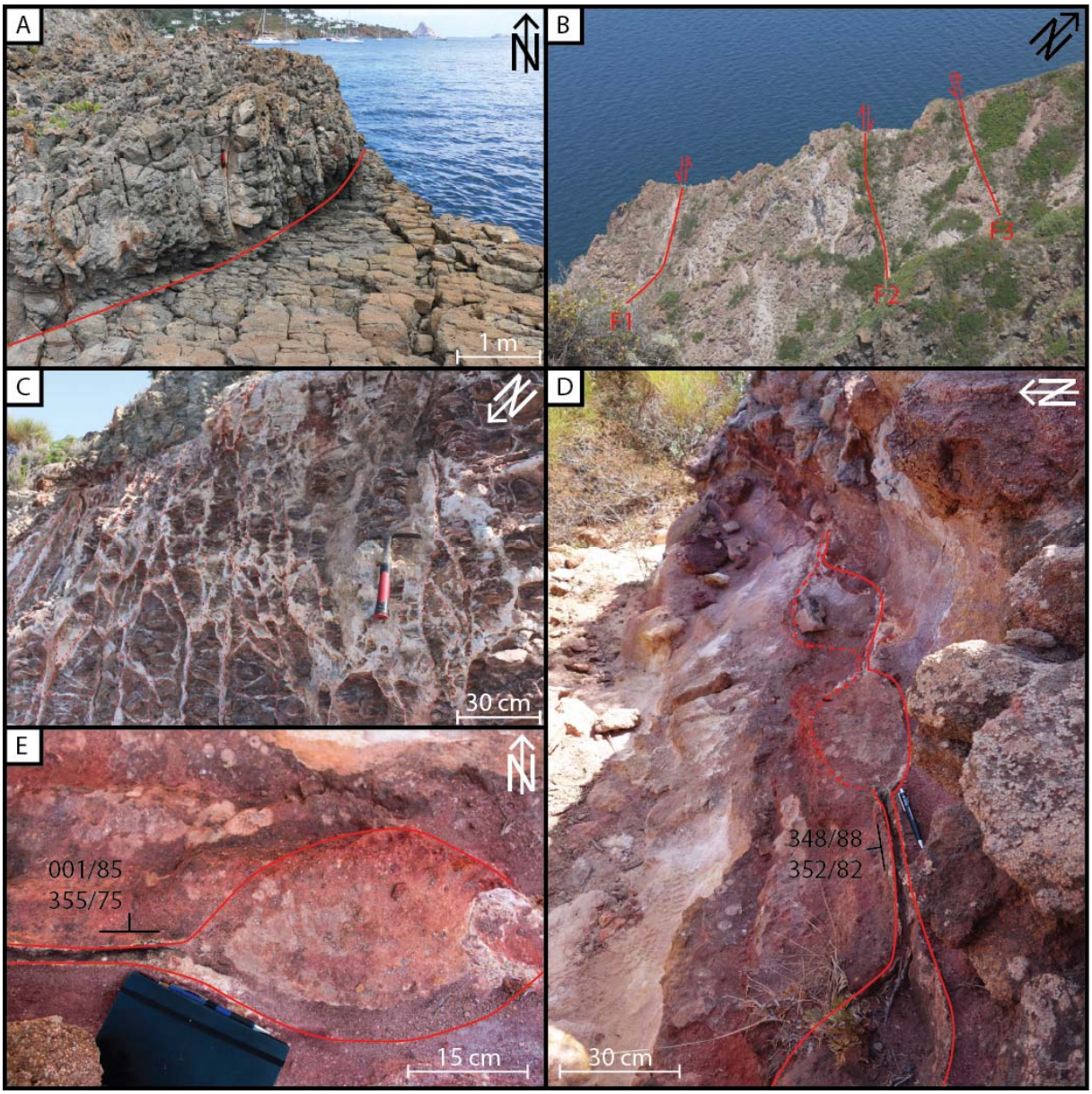

Figure 9: A – Normal fault at Punta Milazzese. The fault cuts through the fan-shaped, jointed volcanic rocks almost perpendicularly. B – Normal faults along the western cliffs of Panarea Island. All of these fault show a NE-SW orientation. Besides the three pictured faults, a fourth one could be identified farther up the cliffs, near the highest peak of Panarea, Punta del Corvo. Due to the steepness of the cliffs along the western flanks of Panarea, the faults could not be investigated in detail. C – Silicified honeycomb structures near La Calcara bay. These structures appear to trace initial pathways of hydrothermal fluids through the surrounding host rocks. While some, nearly upright oriented sections are thicker, the intersecting portions are thinner and more porous. Along the boundary of the dykite material and the dacitic-andesitic host rock, signs of hydrothermal alteration can be recognized. D – Preserved paleo lineament structure near La Calcara bay. The structure shows a N-S orientation. The side walls are nearly upright. This structure is located along a transition of two different tuff strata. E – Preserved paleo bowl structure of a lineament structure near the prehistoric village of La Calcara. The bowl is filled with sediments of reddish colour. The initial walls of the bowl structure prevail light coloured cements.

Weathered rock surfaces show a red colouration. Along the zone of fluctuating water levels, washed out areas can be observed. Alteration, probably due to the emanation of hydrothermal fluids, is visible at variable spots. At the northern edge of Bottaro, where the islet runs into the sea towards the dive location Bottaro North, decimetre large basaltic xenoliths crop out in between the andesitic-dominated rock. At the transition of these two rock types a whitish, greasy, chalk-like material can be found which is similar to the alunite found at La Calcara. In addition, a massive, brown coloured tuff crops out at the southern portion of the islet which contains fragments of glass (mm-scale) and basaltic xenoliths reaching up to 1 dm in diameter. The tuff also contains rounded portions of ashes and pumice which reach up to several centimetres in size. The tuff also shows signs of hydrothermal alteration. The uppermost portions of Bottaro islet are covered with a mm-thin layer of sandy sediment. Well-rounded surf conglomerates can be on the shorelines of Bottaro islet.

Along the south-western shore an approximately 60 cm thick, white coloured dyke runs into the sea (Figure 10 D). The structure shows intense silicification which makes it massive and brittle. As observed at other locations (e.g. La Calcara bay, BW, CAV) the silicified rock, also referred to as Dykite (STANULLA, 2021), appears much more resistant to chemical alteration processes as the surrounding rocks are highly altered. Optical microscopy hints on a high-temperature alteration of quartz. According to DEKOV ET AL. (2013) the material is nearly entirely composed of SiO_2. The dykite of Bottaro has formed honey-comb structures at some spots where thin bands of the rock intersect thicker bands at various directions (Figure 10 B).

The islet of Lisca Nera which only comprises small rock portions emerging from the sea is made up of lava flows of dacitic to andesitic composition (CALANCHI ET AL., 2002) in which volcanic xenoliths are embedded.

Along with Lisca Bianca, Dattilo islet is the largest among the islets to the east of Panarea. Several smaller rock portions crop out of the sea at its western shore. The main portions of Dattilo are made of dacitic lavas. Slope debris can be spotted at several spots along the coastal line. Hand specimen taken during a dive on the northern shore of Dattilo showed a high amount of volcanic xenoliths. The eastern side of the islet comprises highly altered dacitic breccias. The rocks of Dattilo islet are generally altered intensely due to hydrothermal fluids. The upper portions of the islet shows several spots where native sulphur covers the host rock. Well-rounded sea shore deposits of variable size can be found at several spots around Dattilo.

Panarelli, located in the north-west of the submarine crater, resembles Lisca Nera. After CALANCHI ET AL. (1999), these rocks are mainly composed of andesites.

The islet of Lisca Bianca prevails dacitic to andesitic lavas showing various degrees of alteration which have formed flow bands dipping at a gentle angle into the sea to the east. In addition, massive tuffs of brown colour crop out in the southern part of this islet. As ESPOSITO ET AL. (2006) and CAS ET AL. (2011) state, networks of alunitic veins run through the host rock. Sea shore deposits lay along the shore line of the islet.

Structural data

Throughout the Island of Panarea, several areas can be found which indicate ongoing hydrothermal activity. As the hydrothermal fluid have their source in the magma chamber underneath the Panarea volcanic system, the emanation point must be linked to tectonically active structures. Prominent spots are the plug domes in the southern portion of the island as well as the bay of La Calcara in the north-east. Dykes cutting through the northern cliffs of Panarea are supposed to be linked to tectonic structures as well.

The area around the bay of La Calcara prevails various features that can be linked to hydrothermal and hence also tectonic activity. On the northern edge of the beach, uprightly rising SiO_2-rich structures indicate two orientations along which they formed and sulphurous minerals evolved: 277/75 and 324/72. South of the beach of La Calcara columnar joints oriented nearly upright form a line running into the sea. The general NE-SW strike direction of these joints coincides with structures near the prehistoric village of La Calcara. There, several preserved degassing structures, both bowls and elongated lineament structures, prevail a general N-S orientation of 354/83. The silicified degassing pathways in the vicinity of the paleo structures show a variety of orientations where the largest and thickest ones dominate over the others with an average of 060/74. Smaller structures show a 091/74 or a 025/64 trend.

The domes of Castello and Punta del Tribunale are located along a NW-SE trending fault. Another volcanic crater along this fault line is suggested by CALANCHI ET AL. (1999) on the western shore, between Punta Scritta and Torricella. As this portion could not be investigated in detail, the suggested feature being a part of the fault system can neither be confirmed nor rejected.

The cliffs along the western coast of Panarea Island are cut by four normal faults running in a NE-SW direction (Figure 9 B). They all show a general NE-SW strike direction. Due to inaccessibility precise data could not be gathered. Dipping angles appear rather high (> 70 °). They extent over a length of several decametres. According to LUCCHI ET AL. (2013b) the displacement of the uppermost fault measures 80 m. The authors suggest a horst- and graben system due to opposite vergences of the faults.

Another normal fault is located at Punta Milazzese. While one part of the jointed andesites seems to be built in a fan-shape, another part of them runs nearly perpendicular to them directly through the fan (Figure 9 A). At the border of these two parts, a whitish and soft material can be located between the joints resembling chalk. As similar structures could be observed along the western beach at Caletta dei Zimmari it can be assumed that the fault continues in the submerged portions of Panarea.

The banded lava flows of Bottaro islet prevail a gentle dipping to the south-west. The overall strike direction of the dyke along the islet's western shore is 150-330 ° (Figure 10 D). Looking closer, it is obvious that the dyke is made of multiple band of SiO_2-rich material which mostly runs parallel in the main strike direction. However, most of the bands are also intersected by thinner dykite bands (Figure 10 B). These thinner bands often show strike directions of 030-210 °. While the main bands prevail dipping angles > 80 °, the intersecting bands often

show dipping angles below 20 °. Another fault cuts the dacitic-andesitic host rock of the islet of Bottaro at its southern tip which has an average orientation of 333/83.

The dacitic-andesitic rocks of Bottaro islet are cut by another fault of volcanic rock composition in the southern portions. In contrast to the dykite fault along the western shore, this one prevails a strike direction of 090-270 °. Dipping angles are rather high (> 80 °), but could not be measured as the surrounding rocks crop out higher than the fault and do not display an even rock surface which would ensure correct measurements.

As native sulphur as well as hydrothermal alterations were found along the shore of Bottaro islet it can be assumed that these observations occur mainly along tectonically active structures. Due to the inaccessibility of the other islets during the conducted field works this assumption could not be investigated further.

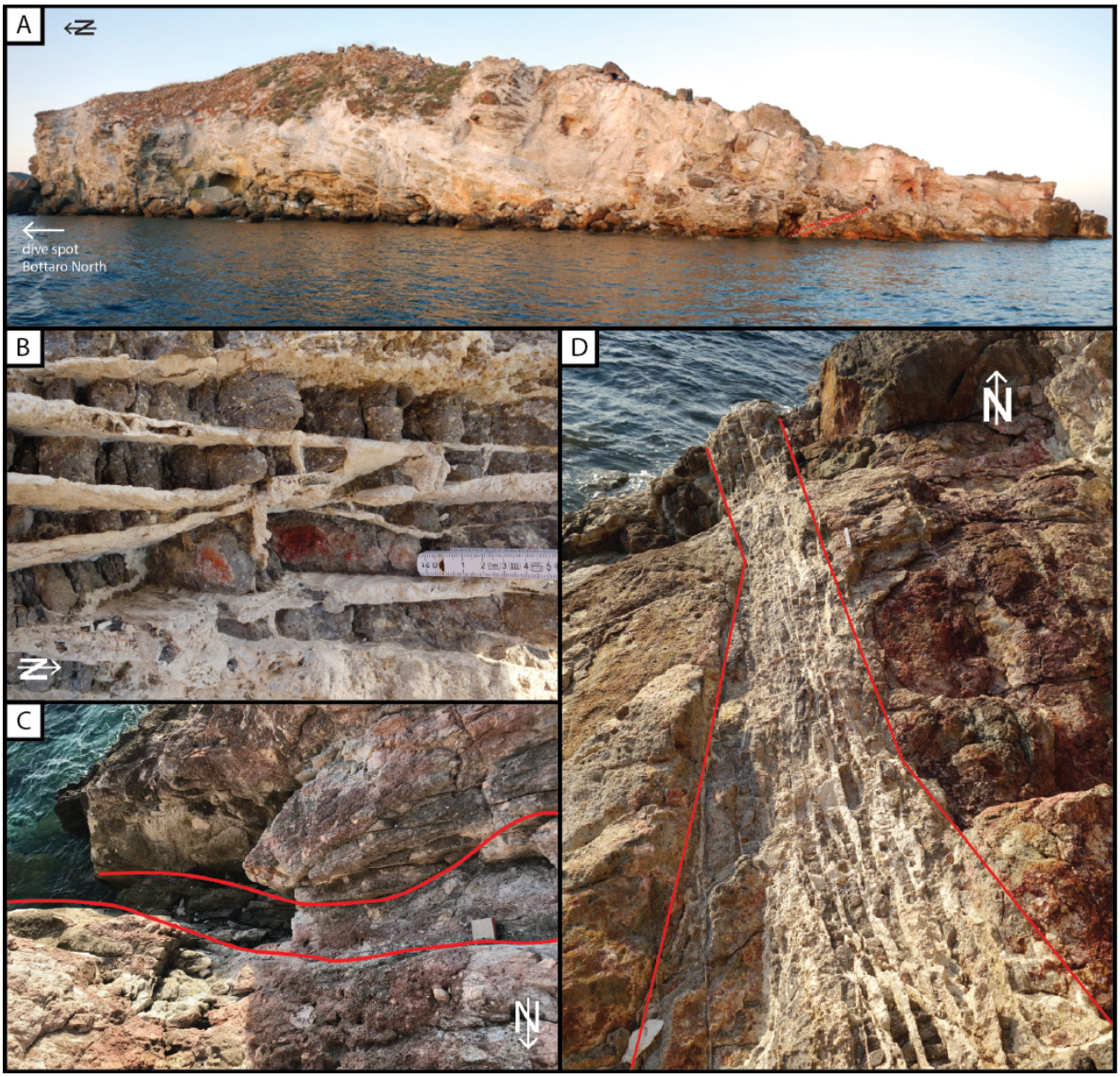

Figure 10: Bottaro islet. A – Overview of the islet's western flank. To the south the islet runs continuously into the sea with a gentle slope. To the north it also has a slope. Yet, this one is cut off on its tip. The western and eastern flanks are made of steep, hardly accessible slopes. Well-rounded sea shore deposits lay on the entire

shore line. B – Close-up image of the dyke along the western flank. The severely weathered dacitic-andesitic host rock is cut through by the SiO_2-rich dykite which formed honeycomb structures. C – Fault on the southern edge of the islet cross-cutting the dacitic-andesitic host rock in a 090-270 strike direction with steeply dipping walls. D – Overview of the dyke which runs into the sea with a general strike direction of 030-210 °.

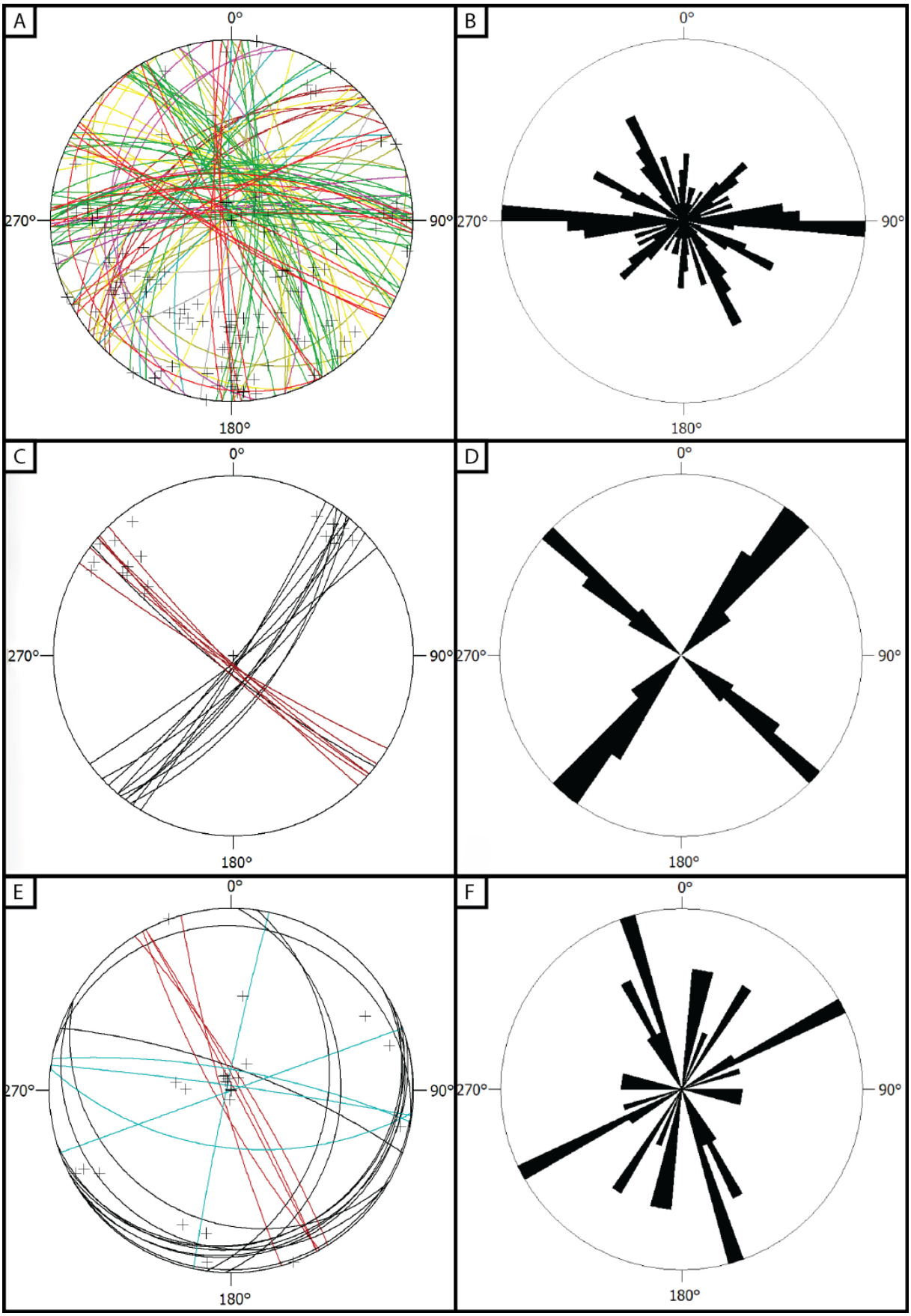

Figure 11: A – Equal-area projection of the lower hemisphere of major structures at La Calcara bay. Dark red – Outcrop 1, olive green – Outcrop 2, purple – Outcrop 3, yellow – Outcrop 4, blue – Outcrop 5, green – Outcrop 23, light red – Outcrop 38, crosses represent pole points. Most of the structures prevail high

dipping angles (> 50 °). B – Rose diagram of the strike directions measured at the bay of La Calcara; N = 111. Dip directions are not considered. The diagram shows a major strike direction with an orientation of 090-270 °. Further prominent strike directions are 150-330 °, 060-240 °, and 120-300 °. Several minor strike directions can be recognized. C – Equal-area projection of the lower hemisphere of major structures at Capo Milazzese. Red – fault, black – columnar joints, crosses represent pole points. Dipping angles are relatively high (> 60 °), yet the angles of the fault are slightly higher. The fault intersects the surrounding columnar joints almost perpendicularly. D – Rose diagram of the strike directions measured at Capo Milazzese; N = 18. Dip directions are not considered. The diagram shows two major strike directions: 130-310 ° and 035-215 °. As shown in C, the values indicate that the fault is cutting through the host rock as also observed in the field. E – Equal-area projection of the lower hemisphere of major structures Bottaro islet. Black – western flank, blue – cave, red – dyke, crosses represent pole points. F – Rose diagram of the strike directions measured at Bottaro; N = 22. Dip directions are not considered. The diagram shows two major strike directions: 150-330 ° and 060-240 °. Several minor strike directions can be identified. Yet, the dyke on the western flank of the islet is not represented although this structure is among the most prominent on the islet.

4.2 Submarine investigation sites

4.2.1 Area 26

Mapping

The majority of the sub locations are located in the southern part of Area 26 near buoy 2. The precise distances and directions from buoy 2 can be found in Table 6.

3-Bowls can be found close to the southern buoy. The bowl structures are arranged in a triangular shape where each of the cavities is between 3 to 4 m apart from each other. They measure 1-1.5 m in length and 0.6-1.3 m in width. Each of the bowls is at least 0.3 m deep, although it is assumed that they reach much further into the ground.

Hot Bowl west of buoy 2 is a bowl-structure next to a Posidonia field that measures 1.8 m in length and 0.75 m in width. Precipitation ridges run from the bowl into various directions.

First excavated in the 2017 field trip to Panarea, the sub location *Brodor* is a spot of intense hydrothermal fluid discharges. The structure has a slight oval shape and measures only about 1 m^2 in size. Hydrothermal fluids discharge through tubes and cones (STANULLA, 2021).

Table 6: List of distances and directions for the most prominent sub locations at Area 26 measured from buoy 2 (UTM 33S 509111 E/14276753 N) in the southern region of the submarine investigation sites. Since the Mouth is located directly at buoy 1, individual coordinates are not needed for this sub location.

Sub location	Distance from buoy 2	Direction from buoy 2
Hot Bowl	22,0 m	265 °
3 Bowls		
Bowl A	14,0 m	65 °
Bowl B	11,0 m	85 °
Bowl C	7,0 m	65°
Lineament (southern edge)	19,0 m	0 °
Brodor	14,0 m	330°
Hobbit Hills	59,0 m	300 °
“Lava” tongue	42,0 m	10 °

Lineament is an elongated feature that is about 15 m long and up to 50 centimetres wide. It can be found about 20 m north of the southern buoy, close to *Brodor* and *3-Bowls*. The structure comprises several elongated bowls which can be up to several decimetres long. These bowls are connected by precipitation ridges. Similar structures to Lineament can be found in the west of Area 26. However, these are all distinctly smaller. *"Lava" tongue* is located almost in the middle of both buoys.

Geology

Area 26 is mainly characterized by sandy plains on which Posidonia fields grow (Figure 12). The sediment at is made of pyroclastic, medium- to coarse-grained sand and clasts of fine to medium gravel size in between.

The area comprises a variety of hydrothermally induced structures whose walls are consolidated by sulphuric cements. Most of these secondarily formed structures are covered with recently transported sediment which is why these structures can often only be identified due to white bacterial mats growing on top of them. The sediment cover can be up to several decimetres thick. Besides covering a great part of the plain, it can also be found as a filling within the structures.

3-Bowls can be found close to the southern buoy. After the excavation of one of the bowls to a depth of 1.5 m below the sea floor, a stratified sulphur-cemented sandstone was recognized which forms the bowls' walls. They are filled with massive sulphide ore aggregates, pyroclastites and clay-like materials in the deeper parts of the bowls (Figure 13 B). Gas-dominated hydrothermal fluids are being exhaled at these structures. Thin sulphur-cemented structures, also called precipitation ridges, connect these cavities with each other. Besides, these ridges also run into different directions from the outskirts of the bowls. Through one of the ridges, *3-Bowls* is connected to the approximately 15 m long *Lineament* structure north-west of it. In addition, these ridges also connect small bowl structures (only few dm^2) that have developed in the centre of the Posidonia field that borders to the 3-Bowls. Within some of the structures such as *3-Bowls*, massive sulphide ore precipitates of several square decimetres in size occur as a consequence of the emanation of H_2S enriched which is enriched with metal ions (KÜRZINGER, 2018).

The walls of *Lineament* are made of sulphur-cemented sandstone. Different kinds of discharge features could be found when the structure was excavated (STANULLA, 2021). Similar to *3-Bowls*, the walls of Lineament are composed of sulphur-cemented sandstone. Mixed fluid outlets, although fairly weak, can be observed along the walls.

"Lava" tongue is located nearly in the middle of the two descending buoys at Area 26. Although the name indicates characteristics of a lava rock body, this feature is made up of homogeneous tuff around which massive sulphide ores can be found. Highly acidic hydrothermal fluids are being discharged from vents and several small-scaled tubes or channels.

Structural data

At Area 26, only few aligned fluid vents can be found throughout the sediment plane. However, some are exposed near the southern buoy. These lines show a strike direction of 30 ° or 330 °. Information on structural data can mostly be derived from larger structures as most of the area is covered with recent sediment.

Bowls A and B of *3 Bowls* are arranged along an overall NNW-SSE line while bowl C is located west of bowl B (Figure 13 A, Figure 15). Precipitation ridges generally show high dipping angles (< 50 °). The strike direction varies between 030-210 ° and 060-240 ° between bowl A and B. Intersecting ridges prevail orientations of approximately 090-270 °. A precipitation ridge running from the south-east of bowl B has a strike direction of 150-330 °.

Due to the formation of a secondary tube complex at *Brodor* (cf. STANULLA, 2021) these discharges cannot be directly linked to one of the prominent large-scale geological structures of this submarine investigation site. The tubes and cones do not show any preferential orientation.

The structure of *Lineament* itself shows a general orientation of 130-310 ° (Figure 14). The precipitation ridges in between the bowls are oriented nearly upright whereas the bowls' walls appear to bulge out due to subrosional processes (Figure 16). Hence, their shallower orientation cannot be referred to as the initial orientation.

"Lava" tongue shows an overall E-W orientation where it strikes out of the surrounding recent sediment cover. Thin fissures run through the top of this structure. These intersecting fissures show general orientations of 150-330 ° and 000-180 ° (Figure 15). The fissures' angles are 80 ° or higher. Fluid vents are arranged along lines with orientations of 090-270 ° or 150-330 °.

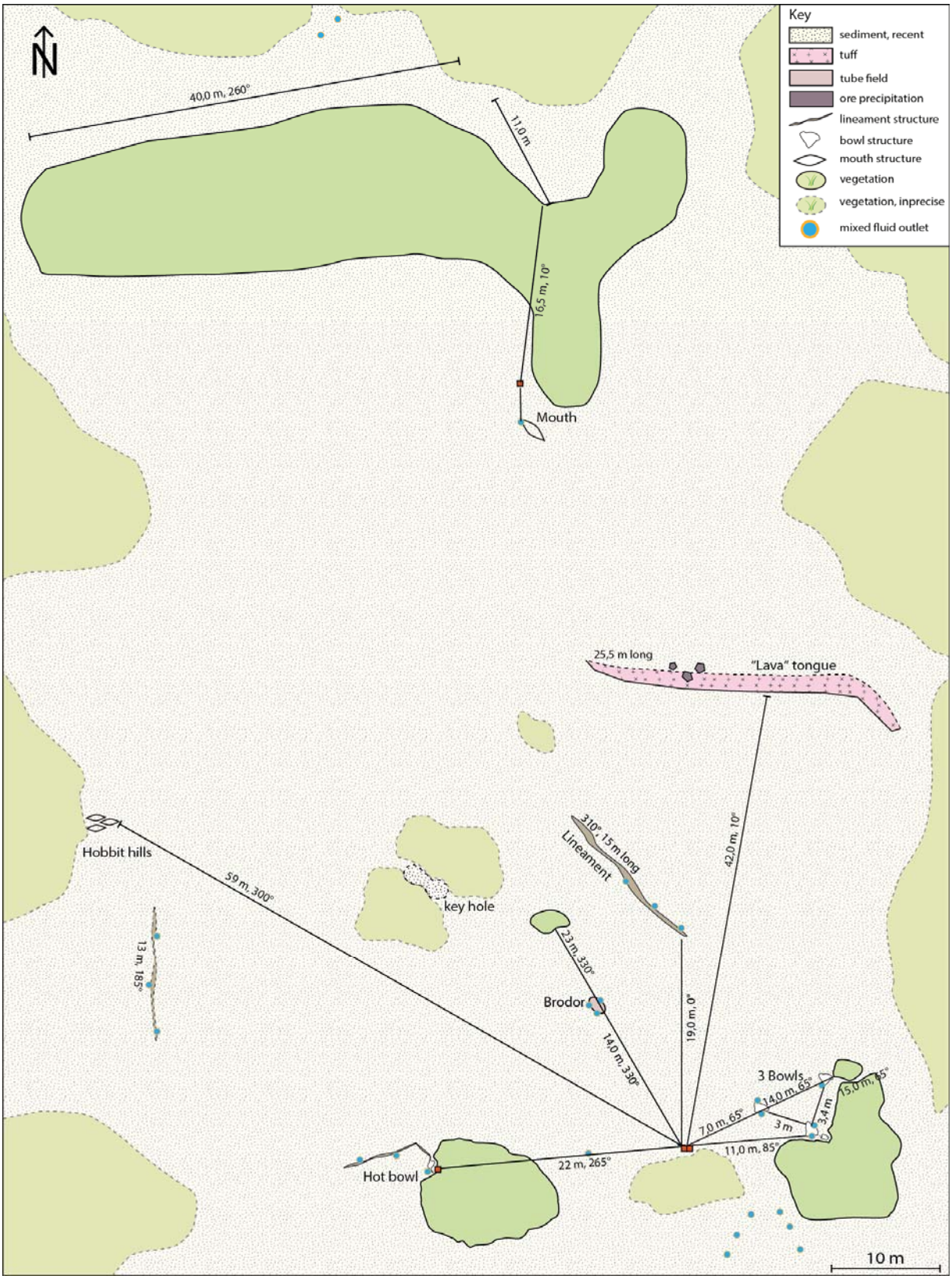

Figure 12: Overview sketch map of Area 26. The most prominent structures which were of interest for the working groups of the SDC were mapped in detail. Distances and orientations are given from buoy 2 in the southern part of Area 26. Posidonia fields (green) are mostly interpolated.

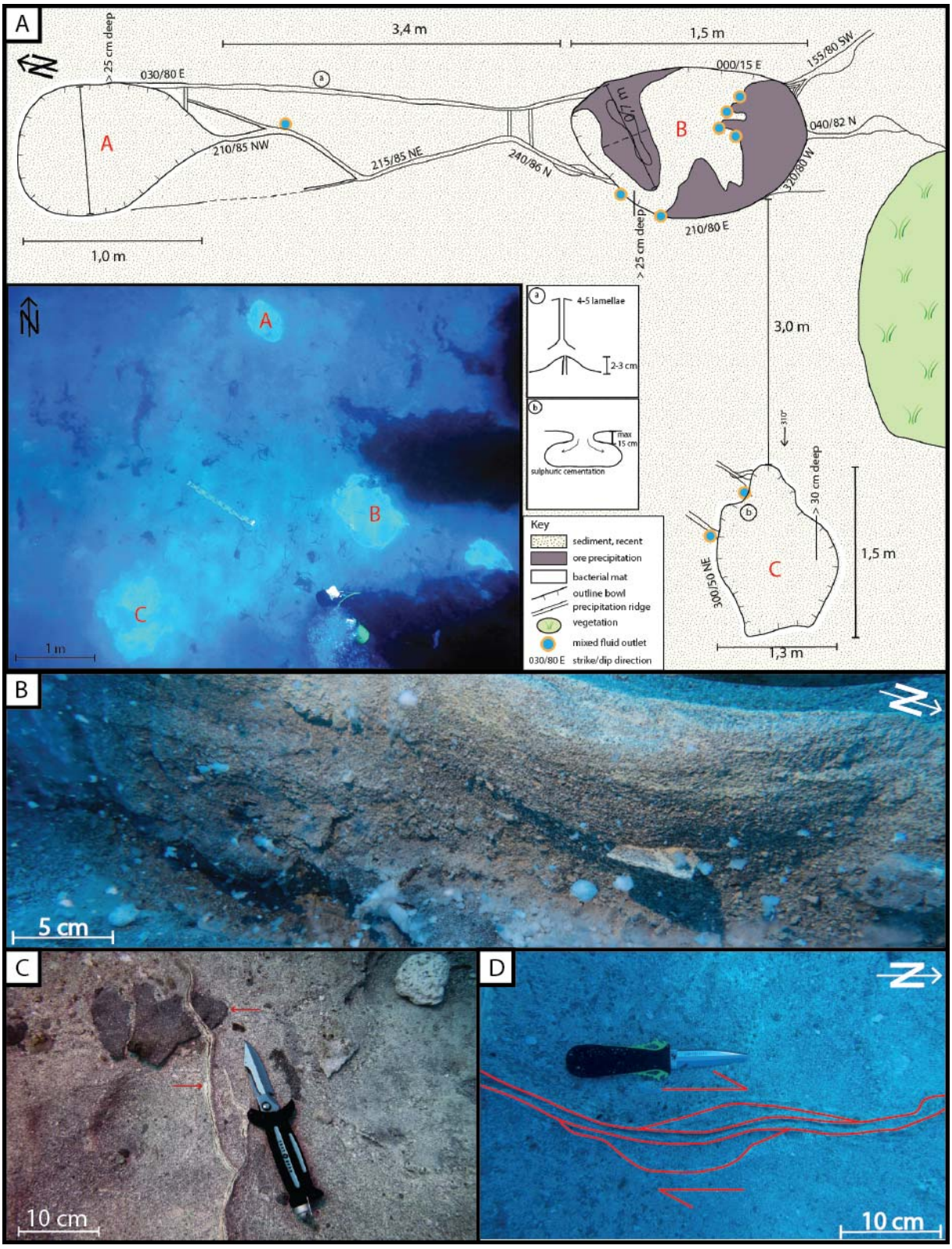

Figure 13: *3 Bowls*. A – Sketch map of the *3-Bowls* structure in the southern region of Area 26. The bowls are connected with each other by thin precipitation ridges. B – Profile view of a stratified bowl wall. The wall is characterized by a medium rained sandstone whose cements are made of sulphuric mineral precipitations. Single large clasts are contained as mass flow deposits (ADAMEK ET AL., 2019). C – Sulphur bearing ore aggregates can be found within the bowl as well as along the small ridges that connect the bowls with each other. D – Along the ridges hints on a sinistral shear structure are given. Knife for scale, pointing north. (Photography: B, C – R. Stanulla)

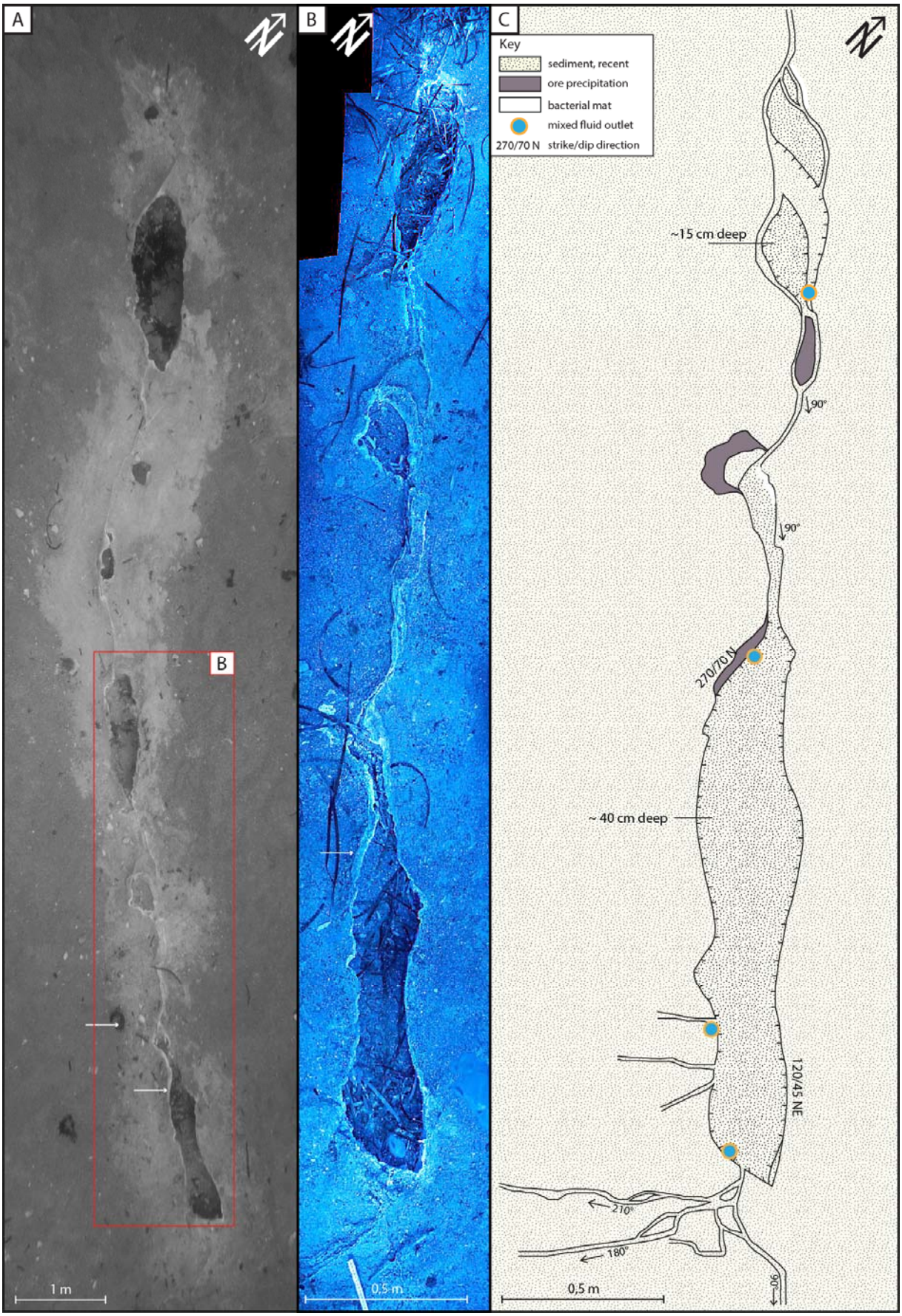

Figure 14: *Lineament*. A – Overview picture of the excavated Lineament. B – Close-up of the south-eastern part of the structure. Overlying bacterial mats and recent sediments were removed at some spots. The bowl

structures along the lineament are up to 40 cm deep and partly filled soft sediment and Posidonia remnants. Small precipitation ridges run into various directions from the southern edge. Sulphuric ore aggregates were found at various spots along the structure. C – Simplified sketch of *Lineament*. Few hydrothermal fluid vents are located along the rims of the bowls. Although from top view not visible, the walls of these bowls are covered with sulphuric precipitations. (Photography: A – R. Stanulla)

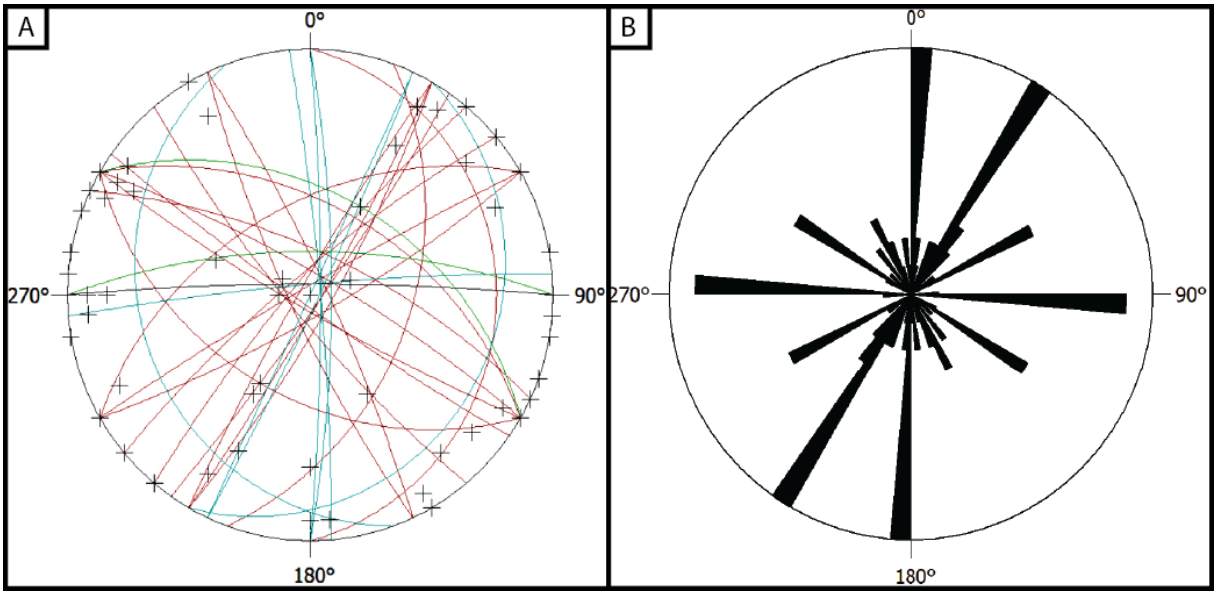

Figure 15: A – Equal-area projection of the lower hemisphere of major structures at Area 26. Red – *3-Bowls*, blue – *Lineament*, green – *"Lava" tongue*, crosses represent pole points. While the southern structures *3 Bowls* and *Lineament* show variable strike directions ranging between 030-210 ° and 060-240 °, "Lava" tongue displays mainly N-S striking structures with high dipping angles which are intersected by few E-W oriented fissures. B – Rose diagram of the strike directions measured at Area 26; N = 66. Dip directions are not considered. The diagram shows two major strike directions: 000-180 ° and 030-210 °. Minor strike directions of the structures are 090-270 °, 060-240 ° and 120-300 °.

Further data

Both water- and gas-dominated fluid discharges can be observed at Area 26. Most of the vents can be found in the vicinity of the large structures, such as *Hot Bowl*, *3 Bowls* or *Lineament*. The majority of the pulsating and irregularly discharging vents are presented as single spots of class A to B (STEINBRÜCKNER, 2009). Only few locations, such as *Brodor*, can be distinguished where numerous vents (up to 30) are concentrated in a small area and flow-rates are higher than in the surrounding regions. Posidonia roots possibly act as a pathway for hydrothermal fluids.

Numerous gas dominated discharges are located around "*Lava" tongue*. These distinct vent points are characterized by higher flow-rates (class C) and an acidic fluid composition. In contrast, locations such as the *Mouth* show a rather water-dominated discharge behaviour which can be recognized due to the schlieren which are emitted at the foot of the structure.

Larger structures are usually covered with bacterial mats (e.g. *3-Bowls*, *Lineament*). Although it was not possible to excavate all of the structures found at Area 26, the location of them is

well indicated and their spatial extent outlined precisely because of the white bacterial mats. Even when excavation was conducted, the mats quickly rebuild themselves within the structures where temperatures were increased. At *3-Bowls*, temperatures around 60 °C could be measured in the sediment cover of the cavities.

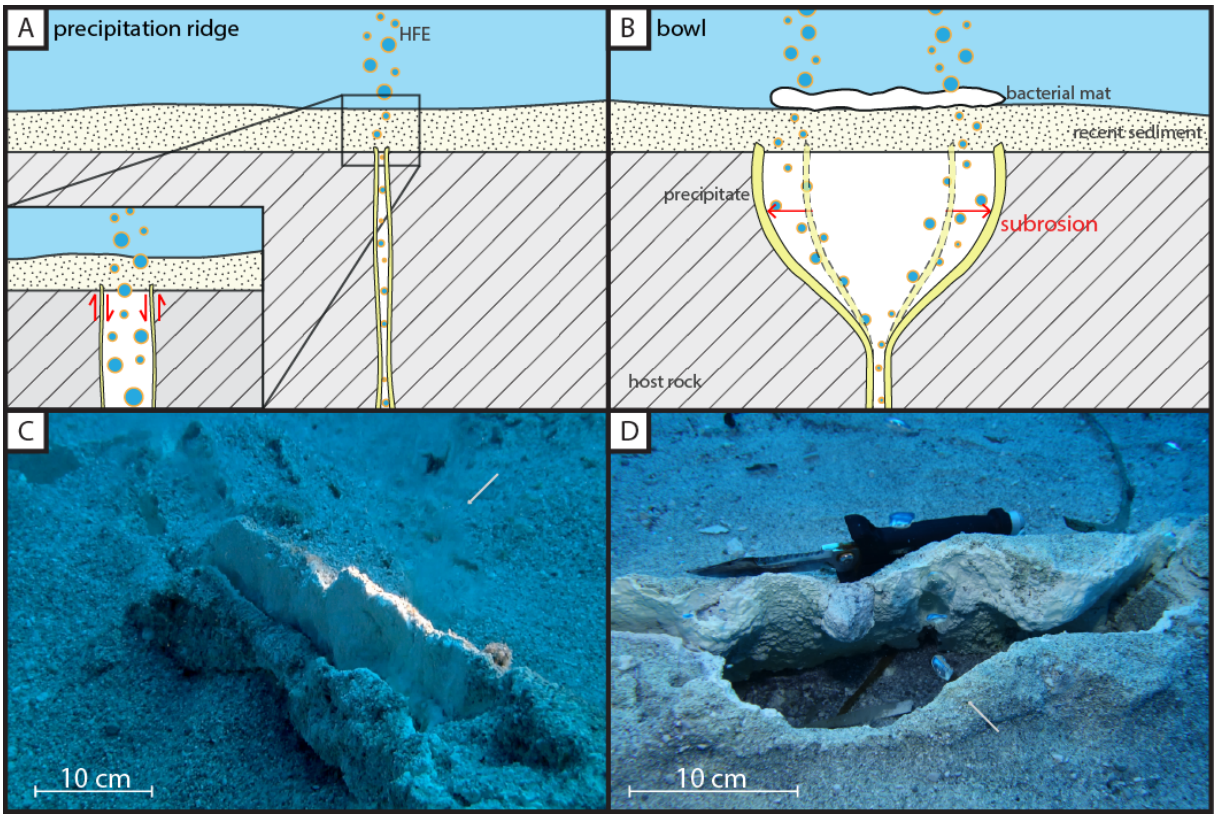

Figure 16: A – Development of precipitation ridges along crevasses or faults in the host rock. HFE: Hydrothermal fluid exhalation. B – Formation of a bowl structure along an initial precipitation ridge. The cavity is a result of periodic processes of subrosion and leaching due to the hydrothermal fluids. These processes lead to the destabilization as well as the collapse of the precipitate walls. The structure undergoes a process of deceleration because of the mineral precipitations (Adamek et al., 2019). C – Precipitation ridge at *Hot Bowl*. Laminated sulphurous precipitates have formed along the weakening zone where water-dominated hydrothermal fluids (arrow; fibrillating water) are still emanated. D – Early-stage bowl along the *Lineament* structure. Due to the discharged fluids (arrow) the initial precipitation ridge has undergone a subrosional processes leading to the bulging of walls. Knife for scale. (Photography: C – A. Trepte, D – R. Stanulla)

4.2.2 Black Point

Mapping

At Black Point, the most significant spots in the surroundings of the shallow water grey smoker in the eastern part of the spot were mapped. The buoy of the INGV as well as its ground weights in the outer crater were mapped, but since these features are man-made they are not content of the map of this location.

The inner crater extends approximately 25 m in N-S direction and 20 m in E-W direction. Within the crater, fluid outlets were mapped which could be found throughout the sediment

plane (Figure 17). Furthermore, the highest and deepest points of the inner crater wall were measured at distinct spots. Details of the grey smoker itself have already been known (HAMEL, 2010), hence mapping of it was not conducted again. The inner crater rises slightly to the outer portions from 23.5 m up to 22.8 m in the western part.
The outer crater is filled with Posidonia fields. These fields were sketched but not measured individually. Small sediment fields are exposed in the northeast and in the west where hydrothermal fluid discharges can be observed. At these spots, bacterial mats have settled. The most prominent structures were added to the map. The rims of the outer crater rise up to 20.0 m in the south. In contrast to the rest of the outer crater, no distinct rim can be found in the south. Instead, the sea ground rises slightly producing a smooth slope which ends in a large Posidonia field.

Geology

The seafloor of the two craters is covered with light coloured sand and gravel. The sediment fills measure several decimetres. The underlying host rock could not be found when removing the upper portions of the sediment. Throughout the outer parts of this location, some well-rounded, volcanic hard rocks of (deci-)metre scale could be found. However, these rocks could not be defined further due to the severe alteration they have undergone. The light brown coloured walls of the crater are made up of tuffite which resembles the tuffite-rocks at Area 26 and Hot Lake. the rock is characterized by medium to coarse sand. The surfaces of the crater walls are washed out at some spots.
The grey smoker Black Point is composed of sulphurous minerals, such as galena, pyrite/marcasite, and sphalerite (BECKE, 2009). Mineral precipitations also occur in the surrounding area of Black Point, especially to the east where several smaller rocks with similar precipitations can be found.

Structural data

Due to the sediment filled craters of Black Point, it was only possible to measure strike directions of aligned fluid outlets assuming that they display structures below the sediment cover. Some of these hydrothermal fluid discharges are surrounded by whitish bacteria mats which therefore highlighted the direction additionally.
The majority of these fluid lines displays a general strike direction of 000-180 ° (Figure 18). Further fluid discharges have a 060-240 ° or 090-270 ° orientation which could mainly be observed in the eastern and southern portions of the location. A few lines were found with a strike direction of 030-210 °. The ore bodies distributed around the main emanation point of the grey smoker do not show a preferential orientation.

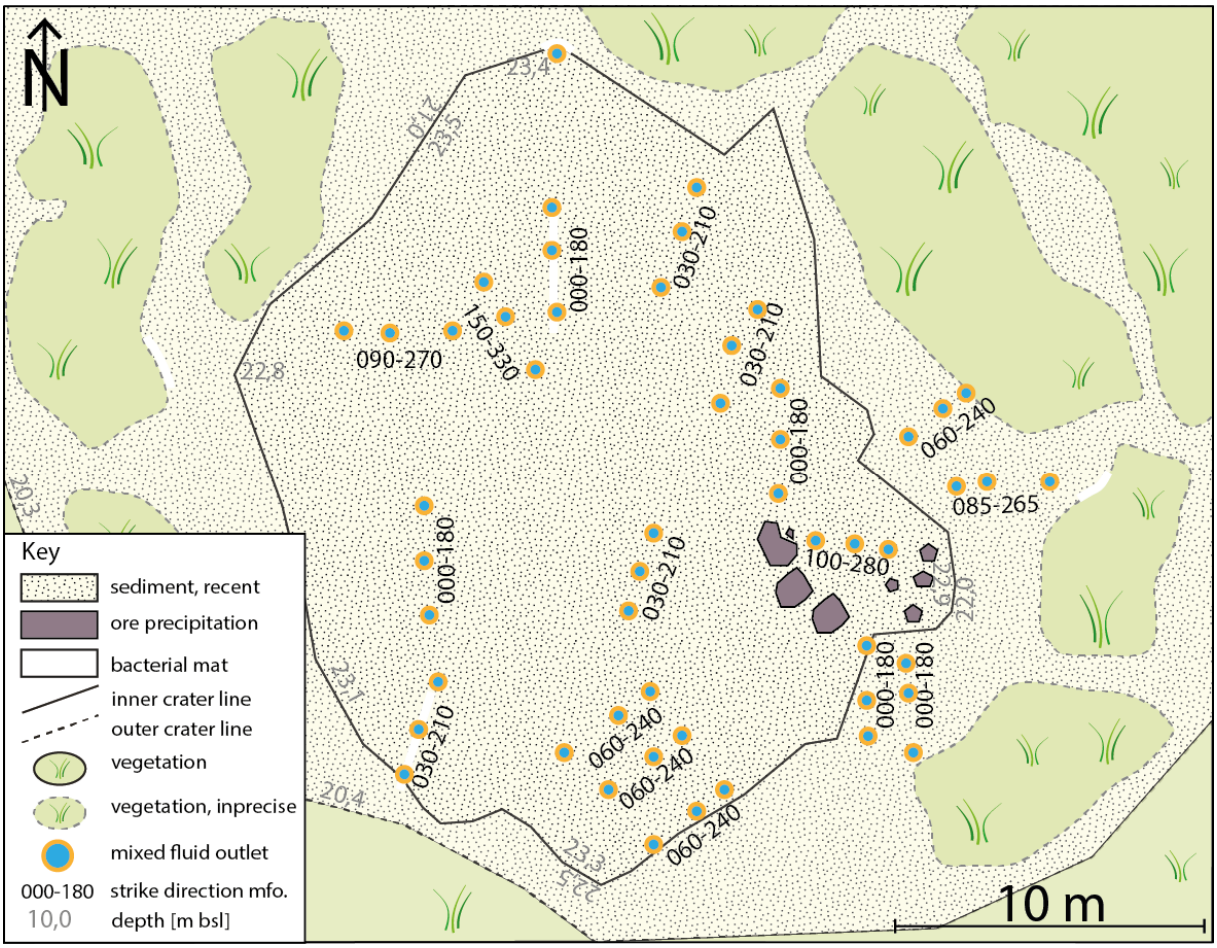

Figure 17: Sketch map of Black Point. The shallow water grey smoker (ore body) is located in the south-east of the sediment filled inner crater (solid line). Aligned fluid outlets (dots) along which bacterial mats (white) have partly settled. The outer crater (dashed line) is mostly overgrown with Posidonia fields (green). Instruments such as the buoy of the INGV as well as its ground weights were not added to the map. Depths of the crater rims are given in light grey: numbers within the crater display the foot of the rim while numbers on the outer side represent the upper part of the wall.

Further data

Considering the various points of investigation in the submarine area east of Panarea, the highest temperatures could be measured at Black Point. Although a general cooling trend could be observed for the hydrothermal fluids between 2016 and 2018, temperatures can reach up to 132 °C which resembles the boiling point 23 m bsl (personal communication with B. Merkel).

Vents throughout the craters show pulsating emanation of the gas-dominated fluid outlets. In contrast, water-dominated spots show a constant fibrillation of the water.

The water-dominated fluids emanated at the grey smoker show an elevated mineralization with low pH-value compared to fluids at other locations (STANULLA, 2021). Gas-dominated fluid outlets (class A-B; STEINBRÜCKNER, 2009) could only be documented in the centre of the crater.

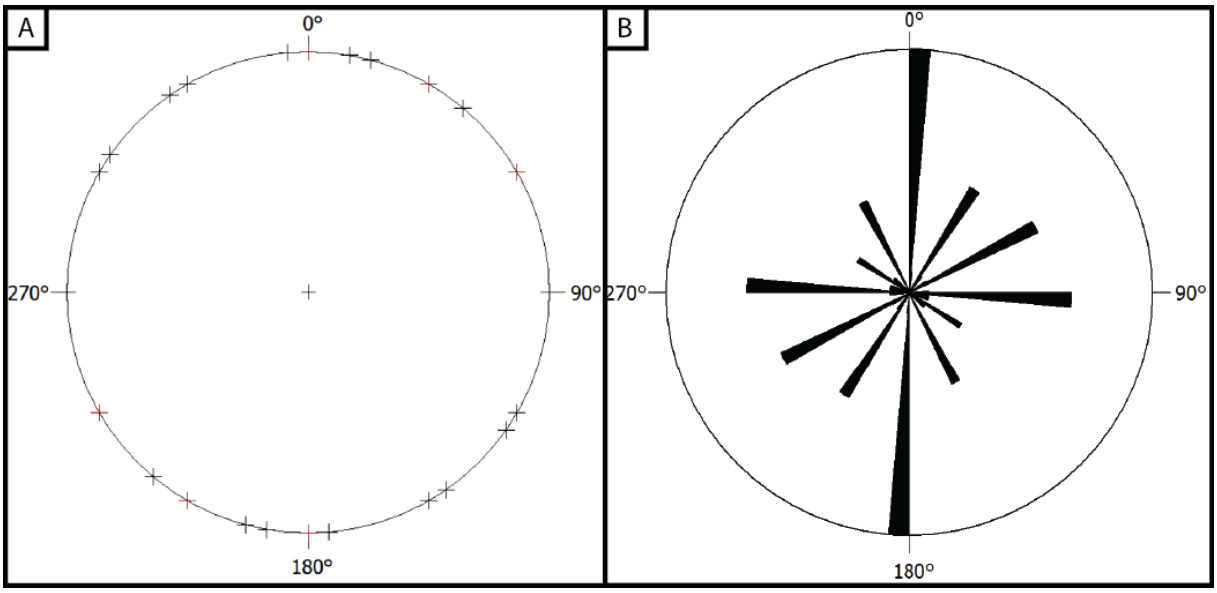

Figure 18: A – Equal-area projection of the lower hemisphere of structures at Black Point. Since no dip could be measured, only the pole points (crosses; black – inner crater, red – outer crater) could be added to the diagram indicating the strike direction. B – Rose diagram of the strike directions measured at Black Point; N = 48. Dip directions are not considered. The diagram shows a major strike direction of 000-180 °. Minor strike directions of the structures are 030-210 °, 090-270 ° and 060-240 °.

4.2.3 Bottaro North

Mapping

During the underwater survey to Bottaro North, the overall morphology and appearance mapped in the previous years by members of the SDC could be confirmed. In addition to the existing map, geological features were added as well as the strike direction of the aligned fluid emanation points found at this location.

Geology

Bottaro North is characterized by a central gravel field that is surrounded by allochthonous large boulders (Figure 19). The dacitic-andesitic boulders, possibly resulting from landslides of Bottaro islet, can reach several meters in diameter. The fine- to medium-grained, sub-rounded gravel lies on top of a polymictic conglomerate which is cemented by sulphuric precipitations. Bacterial mats cover the sediment near weak fluid exhalation points. Sulphurous mineral precipitations can be observed near the vents. Other discharge structures could not be observed.

North-west of Bottaro North, towards Fumarolic Field, silicified crevasses can be found which indicate former degassing structures. The whitish material, stated as Dykite (STANULLA, 2021), is compact and brittle and rises clearly from the surrounding volcanic host rock. Along this lithology small hydrothermal fluid discharges can be spotted.

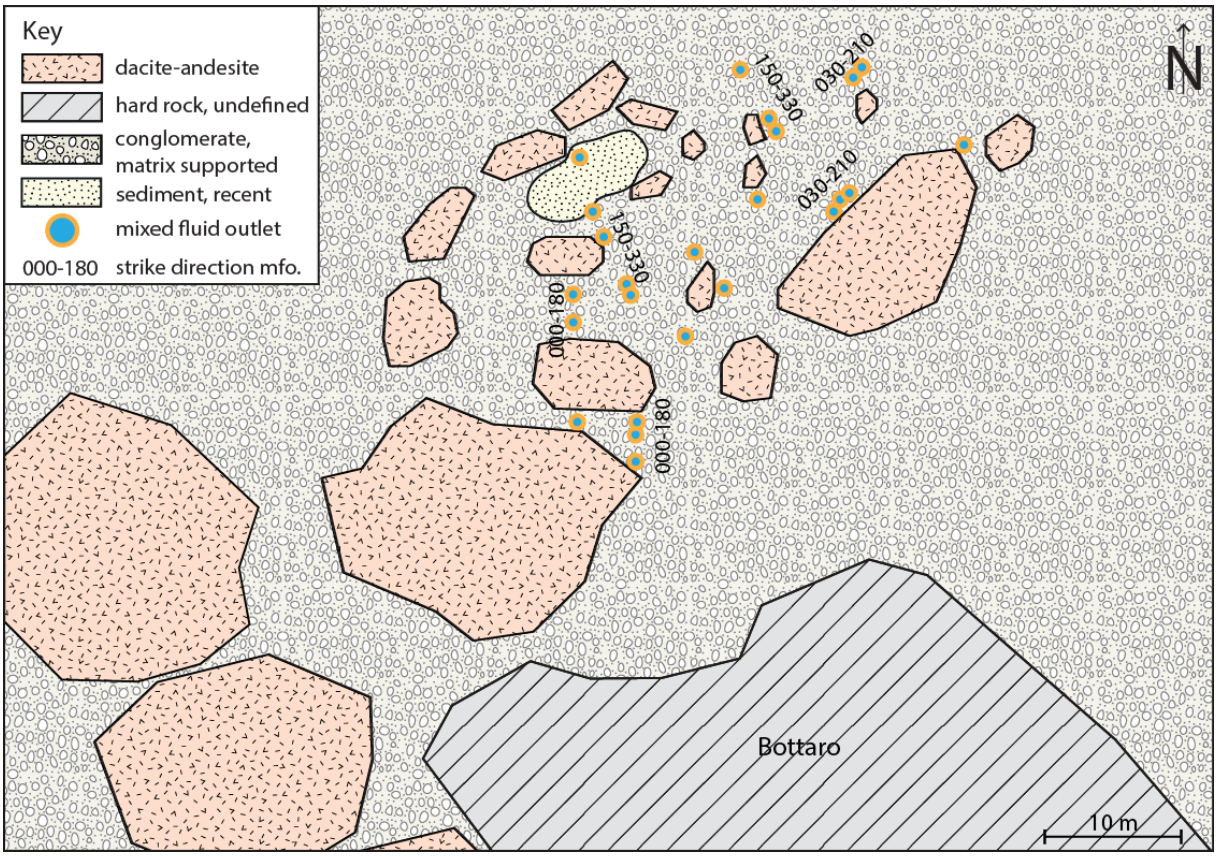

Figure 19: Sketch map of Bottaro North. A central gravel field (yellow) is surrounded by loosely arranged boulders of mainly dacitic-andesitic composition (red) at the northern shore of Bottaro islet. Fluid vents are arranged in lines indicating the strike direction.

Structural data

Due to the cover of the location with loose sediment, no structures could be found at the main location of Bottaro North where strike and dip directions could be measured. Yet, fluid vents are partly arranged in line-like structures which can mainly be found south and east of the gravel field. These lines mainly indicate strike directions of 150-330 ° (Figure 20). 000-180 ° as well as 030-210 ° are subordinated strike directions. A fracture east of the gravel field, partly refilled with sulphurous precipitates, was found in the dacitic host rock with an orientation of 005/83.

Although only few surfaces were found where measuring the silicified structures to the north-west was possible, the general strike direction of the dykite material is similar to the major strike direction (150-330 °) around the gravel field. Dip directions are generally higher than 70 °.

Further data

Hydrothermal fluid discharges at Bottaro North are mainly gas-dominated. While the majority of these vents can be characterized as class A to C (STEINBRÜCKNER, 2009), there are single

emanation points of class E. Fluids appear to be emitted at a constant flow-rate. The strongly exhaling vents are especially located in the east and in the south.

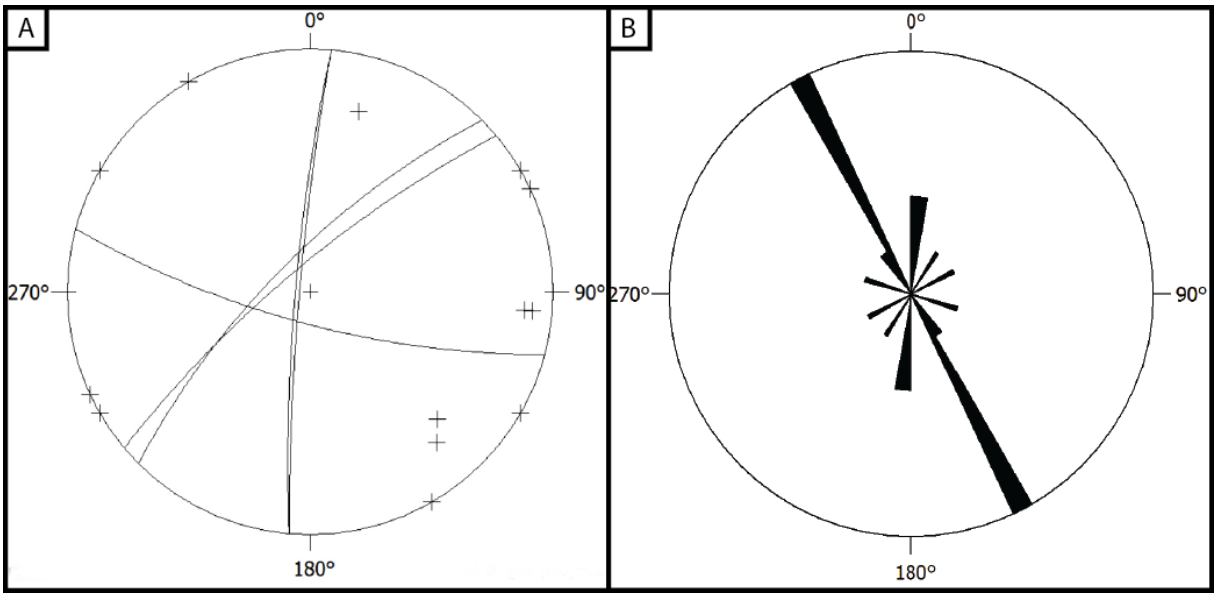

Figure 20: A – Equal-area projection of the lower hemisphere of structures at Bottaro North. Black – silicified structures (north-) west of BN, crosses represent pole points. B – Rose diagram of the strike directions measured at Bottaro North; N = 14. Dip directions are not considered. The diagram shows a major strike direction of 150-330 °. Minor strike directions of the structures are 000-180 ° and 030-210 °.

4.2.4 Bottaro West

Mapping

As the location's map proposed by the SDC had only contained the main crater as well as its surroundings, the mapping campaign was expanded to the north following prominent structures. Mapping was mainly conducted during the 2018 field campaign.

Bottaro West's central part represents a submarine crater with an elliptical shape that extents about 10 m in its NE-SW axis and about 12 m in its NW-SE axis (Figure 22). Depths along the crater rims were added. Small fields of Posidonia are located in the northern part of this crater. Throughout the outer crater as well as in the outer portions, several blocks of hard rock can be found. The number of blocks increases to the east. Fluid discharges distributed in the southern portions of the crater are surrounded by small amounts of whitish bacterial mats.

Northwest of the crater, another elliptical shaped gravel field can be found. This second crater is about 12 m long and 8 m wide at its broadest position. Weak hydrothermal fluid discharges can only be observed in the north-eastern portion of this field. At its southern margin a light-coloured hard rock forming a triangular shape is located which is why this location was given the name *Dragon tooth*. Going further to the northwest, several rock portions of various size can be observed between the dense Posidonia fields. A particular spot was named *Gimli* due to the axe shape of the approximately 3 m high rock when looking at it from the east or west. It is situated on a round sediment field measuring 4 m in diameter. This structure, mostly

overgrown with biota, is located NW of the northern crater. Following the north-west direction further, other hard rocks similar to *Gimli* can be located. Yet, these structures were not mapped due to limited time available.

Geology

Recent sediment can be found in the initial craters at Bottaro West. It can be interpreted as a polymictic sand. Its angular grains vary between medium and coarse size. Fine- to medium grained, angular gravel is also contained in the sand plains of the crater fields.

Underneath the sediment within the main crater a sulphur cemented, polymicitc conglomerate crops out at some spots within the crater. Grains are sub-angular. As it could be found in the midst of the Posidonia field in between main crater and the northern crater as well as in the vicinity of *Dragon tooth* it can be assumed that this lithology expands over the entire location.

Most of the blocks at this location are of volcanic composition, similar to the dacitic blocks found at Bottaro North. Most of the rocks show severe alteration which is why mineral or rock determination is difficult. As STANULLA (2021) states, individual minerals could be determined in thin sections as Plagioclase, Biotite, and Quartz due their shape. Chemical characterization of these samples was not possible.

Rock material from structures such as *Dragon tooth* or *Gimli* differs from the volcanic rocks distributed in this location. The majority of the rock is made of a whitish, hard and brittle material. This silicified rock, also referred to as Dykite (STANULLA, 2021), is associated with the dykes that run through the investigation area. According to DEKOV ET AL. (2013), the dykite material is mainly made of SiO_2. Both *Gimli* and *Dragon tooth* are not made of a compact rock mass but of thin layers of rock which are arranged in various directions in whose centre altered volcanic host rock remnants can be found (Figure 21). As a result, these rocks form polyhedral structures that resemble honeycombs.

Structural data

In contrast to other locations, the majority of the gas-dominated vents in the southern part of the main crater are not arranged in lines. The few aligned fluid discharges show a general strike direction of 060-240 °. In the northern part of the main crater strike directions range between 120-300 ° and 150-330 °. In the northern crater vents are commonly aligned with a 150-330 °, sometimes also with 000-180 ° orientation.

Structural data could not be recorded for the volcanic hard rocks as well as the conglomerate underneath the soft sediment cover. Data was derived from the largest and thickest layers of the dykite honeycombs. Minor intersecting layers were not measurable due to the size of the clinometer applied. At *Dragon tooth* the average orientation is 357/80. In contrast, the structures at *Gimli* show two main direction intersecting each other repetitively: 030/47 and

330/17 (Figure 23). Compared to similar structures in the submarine investigation area, the dipping angles at this structure can be rather small.
Several smaller portions of dyke material crop out at the western edge of the main crater. As the covering soft sediment was not removed sufficiently, only the general strike direction of 090-270 ° of these rocks could be followed.

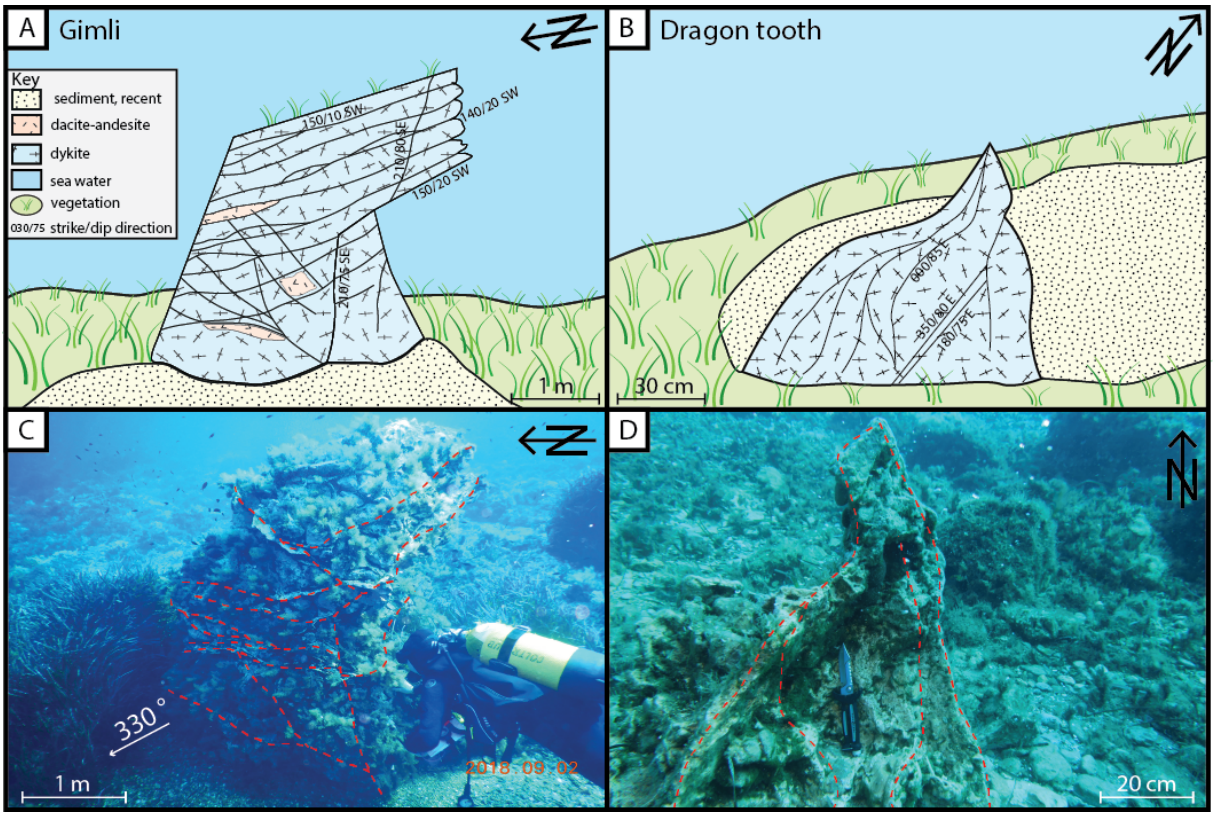

Figure 21: Silicified structures at Bottaro West. A – Simplified sketch of *Gimli*. The structure, located at the margin of a sediment field, is densely overgrown with biota. It is mainly composed of SiO_2-rich dykite which outlines initial fluid pathways. Although strongly altered the volcanic host rock is still visible at some spots. The majority of the silicified structures show strike directions of 150-330 ° and moderate dipping angles of 20 ° or less. B – Simplified sketch of *Dragon tooth* at the margin of another sediment field near the main crater. This dykite structure as well traces initial fluid pathways. Here, dipping angles are 80 ° or higher with N-S oriented strike directions. C – Overview image of *Gimli*. As biota covers most of the formation, silicified structures were traced exemplarily (red lines). D – Overview image of *Dragon tooth*. The thickest and most prominent silicified fluid pathways (red lines) are outlined. (Photography: D – R. Stanulla)

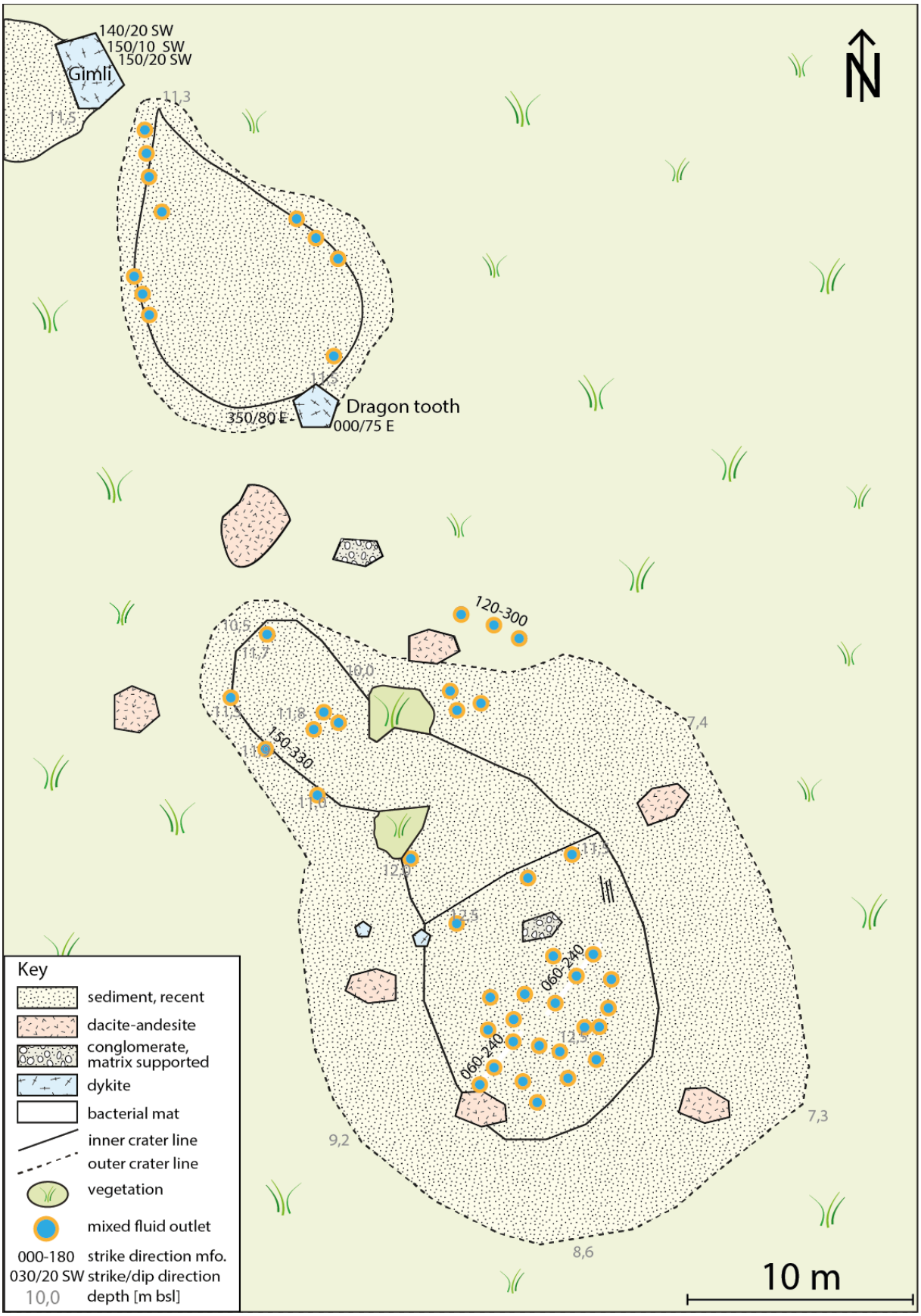

Figure 22: Sketch map of Bottaro West. The main crater in the south is covered with recent sediment (yellow) which lies on top of a matrix supported conglomerate (light brown). Dacitic-andesitic boulders (light red) are distributed throughout the area. To the north a second crater is located on whose southern edge *Dragon tooth*

(blue) can be found, a silicified structure. Further to the north-west, *Gimli*, an additional SiO_2-rich structure is located. Hydrothermal fluid vents are often distributed in the area, yet they are seldom arranged along clearly identifiable lines. The craters are bordered by densly growing Posidonia fields (green).

Further data

For the majority of the gas-dominated class A-B vents (STEINBRÜCKNER, 2009) a slow, but constant emanation could be observed. As observations from the previous years have shown, the overall amount of emanation points within the main crater of this location has decreased. No elevated temperatures at the vents could be measured in the field trip in 2018.

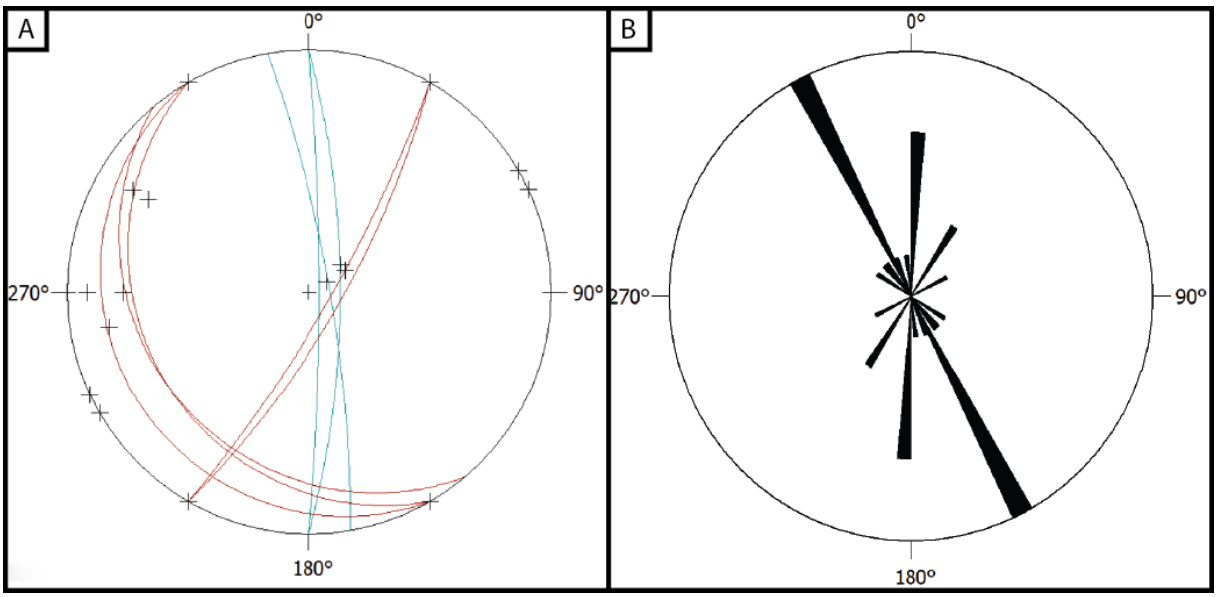

Figure 23: A – Equal-area projection of the lower hemisphere of major structures at Bottaro West. Black – silicified structures at *Dragon tooth*, red – silicified structures at *Gimli*, crosses represent pole points. B – Rose diagram of the strike directions measured at Bottaro North; N = 18. Dip directions are not considered. The diagram shows a major strike direction of 150-330 °. Minor strike directions of the structures are 000-180 ° and 030-210 ° as well as 060-240 °.

4.2.5 Cave

Mapping

As Cave is a rather new working location for the SDC, only a sketch of the location by J. Engel existed from the previous years. During the dives at Cave, this sketch was adjusted and scales were added.

The collapsed cave expands about 8 m in its length axis and is approximately 3 m wide. It is about 2 m deep. On the northern rims lay large, poorly rounded boulders of metre scale. In the east an overhang can be spotted which is about 1.1 m long and 1 m wide (Figure 24). The seafloor within the depression is covered with a decimetre thick layer of dead Posidonia leaves. Bacterial mats can be found at various spots throughout the structure. The initial cave

in the southern part of the depression reaches about 1 m into the host rock. As the exhaling air of divers disperses the dense bacterial mat cover in this cave, it is hard to explore it further. Outside of Cave's depression large blocks and boulders are scattered which can reach up to several metres in diameter. Following the general direction of the depression further to the south for approximately 100 m, the slope rises up to about 10 m. The area southeast of Cave is characterized with large and dense growing Posidonia fields in between which recent sediment covers the sea floor. The sediment ranges from medium-grained sand to coarse gravel. Underneath different kinds of hard rocks crop out. In addition, aligned hydrothermal fluid vents can be found. The area to the north of Cave has not yet been investigated by divers from the SDC.

Geology

The bottom of the depression is made of conglomerate similar to the one at Bottaro West. It is polymictic and prevails sulphuric cements. In addition, sulphide ore clasts are incorporated in between the rounded to sub-rounded clasts.

The surroundings of Cave, including the large boulders and blocks, are made of volcanites, similar to the dacites of Bottaro North. The rocks show severe alterations which is why a precise determination is not possible without laboratory investigations. Along the western side of the depression a dyke intersects the volcanic host rock. The dykite (cf. STANULLA, 2021) is characterized by a high grade of silicification making the rock extremely hard. The SiO_2-rich (DEKOV ET AL., 2013) millimetre to centimetre thick ridges form honeycomb structures. At some spots, small vents can be identified in or along the ridges from which hydrothermal fluids are discharged. Although much smaller in size, the dykite crops out at various spots in the southeast of Cave.

Structural data

The depression of Cave itself shows a general strike direction along its long axis of 150-330 °. This orientation is also displayed at smaller scale in from the dykite honeycomb structures within the depression (Figure 25). Dipping angles within the collapsed cave are at least 76 ° or larger.

Only few aligned gas-dominated fluid vents could be found in and around the depression of Cave. The ones found do show different strike direction which is why a dominating direction cannot be stated.

Silicified structures south of Cave are generally found along the general strike direction of 150-330 °. Yet, the strike directions the structures display vary clearly. Common strike directions south of Cave are 000-180 °, 030-210 °, as well as 090-270 °. Dipping angles are variable, but often the structures are oriented nearly upright.

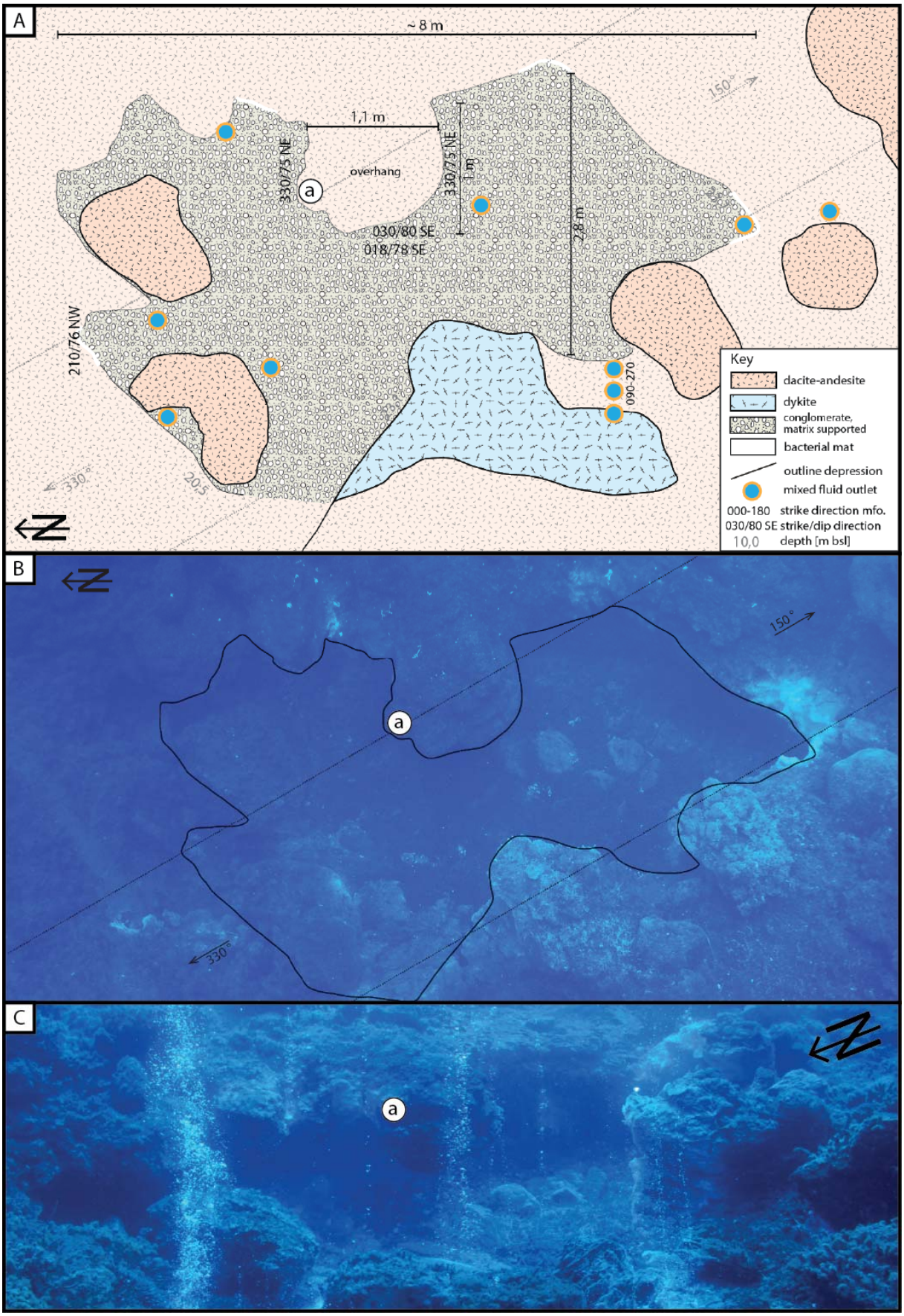

Figure 24: Overview of Cave. A – Sketch map of the of the depression and its surroundings. The depression, filled with conglomerates at the bottom, is arranged along a 150-330 ° striking dyke. Several mixed fluid outlets are

distributed throughout the depression. B – Overview image of Cave. The southern cave is highlighted by bacterial mats covering the dacitic-andesitic host rock. C – View from the north western edge into the depression of Cave. Several fluid outlets can be observed. In their vicinity bacterial mats cover the rocks. (Photography: C – R. Stanulla)

Further data

No long term investigations have been made yet at Cave by the SDC for this location is rather newly known. Gas-dominated, class A-B fluids (STEINBRÜCKNER, 2009) in the surroundings of Cave appear to be emitted at constant, but pulsating flow-rates. Flow-rates along the dykite seem slightly higher than in the depression. Water-dominated fluids are emanated in the southern cave of the depression.

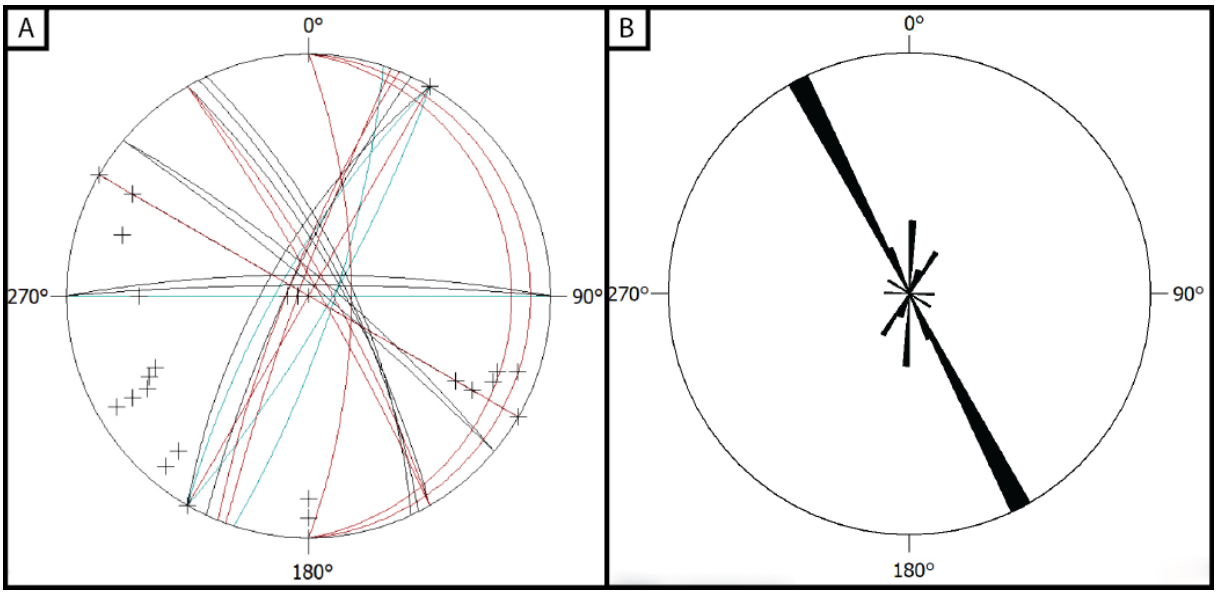

Figure 25: A – Equal-area projection of the lower hemisphere of structures at Cave as well as structures south of the main site. Black – Cave, blue – close surroundings of the depression, red – structures to the southeast of the depression, crosses represent pole points. Dip directions are generally rather high. The orientation of Cave's dykite is consistent with the overall strike direction (150-330 °) of the depression. Structures to the south are rather variable but the overall strike direction of 150-330 ° along which the rocks are located remains the same. B – Rose diagram of the strike directions measured at the investigation site; N = 23. Dip directions are not considered. The diagram shows a major strike direction of 150-330 °. Minor strike directions of the structures are 000-180 ° and 030-210 °.

4.2.6 Fumarolic Field

Mapping

The initial map of Fumarolic Field by the SDC was mainly focusing on the central sediment field. Hence, the surroundings of the spot were mapped more detailed. The field is enclosed by rocky slopes which are rising steeper at the western margin than at the others. To the east and the west, these slopes are covered with densely growing Posidonia. South of this

submarine investigation site, the soft sediment cover becomes less dense exposing the underlying hard rock. Several boulders are distributed in the southern area of Fumarolic field. Throughout the sediment field, smaller boulders can be found which can reach up to several decimetres in diameter. Aligned fluid outlets as well as bacterial mats in their vicinity can be observed across the field, as shown in Figure 26.

Geology

The actual Fumarolic Field comprises a layer of unconsolidated, coarse grained sediment, mainly gravel, which lays on top of sulphuric cemented conglomerates (cf. Bottaro West). The clastic soft sediment layer measures several centimetres. Some of the (sub)rounded pebbles prevail a brown to black coloured coating due to high concentrations of manganese (KÜRZINGER, 2018). Boulders of volcanic composition are distributed across the gravel field.
In the southern area of the location, porous and brittle dacitic to andesitic rocks can be found. These rocks show signs of hydrothermal alteration. Therefore, a precise declaration of the rock or lava type was not possible. Cutting through the volcanites prominent SiO_2-rich, nearly completely silicified (DEKOV ET AL., 2013) rocks of white colour are prevailed. These compact rocks can be up to several metres long and several centimetres broad. At some spots, they show a layered appearance. Gas-dominated hydrothermal fluids are often emanated along the transitions of these layers (cf. Figure 28 B). Honeycomb structures are prevailed in some boulders in the south-east (Figure 28 C). As Figure 28 D shows, the largest of these structures run straight with a defined direction while smaller structures run from or into the larger ones in a rather curvy way through the host rock.

Structural data

Gas-dominated hydrothermal fluid discharges across the sediment field are arranged along lines which prevail the typical strike directions of the working area: mainly 150-330 ° and 030-210 ° but also 000-180 ° as well as 060-240 ° (Figure 27). Yet, considering only the fluid outlets it is not obvious which direction dominates over the others.
Structural data is also given by the silicified structures in the southern part of Fumarolic Field. Due to the general strike direction of 060-240 ° and 150-330 ° the structures in the south-western area would intersect each other. Yet, this is only visible in rare cases (Figure 28 C). In the south-west the dykites rising from the dacitic-andesitic host rock prevail dipping angles higher than 65 °. Most of the structures in the eastern portions resemble the western ones. However, with 25 to 50 ° dip angles are low. A triple junction in the south-east, outlined by the dykite, shows varying strike directions based on the branch as shown in Figure 28 A. Similar to the junction along which the Aeolian Islands are arranged, the southern branch displays a N-S orientation while the eastern branch has an orientation of 030-210 °. The third branch runs with an orientation of approximately 090-240° to the west.

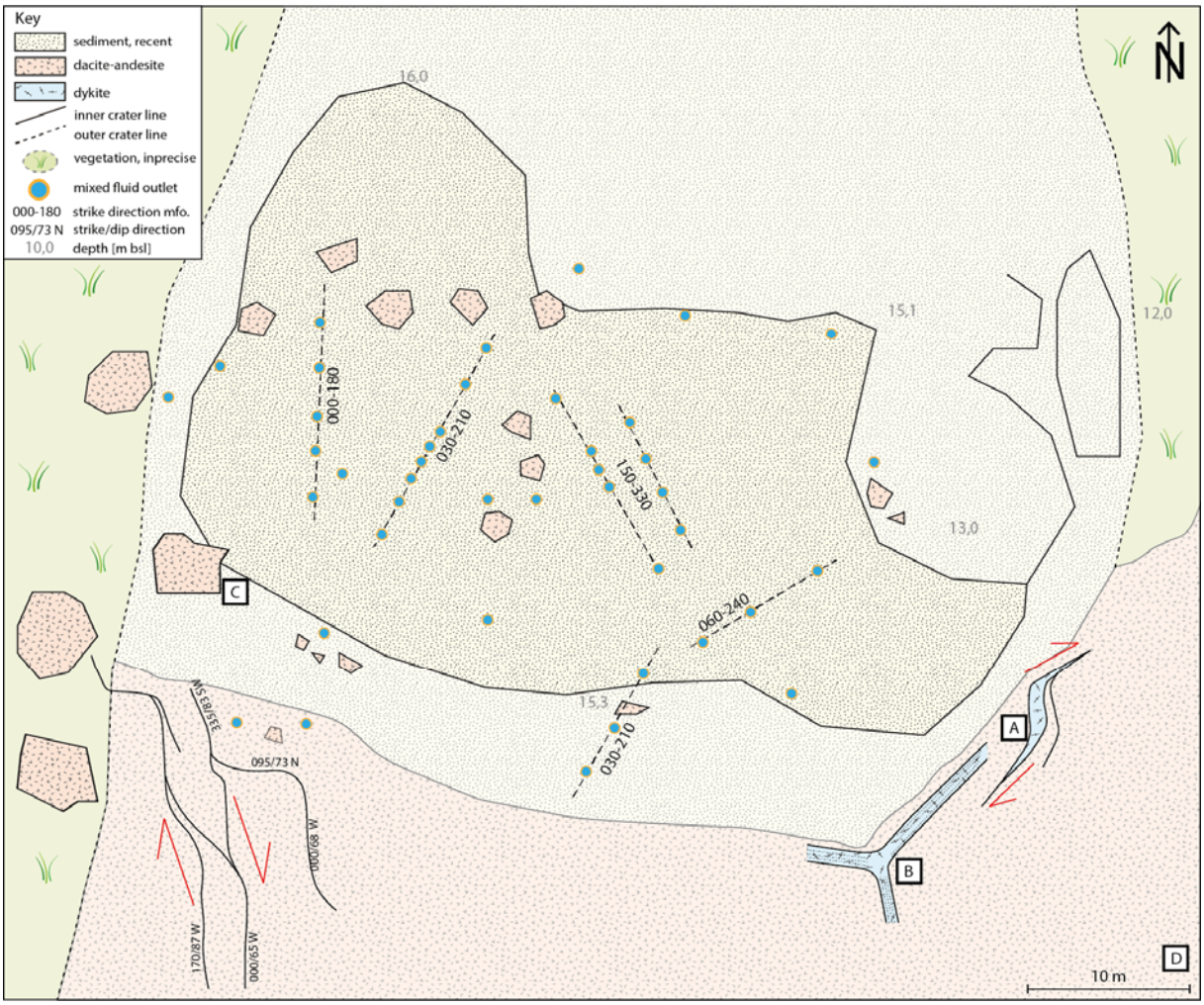

Figure 26: Sketch map of Fumarolic Field. Overgrown slopes (green) border on the central gravel field (yellow) to the east and west. Fluid vents are aligned along typical strike directions. In the south, dacitic-andesitic hard rocks (red) cover the sea bottom. In between these volcanites silicified structures (blue) crop out. Structures of smaller scale are displayed in Figure 28.

A structure of dykite in the south-west of the sediment field indicates a sinistral shear movement (Figure 28 B). As the dykite itself does not prevail any signs of movement it can be assumed that this structure developed prior to its silicification. Yet, due to the alteration of the dacitic-andesitic host rock, no definite indicators of rotation could be found. A similar, sinistrally rotating structure can be found east of the sediment plane.

Further data

Numerous, mainly class B (STEINBRÜCKNER, 2009) fluids vents are distributed across the gravel field of Fumarolic Field. Stronger discharge points (class C) can be found on the western and southern edge of the field. Fluids emanate at constant and moderate flow-rates. However, flow-rates have decreased since members of the SDC have worked at this spot. During the

field trips in 2017 and 2018, most fluid temperatures were similar to temperatures of the seawater. At some spots, temperatures reached up to 45 °C.

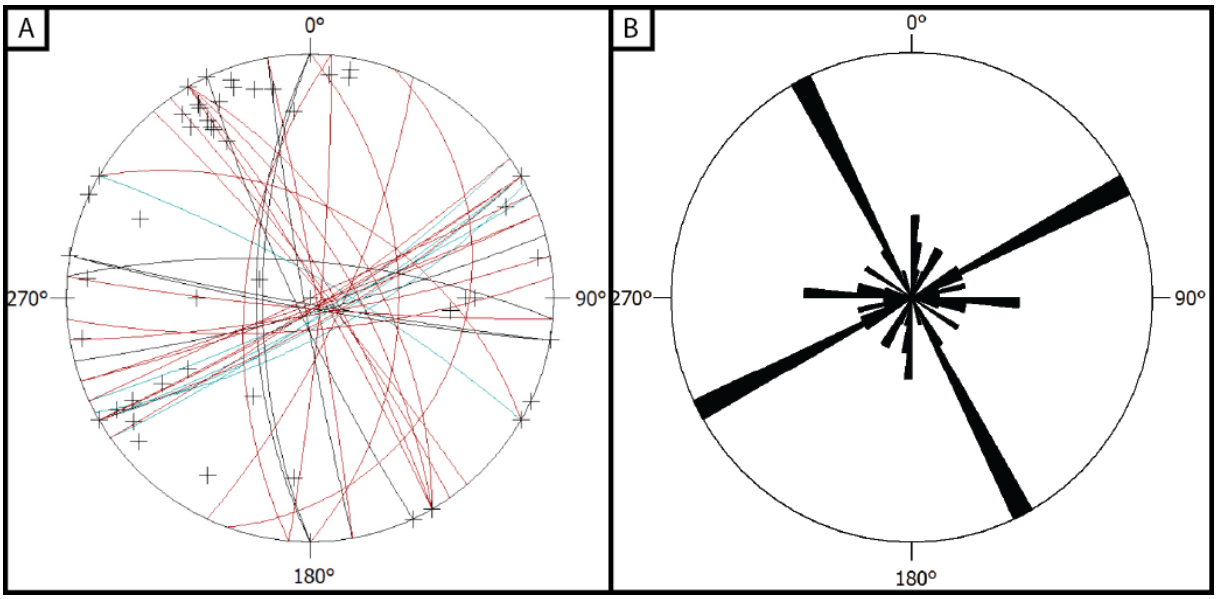

Figure 27: A – Equal-area projection of the lower hemisphere of major structures at Fumarolic Field. Red – structures (south-)east of Fumarolic Field, black – structures to the south-west of the gravel field, blue – structures west of the main gravel field, crosses represent pole points. The majority of the dip directions are rather high. The silicified structures in the south-west prevail an intersecting orientation. In contrast, structures on the eastern area of Fumarolic Field do not show a preferential orientation. B – Rose diagram of the strike directions measured at the site; N = 53. Dip directions are not considered. The diagram shows two major, intersecting strike directions: 060-240 ° and 150-330 °. Minor strike directions of the structures are 000-180 ° and 090-270 °. Structures with a 030-210 ° orientation are rather scarce.

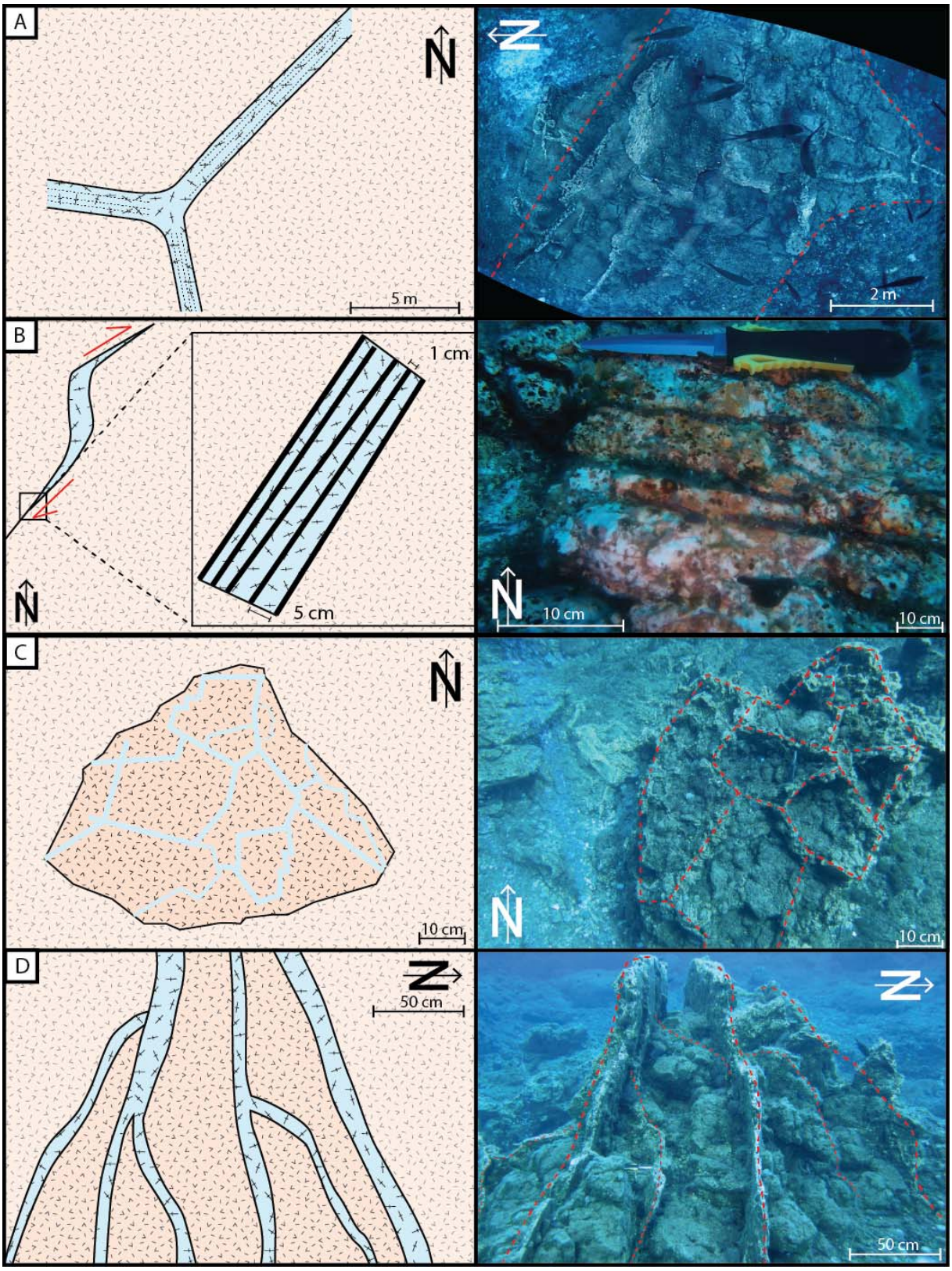

Figure 28: Close-up views of structures at Fumarolic Field. Locations shown in Figure 26. Simplified sketches on the left, exemplary photographs on the right. A – Triple junction in the south-east of FF. Three branches run into various directions. The dacitic-andesitic host rock in between the single layers of the dykite shows signs of severe alteration, possibly due the emanated hydrothermal fluids. B – Close-up view on a silicified structure. It is composed of several bands of 5 cm thickness. In between which these bands, an up to 1 cm thick empy space occurs. Sporadically hydrothermal fluids emanate from these spaces. C – Honeycomb structure on a volcanic

rock south of the gravel field. The bands forming the silicified honeycombs are up to 3 cm thick. D – Massive silicified bands cutting through the surrounding volcanites at high dipping angles. The SiO_2-rich dykites are up to 10 cm thick. Thinner bands intersect the main, 150-330 ° oriented structures.

4.2.7 Hot Lake

Mapping

As a map of Hot Lake has already been proposed in the previous years by the SDC, the mapping campaigns were used to rectify it and add geological information. Hot Lake represents an irregularly oval shaped depression, up to 2 m deep, which measures 10 m in its NE-SW axis and up to 6.5 m in its WNW-ESE axis (Figure 30). Bacterial mats cover the walls of the small grotto that can be found in the southern edge of Hot Lake. Dead Posidonia leaves lay on the ground of the structure. Outside the depression, the ground rises in the southern direction from almost 18 m to about 15.5 m bsl. A few metres around Hot Lake, the sea ground is only covered with some recent soft sediment as well as small amounts of Biota. Further away, large Posidonia fields have evolved.

Geology

The ground of Hot Lake is characterized by a polymictic, matrix supported conglomerate. It prevails sulphuric cements. The clasts are sub-rounded to rounded. On top of the conglomerate lays a cover of recent sediment made of well-rounded sand and gravel which are mixed with the Posidonia remnants.

The depression's walls as well as the surroundings of the depression are built up of two greyish tuffite strata. The transition of the two strata can be seen in the south-western edge of Hot Lake. Surfaces of the tuffite are washed out. Fractures running through the tuffite are filled with native sulphur. Clay lenses are embedded in the tuffite. Due to their ovate shape these lenses are referred to as 'dragon eggs' (KÜRZINGER, 2018). Large boulders of tuffite which are possible remnants of a former collapse of the structure and can reach up to several metres in diameter can be found along the depression's rims as well as inside of it.

Structural data

The long axis of Hot Lake has a general strike direction of 030-210 °. The two branches running from the northern end of the depression prevail a strike direction of 060-240 ° and 150-330 °, respectively.

Only few measurements could be taken inside the depression (Figure 29). They were especially carried out along the fractures in the rock where sulphuric precipitations hint on former hydrothermal activity. The strike directions (between 000 and 030 °) coincide with the overall orientation of the structure. Most of the fractures prevail low or moderate dipping angles. Based on opposite strike directions of 000 ° and 185 ° on the western and eastern wall it can be assumed that Hot Lake resembles the bowl structures at Area 26, although they are

a lot smaller. No gas-dominated fluid vents or bacterial mats could be found with whom further strike directions of nearby fractures could be estimated.

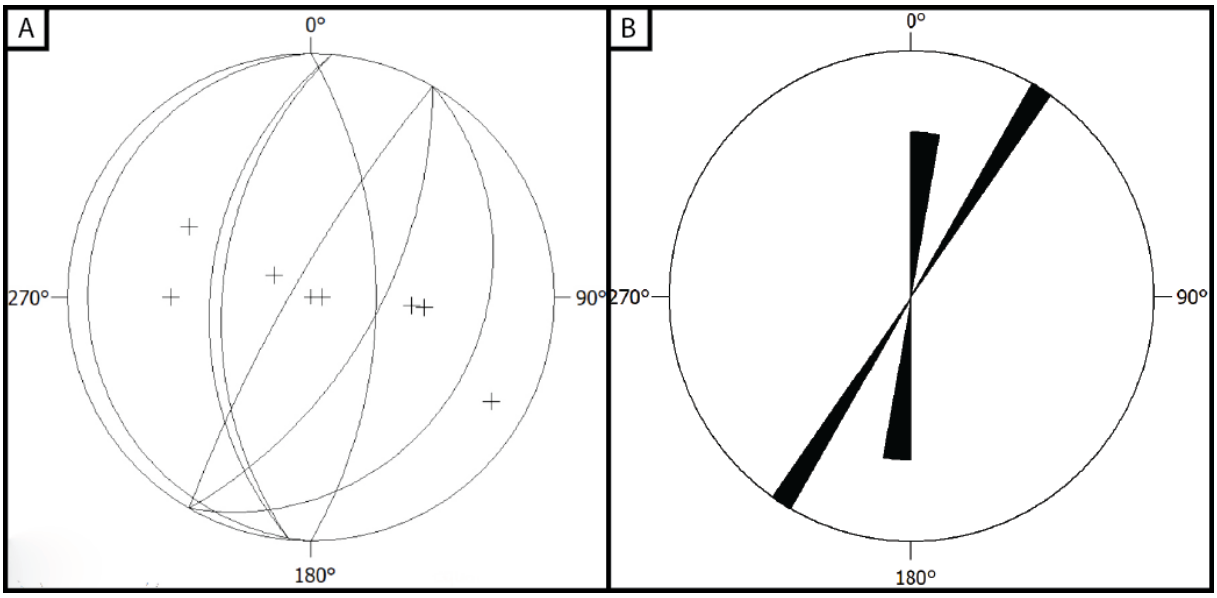

Figure 29: A – Equal-area projection of the lower hemisphere of major structures at Hot Lake. Black lines – walls inside the depression, crosses represent pole points. Dip angles are low to moderate. While the western wall of the structure dips to the east, the eastern wall dips to the west at moderate angles. These dip directions hint on a similarity between the bowl-like structures of Area 26 to Hot Lake. B – Rose diagram of the strike directions measured at the site; N = 7. Dip directions are not considered. The diagram shows a major strike direction of 030-210 ° and a minor direction of 000-180 °.

Further data

According to CANZLER (2013), elevated temperatures up to 80 °C could be measured within the depression of Hot Lake. Yet, temperature measurements during the field trips in 2017 and 2018, where a maximum temperature of 30 °C was noted, indicate a cooling process.

Hot Lake is known for its remarkable chemistry in the emanated hydrothermal fluids. Discharged fluids at Hot Lake used to be mainly water-dominated whereas gas-dominated vents could barely be observed at this spot. A dense bacterial mat cover in the cave on the southern edge of the depression hint on a still active water-dominated fluid discharge. The discharge of hydrothermal water at this spot is disperse and not visible. In 2017, only isolated discharges with low flow-rates (class A; STEINBRÜCKNER, 2009) could be observed in the outskirts of the depression.

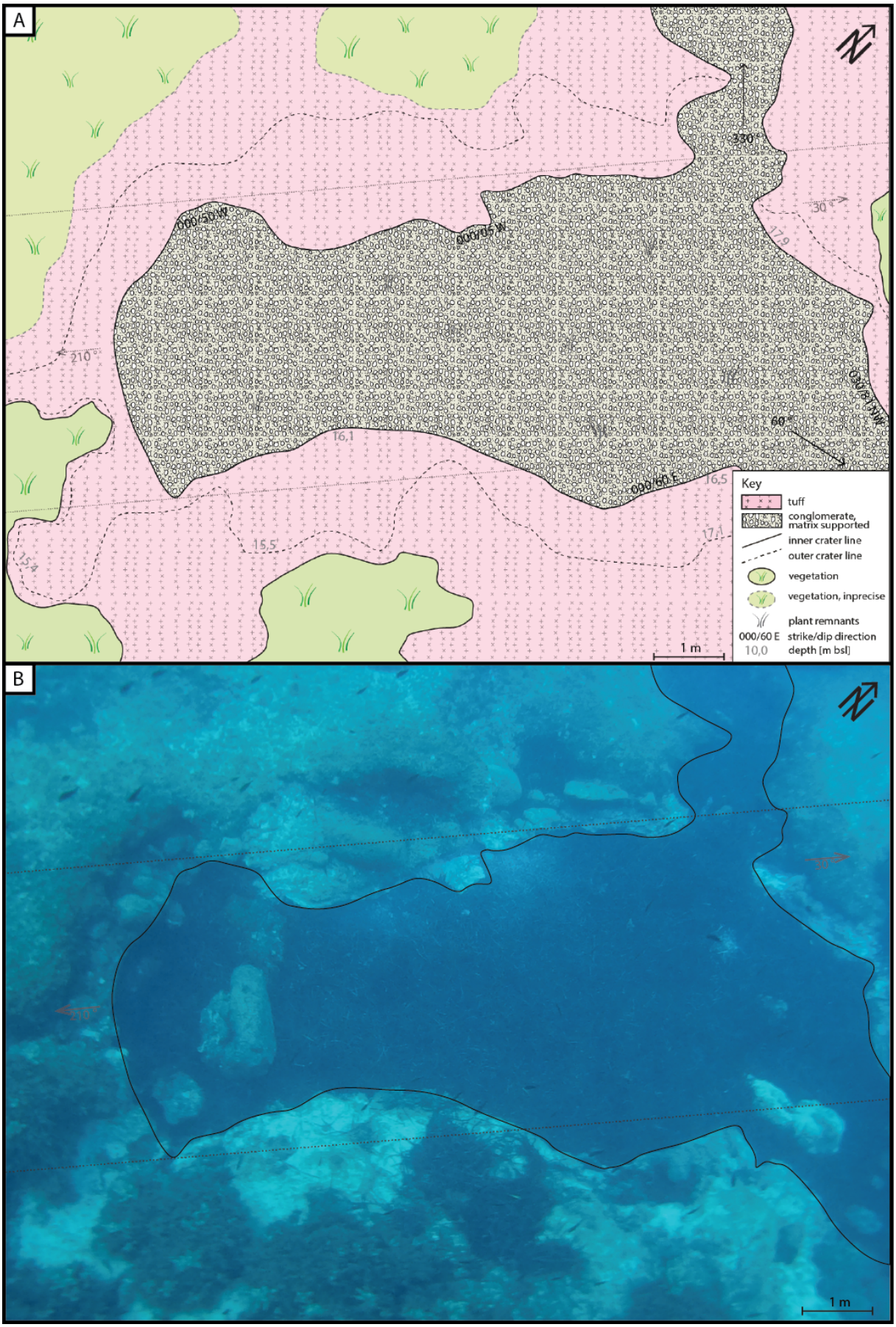

Figure 30: Hot Lake. A – Sketch map of the submarine site. While on the bottom of the depression a matrix-supported conglomerate lays, the walls and the vicinity of Hot Lake is made up of tuffite. Large fields of Posidonia

grow around the depression. No signs of bacterial mats could be found. B – Overview image of Hot Lake. Tuffite boulders lay near the rims. Dead Posidonia covers the majority of the structure's ground.

4.2.8 La Calcara

Mapping

A map of the submarine investigation site has already existed displaying the main working areas such as *New Rock* (NR), *Black Rock* (BR) near B2, and *Octopus Rock* (OR) where large boulders can be found. Several Posidonia fields of variable sizes lie between the fix points. As the field works of the 2017 and 2018 field trips brought up other places of interest, the map had to be expanded (Figure 31).

La Calcara is a spot that is mainly characterized by large plains of soft lose sediment in between which Posidonia fields grow in extended fields. Close to the southern buoy B1 a spot of comparably small size (2.0 x 1.7 m) was found underneath the sediment cover with numerous fluid vents. These vents are emanated from abstracted cones and tubes (cf. STANULLA, 2021) giving the ellipsoidal shaped location the name *Mordor*.

Following the gently dipping area to the south-west for several decametres large boulders can be found about 13-14 m bsl forming a wall-like structure giving it the name *The Wall*.

Geology

La Calcara is characterized by a recent homogeneous, polymictic sand facies of several decimetres thickness. This sand has formed wave ripples which are up to 30 cm high and possibly result from tidal influence due to the proximity to the shore of Panarea Island. An additional facies made of sand prevails a fine-grained matrix whose components mainly consist of weathering products of the volcanic hard rocks found close to the bay of La Calcara. Therefore, Alunites and Smectites are common products found in this facies (KÜRZINGER, 2018; STANULLA, 2021). At some spots, for example towards *The Wall*, thin layers (sub mm-scale) of iron-bearing precipitations cover the recent sand.

Underlying the recent sediment, altered product of volcanic rocks can be found. At the deepest point near *Octopus Rock* which resembles a well-rounded, cemented, sulphide-bearing rock the underlying sediment is characterized by an altered tuffite in which clays and silts are common. Sulphide ore precipitations, most likely Pyrite/Markasite, are common within this facies. Small degassing structures were found across the uncovered facies. At this spot, numerous samples were taken. It appears that precipitates have newly formed.

The newly discovered sub location *Mordor* prevails a sedimentary rock with clasts of sand and fine gravel. Cements are iron-bearing. In addition, white mineral crusts are incorporated which resemble the dykite material at other submarine sites. Abstracted tubes and cones have built up as a consequence of the emanated hydrothermal fluids.

The Wall is made up of surf conglomerates. The well-rounded boulders can reach more than 1 m in diameter.

Figure 31: Sketch map of La Calcara. Due to its large spatial extent, sub locations were set up (e.g. *NR*, *BR*, *Mordor*, *The Wall*, …). Two ascending buoys (B1, B2) were installed to ensure short travel times to these locations. The area dips slightly to the east which is why *The Wall* represents the shallowest point at 14 m bsl and *Octopus Rock* (OR) is located almost 10 m deeper. The area in between these spots is mainly characterized by large sandy plains (yellow) intersected by Posidonia fields (green). As they were not entirely mapped in detail, these fields are marked as imprecise in the map. Few hydrothermal fluids are scattered throughout the Area. Yet, secondary structures, such as bacterial mats and cones indicate a high hydrothermal activity underneath the sand cover (see Figure 33 and Figure 34 for detail).

Structural data

As the majority of La Calcara's area is covered with a thick layer of recent sediment, structural data could mostly be derived from secondary structures. At La Calcara, such secondary indicators are especially bacterial mats and discharge features, like sand cones. Furthermore, iron-bearing mineral precipitations can be found near these structures. Hydrothermal fluid exhalations arranged along lines are scarce. Concentrated spots, such as *Mordor*, can be found

where numerous fluid vents are distributed on a generally small area. However, no preferential orientation could be identified along which they are arranged.

Near the southern buoy B2 numerous bacterial mats can be found. In contrast to other locations, the mats are arranged in line-like structures which partly extent over several metres. These bacterial mats are not influenced by the sand ripples of this location. It can be assumed that the mats trace structures, such as fissures, in the host rock underneath the sandy cover (ADAMEK ET AL., 2020). That way the strike direction can be derived (Figure 33). The bacterial mats indicate a network of structures which partly intersect each other. Numerous lines prevail a strike direction of 000-180 ° or 030-210 °. But orientations of 060-240 ° and 090-270 ° are also common (
Figure *32*).

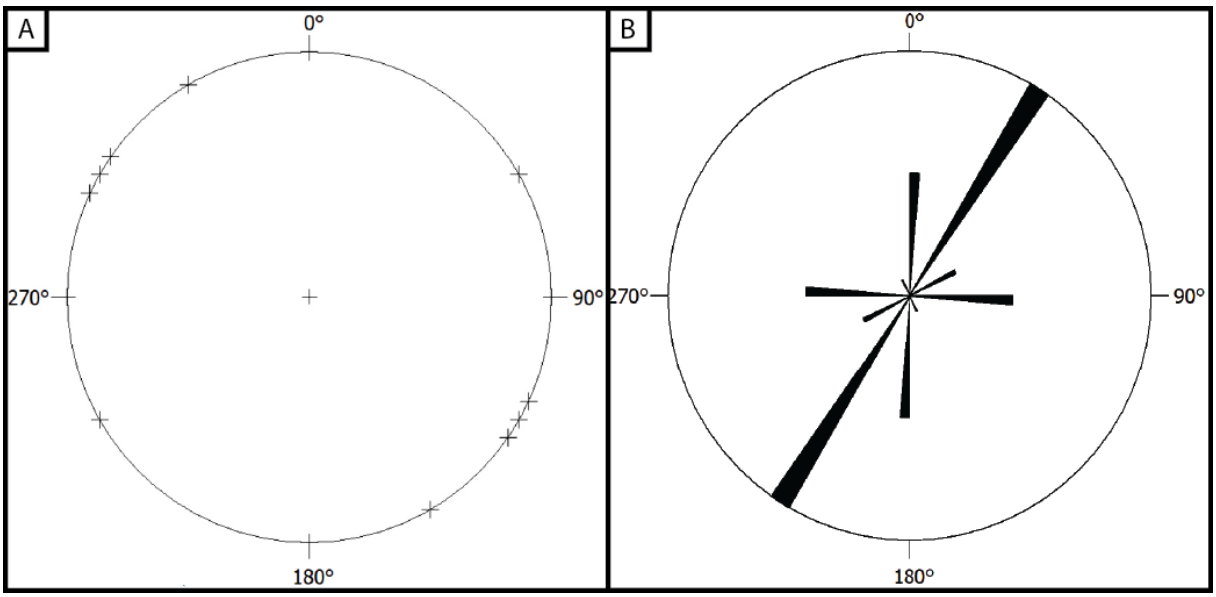

Figure 32: A – Equal-area projection of the lower hemisphere of major structures at La Calcara. As no dip directions could be measured only pole points of the strike directions are displayed. B – Rose diagram of the strike directions measured at the site; N = 31. Dip directions are not considered. The diagram shows a major strike direction of 030-210 ° and minor directions of 000-180 ° and 090-270 °. Yet, it cannot be stated clearly that one direction dominates over the others due to the low flow-rates and the thick sediment cover at this location. Secondary structures, such as bacterial mats and unconsolidated cones (cf. STANULLA ET AL., 2017), hint on the strike directions of underlying tectonic structures.

Taking the number of secondary indicators as well as their spatial extension into account, the existence of a large-scale structure can be assumed. It extends over several decametres. Tracing its outlines, the structure appears to have a sinistral shear sense. Figure 35 displays a part of this structure along which temperature measurements were carried out. A second, similar structure can be assumed farther to the north of La Calcara, due to the same indicators (Figure 31).

Unconsolidated cones can be found at various spots of the western portions of La Calcara, especially near towards *The Wall*. The cones form concentrated fields of individual structures, often close to the outer edges of Posidonia fields. Similar to the bacterial mats, a number of

these cones are arranged along lines (Figure 34). Typical strike directions are 000-180 ° and 060-240 °.

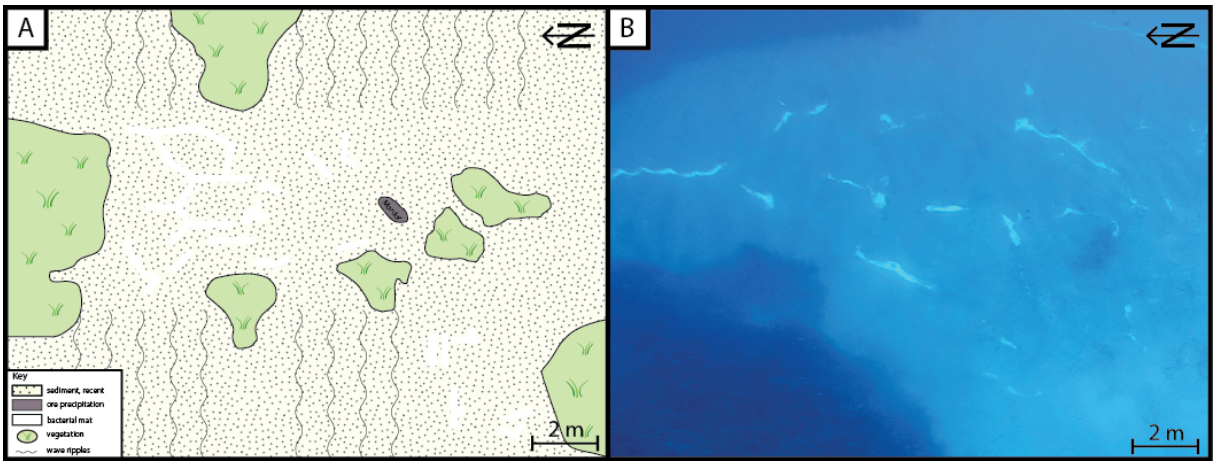

Figure 33: Bacterial mats tracing the strike directions of structures covered by a decimetre thick layer of sand and gravel. A – Sketch of a sediment plain (yellow) near Mordor where bacterial mats point out structures underneath the sand cover. Typically, the mats show strike directions of 000-180 °, 030-210 °, and 060-240 °. B – Overview image of bacterial mats settling along linear structures which coincide with recurrent strike directions typical for the area.

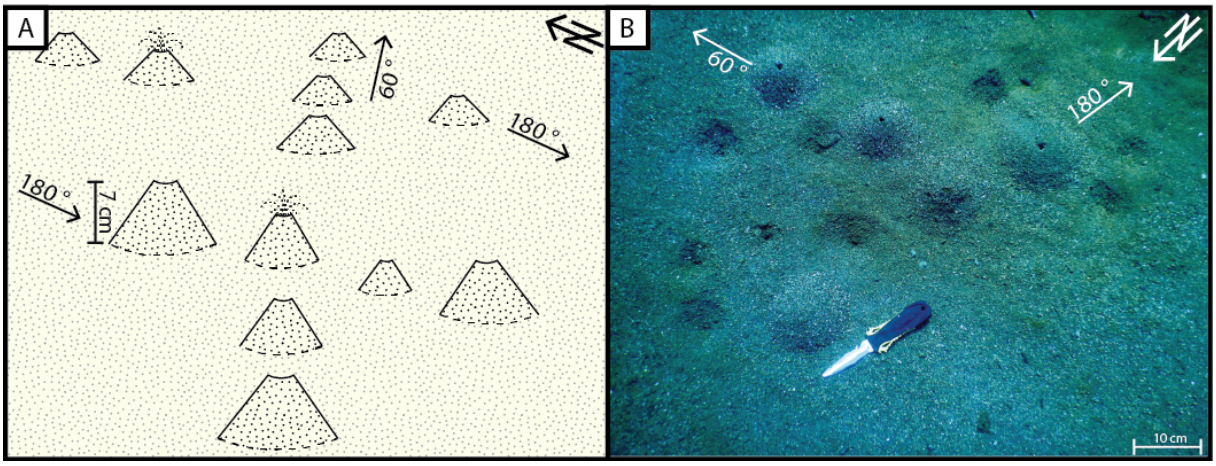

Figure 34: A – Sketch of sandy cones arranged along directions of 000-180 ° and 060-240 °. These directions coincide with usual strike direction in the working area and can thus be assumed to display structures underneath the sediment cover. Some cones still show hydrothermal activity by emanating gas-dominated fluids at low flow-rates (STANULLA ET AL., 2017). By doing so, sand becomes ejected as well. B - Unconsolidated cones aligned along typical and recurrent strike directions. Knife for scale, pointing north.

Further data

Fluid temperatures can be very high at La Calcara. In 2017, 130 °C were measured at the sub location *Mordor*. Fluids are highly acidic and can be both water- and gas-dominated.

The investigation site is characterized by numerous discharges which are widely distributed throughout the sand plains. When the sediment cover is removed, one of the discharge points

might turn out to be a spot of a number of vents in the underground. As most fluids are emanated at low, sometimes also unsteady flow-rates (class A-B; STEINBRÜCKNER, 2009) they become dispersed by the decimetre thick sediment cover. Only few spots, such as *Mordor*, show a concentrated number of stronger fluid outlets across a rather small area.

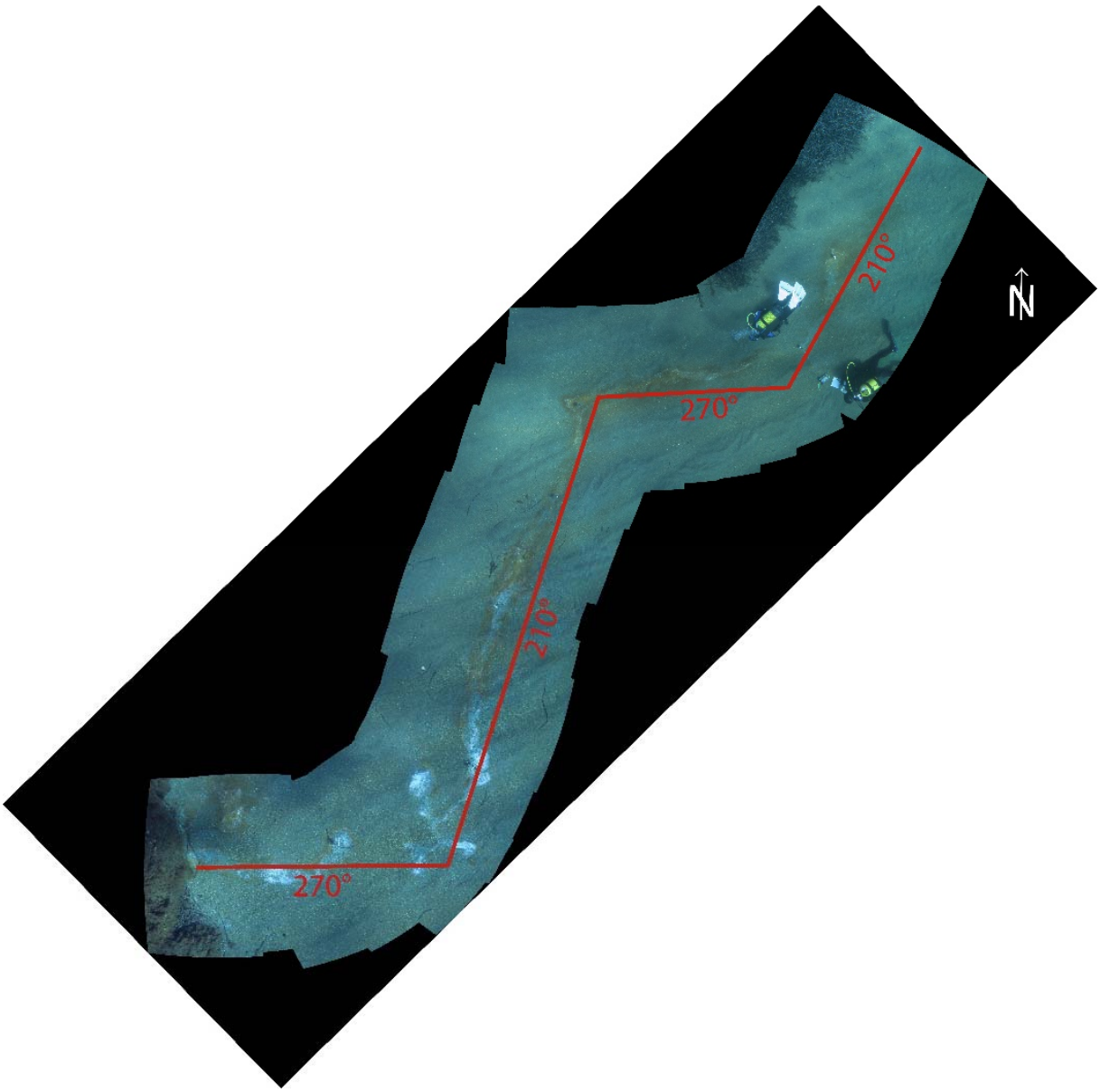

Figure 35: Stitched image of a branch of a supposed shear structure in the south-eastern sector of La Calcara. Temperature measurements were conducted along this structure. At various spots, unconsolidated cones as well as bacterial mats can be found which are arranged along lines coinciding with the strike direction (ADAMEK ET AL., 2020). In addition, mm-thin iron-bearing mineral precipitations lie on top of the sand cover. Few hydrothermal fluid exhalation points can also be found. All secondary structures indicate on a large-scale tectonically influenced structure underneath the sandy cover. (Photography: SDC)

4.2.9 Point 21
Mapping

Mapping at Point 21 was continued based on the existing sketch by the SDC which mainly displayed the *Scarp wall* along with the strongest hydrothermal fluid vents. The S*carp wall* measures about 5 m height and 30 m length. About 20 m to the east of it, the sea-bottom rises with a steepening slope. Various disperse vents emanate hydrothermal fluids out of the wall which is oriented in a NW-SE direction (Figure 37).
On top of the *Scarp wall* a *Plateau* can be found to the west. It measures about 25 m in its N-S-axis and about 15 m in its E-W-axis. The Plateau is traversed by crevasses through which hydrothermal fluids are emanated. At some spots, bacterial mats cover the rock. To the west, north and south it goes over into densely growing Posidonia fields. In between the Posidonia, aligned fluid outlets can be found along with bacterial mat covers.
South of the *Scarp wall*, the area is mostly overgrown with biota. Due to the biota's relatively small height the structure of the sea-bottom can still be recognized. Numerous crevasses run through the host rock. At most of these crevasses weak fluid vents are aligned. In addition, bacterial mats cover the vents' surroundings.

Geology

The *Scarp wall* and *Plateau* are made of variously altered dacite to andesite. Due to the alteration mineral identification based on optical properties is difficult. However, large minerals from the samples showed typical shapes of plagioclase in thin sections. In addition, single small quartz crystals could be identified. Amphiboles or mica could scarcely be identified. Although much smaller in size the matrix is mainly be composed of minerals similar to the large feldspars.
Numerous fissures and crevasses traverse the rock along which hydrothermal fluids are emanated dispersedly. At some of these vents crusts of massive sulphide mineral precipitations have formed. These built up crusts cover both fractures in the rock as well as larger portions of the host rock itself (ORDOSCH, 2016). Furthermore, native sulphur can be found in the vicinity of some fluid outlets across the wall as well as south of the main area of Point 21.
South of the Scarp wall, erosional canyon can be found. Rock material from the southern portions of Point 21 is heavily overgrown with various kinds of biota. Yet, these rocks show a smaller degree of alteration. While the outer millimetres to centimetres of the material show a white colour and no clear mineral shapes, the inner portions display centimetre large plagioclase crystals within a light grey coloured matrix. Small dark minerals, possibly amphiboles, are distributed in the microcrystalline matrix.

Structural data

The location of Point 21 shows a complex structural setting. As Figure 36 shows no preferential orientation can be defined. It can be stated that dipping angles are rather high which coincides with the optical appearance that most structures are oriented nearly upright. Only fissures within the *Scarp wall* show lower dipping angles. Several prominent strike directions can be identified: 000-180 ° and 090-270 ° along with 030-210 °, 060-240 ° and 150-330 °. Furthermore, unusual strike directions (for this working area) of approximately 120-300 ° were measured. The rose diagram for the values measured at this location displays nearly the same situation as only few aligned fluid outlets were found apart from the rock structures.

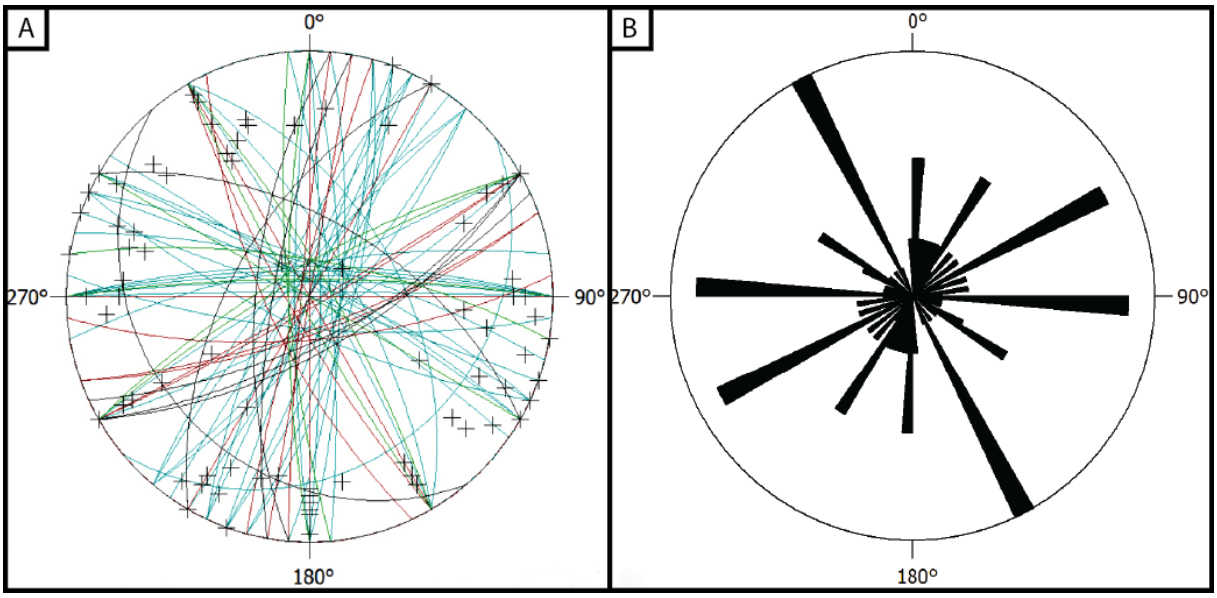

Figure 36: A – Equal-area projection of the lower hemisphere of major structures at Point 21. Blue – structures on the plateau, green – structures to the south of the scarp wall, black – scarp wall, red – eroded vent liens further south, crosses represent pole points. The majority of the dip directions are rather high. None of these individual spots show a preferential orientation. Intersecting directions often occur which confirms the visual estimation of the crevasses from the field work. B – Rose diagram of the strike directions measured at the site; N = 74. Dip directions are not considered. The diagram does not show a strike direction that dominates over the others. Prominent and recurrent strike directions are 060-240 °, 090-270 °, and 150-330 °. Less often measured, but also noticeable are orientations of 000-180 °, 030-210 °, and 120-300 °.

Further data

Long-term temperature measurements were conducted with the help of the FSVG at the class E emanation points (PONEPAL ET AL., 2010). Temperatures reach up to 71 °C.

Fluids at the foot of the scarp wall are emanated at flow-rates of more than 40 l/min (STEINBRÜCKNER, 2009). In contrast, emanated fluids across the plateau have lower flow-rates (class B). The constantly discharged fluids at Point 21 are mostly gas-dominated.

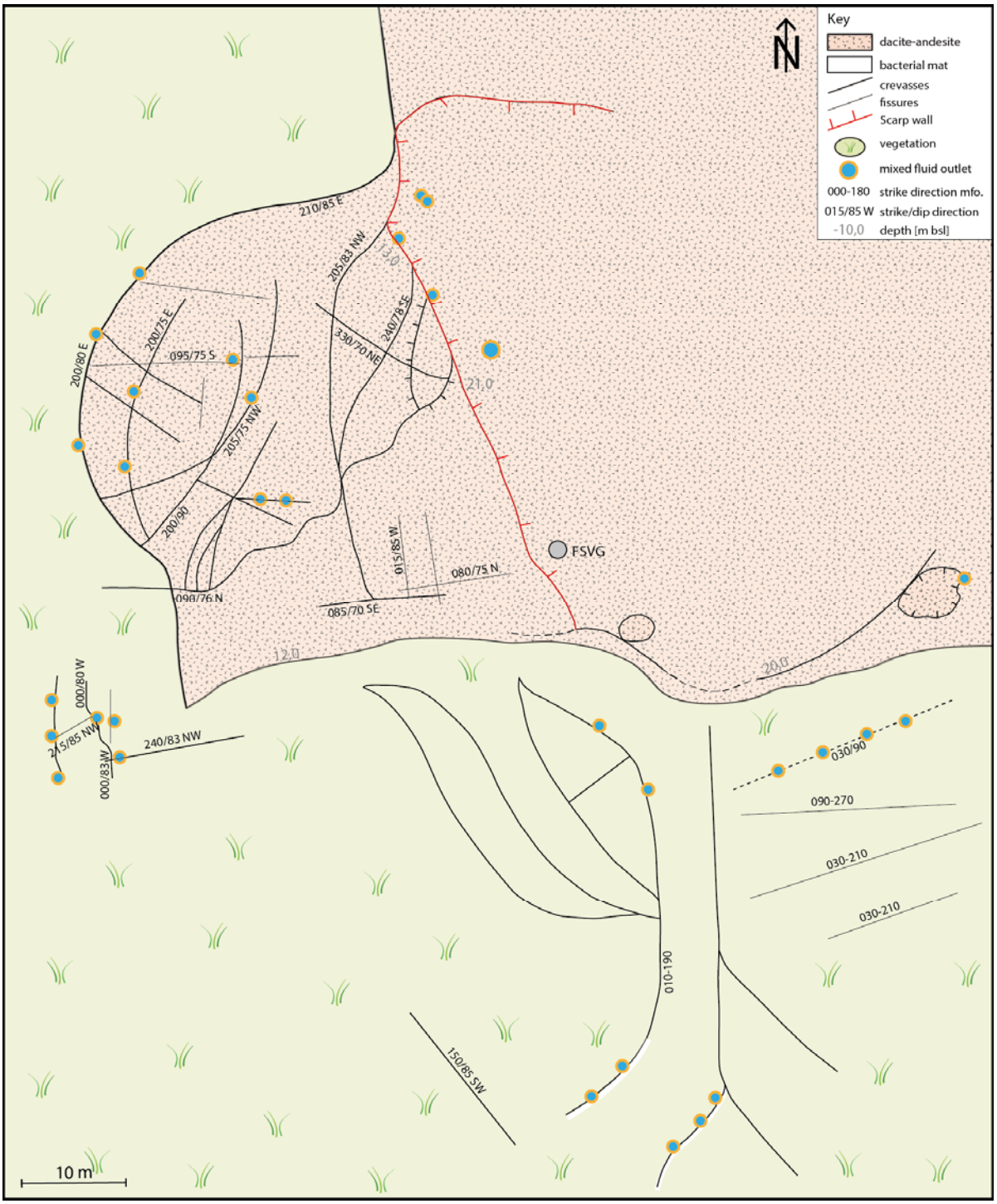

Figure 37: Sketch map of Point 21. Aside the *Scarp wall* and the adjacent *Plateau* to the west, most of the spot's area is overgrown with biota (green). The rock portions are characterized by an intensively altered, brittle dacite to andesite whose minerals can barely be identified. While the foot of the *Scarp wall* is located 21 m bsl, the *Plateau* and surrounding portions of this spot can be found at a depth of approximately 17 m. Fluid outlets are found along fissures and crevasses cutting through the host rock.

5. Interpretation and discussion

As the submarine investigation site La Calcara is located close to Panarea Island and the islet of Bottaro can be seen as the outer margin of the submarine crater east of the main island, the interpretation is split into the two main regions of the working area. Due to the various lithologies recognized, one major point of consideration is the determination of relative ages. Due to mapping campaigns above and below the sea surface the estimation of structures' spatial extent is more precise and gives more insights on the processes that are likely to have taken place.

5.1 Crater east of Panarea Island

Relations between structures and fluids

Although the diving campaigns do not cover the entire area of the submerged crater east of Panarea Island, the conducted investigations allow detailed insight on the environmental settings of this tectonically active region.

The determination of the structures' precise orientations (strike and dip directions) was not always possible at all submarine investigation sites as recent sediment covers the main structures. Various spots were observed where secondary indicators, such as discharge features (cones, tubes), mineral precipitations, (aligned) fluid emanations, and bacterial mats occur. With the help of these features, strike directions of the underlying features can be estimated. However, other fields of interest, as the estimation of the structures' relative age or the determination of their overall size were limited at submarine investigation sites, such as Black Point or portions of Area 26. Measured flow-rates in the previous years by members of the SDC (STEINBRÜCKNER, 2009) as well as the observations in the 2017 and 2018 campaigns do not allow the conclusion that higher flow-rates are automatically linked to larger fractures or other structures through which hydrothermal fluids can discharge. Higher flow-rates are also not linked to the predominating orientations of the structures. Hence, a classification of the dominating and subordinate structures is not given by this method.

Throughout the submarine areas of the Panarea volcanic complex, a number of different hydrothermal discharge features could be observed, such as bowls, widened fractures or silicified pathways. Assuming that all of these features result from initial fractures in the volcanic host rock, certain environmental components appear to influence the formation of one or the other (Figure 38). Besides the chemical composition and physical parameters of the surrounding host rock, the available time for the fracture to evolve is of interest. In addition, physical factors, as temperature, the pressure at certain depths as well as flow-rates, do have an influence on the size and appearance of the variety of discharge features. Furthermore, constructive (e.g. precipitation) and destructive processes (e.g. erosion, subrosion) account to their formation. In some cases, the influence of plant roots is likely as well. In general, the evolution of initial fractures to different kinds of discharge features, as they can be observed now, depends on a number of different environmental influences.

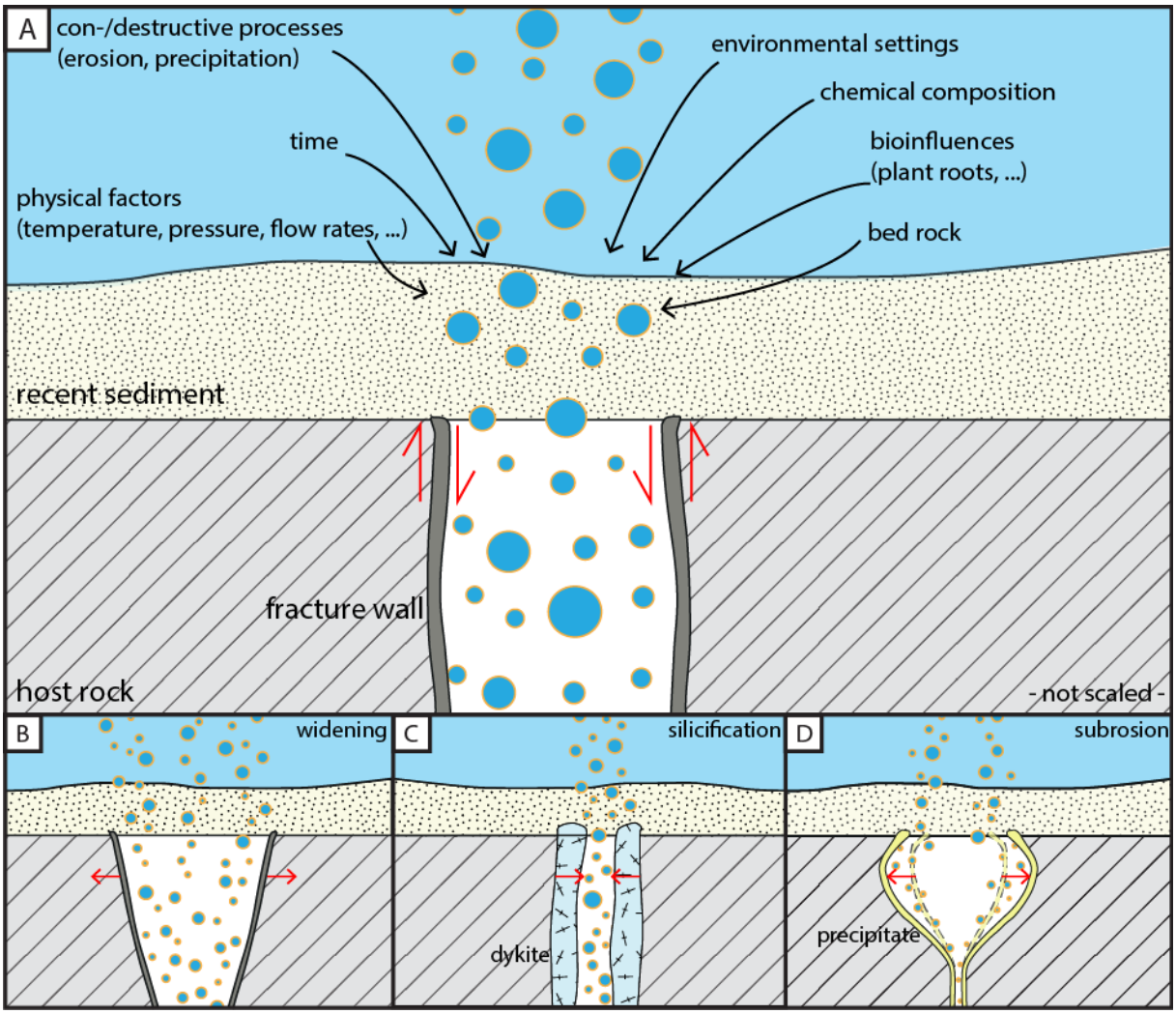

Figure 38: Simplified sketch of a fracture and its possible ways to develop. A – As it can be assumed that all structures found in the submarine area result from initial fractures, the different kinds of development depend on the surrounding components, such as the time given to develop, physical parameters, the chemical composition of the surrounding rocks and the discharged fluids, bio-influences and others. It seems also possible that some fractures remain a fracture. B – Emanating fluids can cause a widening of the initial fracture as acidic fluids dissolve the surrounding host rock along the fracture walls. This case can be observed at Point 21. C – As the fluid composition might change over time, it is also possible that SiO_2-rich components precipitate along the fracture walls leading to a contraction of the fracture and eventually to its closure as observed at Fumarolic Field (cf. Figure 28 B). D – Another possible development is the subrosion of the host rock as fluids dissolve it at deeper levels which leads to the formation of bowls and lineaments as observed at Area 26 and in the bay of La Calcara (cf. Figure 9 D, E; Figure 16). Sulphurous precipitations are characteristic for the side walls of these structures.

A detailed differentiation of younger and older rocks based on discharged features or degassing structures was not possible with the given data derived during field work. Nevertheless, the relative age can clearly be determined at investigation sites where silicified structures were found, as for example at Bottaro West, Cave, and Fumarolic Field. Assuming that the SiO_2-rich structures display former discharge paths of hydrothermal fluids, the surrounding bed rock must be significantly older. As the fractures, which are considered the

basis for all further structures linked to the discharge of hydrothermal fluids, formed most likely during or after the cooling of the volcanic host rock during periods of tectonic unrest, they are consequently younger. Although a precise age determination of the silicified structures could not be found in literature, it can be concluded that these structures are among the youngest in this area.
Assuming that the dykite (STANULLA, 2021) has formed in a submarine environment, the formation of the dykite structures as observed during the mapping campaigns passes several stages:

Stage 1: Initial fracture
After the cooling of the magma, fractures have formed. This might have resulted from cooling processes of the magma as well as tectonic activity in the region. Volcanic fluids, both water and gases, can rise from the magma chamber to the surface (Figure 39 A).

Stage 2: Dykite precipitation
After the development and widening of fractures, SiO_2-rich components precipitated along their walls (Figure 39 B). At the beginning, this fracture wall is rather thin. As the dykite is more resistant to the acidic hydrothermal fluids, the fracture walls do not undergo any erosional processes. As time passes, the walls become thicker. Yet, the pressure of the hydrothermal fluids increases due to smaller area of discharge.

Stage 3: Dykite growth and volcanic rock erosion
Due to their chemical composition, the volcanic host rocks are not as resistant to the discharged hydrothermal fluids as the dykites themselves which leeds to the erosion of the volcanic host rocks (Figure 39 C). This process becomes intensified when the hydrothermal fluids form branches running from the main fracture. The amount of rock surface that gets in contact with the mixed fluids increases as the branches expand. (Note: The orientation of the branches does not coincide with the orientation of the initial fracture.)

Stage 4: Closure of Dykite
Over time, the majority of the initial fracture system along with the evolved branches is filled with precipitated dykite material (Figure 39 D). Hydrothermal fluids cannot pass through these factures anymore. As the volcanic host rock has been eroded, the remaining structures resemble honeycombs in some cases.

As hydrothermal fluids were observed to be emanated from these structures, this process appears to be still ongoing at some spots. The dykite portions in the submarine investigation area indicate that the surrounding rocks have undergone severe erosional processes. The side walls of the dykites prevail even surfaces which are unlikely to form when these structures are surrounded by water. Consequently, the top of the dykites appears to coincide with the initial top of the surrounding rocks. In general, it can be stated that the dykites developed post-

genetically and they are more resistant to the surrounding environmental influences or erosional processes (cf. Figure 21). Taking the formation of dykite material on a submarine environment into account, it can be assumed that the dykite fault at Bottaro islet developed under the same conditions. This hints on a changed sea level during the time of formation.

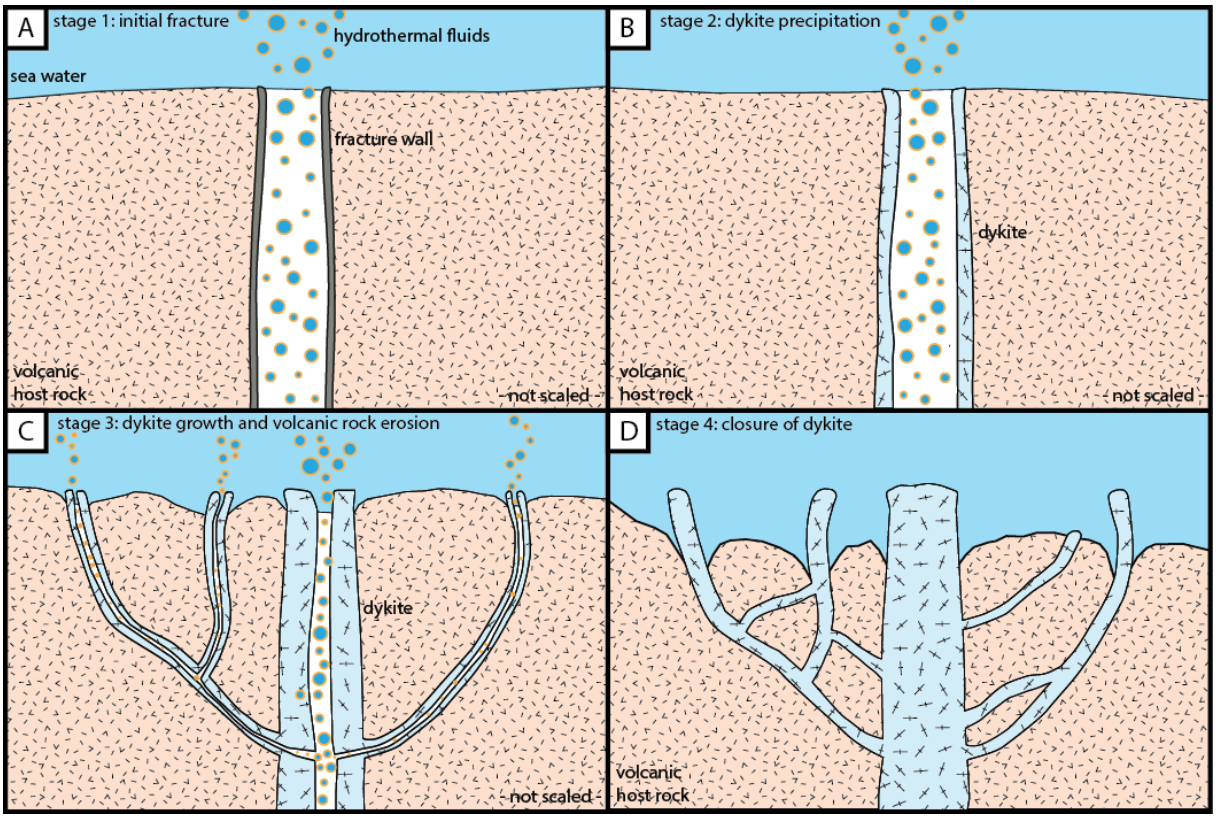

Figure 39: Schematic sketch of how SiO_2-rich dykites form from an initial fracture. A – A fracture runs through the volcanic host rock. Hydrothermal fluids emerge through this facture into the surrounding sea water. B – As time progresses, SiO_2-rich precipitates fall out along the fracture's walls. C – Over time, branches develop originating from the main fracture. The dykite fills larger parts of the fracture. Due to the decreasing opening width of the fracture, hydrothermal gases being emitted through this fracture generate new pathways in order to reach the surface. The surrounding host rock undergoes chemical erosion as the mineral composition is not resistant enough to the acidic fluids. D – Eventually, the fracture will be completely filled with SiO_2-rich precipitates. Hydrothermal fluids cannot flow through the fracture system. As long as the fluids were discharged from this fracture system, the chemical erosion of the surrounding volcanites advanced while the dykite remains more resistant to the fluids and therefor remains its initial expansion. A dykite network has formed (cf. Figure 9, Calcara bay).

Structural notes

The majority of the structures observed in the area of the crater are rather small scaled, reaching up to several metres in length. The dyke of western Bottaro islet runs into the sea at a general direction of 150-330 ° which is why it can be assumed that it can be followed farther to the north-west below the sea level. As the investigation sites of Cave and Bottaro West prevail similar structures along the same strike direction, there are two or three major

structures in the eastern crater. As the dykite structures at Cave and its surroundings could be followed farther to the south-west and the structures of Bottaro west farther to the north-west at a general strike direction of 150-330 ° it can be assumed that these individually observed structures are connected to each other. This observation does not coincide with findings from literature (e.g. ANZIDEI ET AL., 2005 and ESPOSITO ET AL., 2006) where structures in this area were not documented or prevail differing orientations.

While for some locations, an overall dominating orientation can be stated, there are others where structures clearly develop along specific alignments but this orientation does not generally dominate throughout the investigated area of the site. At Area 26 for example, each structure or group of features forms along a clearly distinguishable line while overall they are aligned along varying directions at a larger scale.

The depressions of Hot Lake and Cave, which are two of the major structures within the investigated area, are aligned along weakening zones which coincide with the overall observed fault system. Both features resemble each other in their outer appearance. Assuming that both depressions once represented cave-like structures as still obvious in their outer parts, the cave roofs must have been collapsed at a point where the energy of the emanated hydrothermal fluids as well as their erosional influence dominated over the stability of the roofs or when the roofs have become too thin due to the fluids' chemical erosion.

The severe alteration of the dacitic-andesitic rocks at the location Point 21 in the centre of the submerged crater as well as the high flow-rates with which hydrothermal fluids are emanated at this spot indicate that this location differs from the other locations. Fractures throughout the area of Point 21 do not point out a preferential orientation. In contrast, several orientations appear to be distributed at the same amount. Therefore, Point 21 can be interpreted as a crossing point where structures with opposing strike direction intersect. This observation coincides with bathymetric findings of ANZIDEI ET AL. (2005). Due to these various orientations observed within the crater area, it can be assumed that there are other locations where intersecting features form larger structures due to the instability weakening of the host rock as observed at Point 21.

5.2 Panarea Island and surrounding areas

Throughout the area of Panarea Island and its close surroundings, several large scale tectonic structures, mainly dykes and normal faults, were observed. The majority of these structures coincides with findings from international working groups, e.g. CALANCHI ET AL. (1999), FABRIS ET AL. (2010), LUCCHI ET AL. (2013A). The structures prevail either an NW-SE trend or a NE-SW trend whereas N-S trends are scarce.

In addition to these large-scale structures, degassing structures similar to the ones in submarine areas, especially Area 26 and Cave, were observed. While dykes and normal faults occur in volcanites, the preserved degassing structures were only observed in sedimentary rocks. As for the submarine structures, the development of such features within the surrounding host rock required the existence of a tectonically induced fracture through which

hydrothermal fluids can ascend from the magma chamber to the surface. As STANULLA (2021) states, such features cannot form in volcanic rocks because surrounding conditions, such as time, chemical composition and physical parameters, do not support the development of slowly developing degassing structures.

As stated in the previous chapter, the dykites appear to have formed in a submerged environment. The same applies for degassing structures, such as bowls and lineaments. Consequently, it can be assumed that the area above the bay of La Calcara once belonged to the submarine portions of the Panarea volcanic system. As LUCCHI ET AL. (2007) and LUCCHI ET AL. (2013b) state, several paleo-shorelines can be recognized as brown tuff terraces. These terraces, found at different elevations between 5 and 120 m asl, indicate sea-level changes within the last 150 kyr. It is likely that the area of the Aeolian Islands along with Panarea Island have experienced both processes at the same time. However, it is not clear, to which extent the island has undergone an uplift and the sea-level has changed.

Although the spatial extent of the subaerial degassing structures is rather small it can be assumed, that a tectonic structure follows the general direction farther into the sea. As the sand cover at the submarine location La Calcara does not allow to determine the nature of the structure more detailed, the number of secondary indicators (tubes, bacterial mats, mineral precipitations, fluid emissions) hints on a large expansion of this underlying structure.

6. Conclusion

6.1 The Panarea system in the geological context of the Aeolian Islands

The crater east of Panarea Island is among the most investigated areas of the Aeolian Island group as the submarine and subaerial structures prevail detailed information on the environmental settings of this tectonically active region.

At the beginning of this thesis, the author stated the following hypothesis with the aim to focus on the neotectonic inventory and a comparison of submarine and subaerial structures (cf. Page 15):

- The submarine and subaerial neotectonic inventory of the Panarea system resemble each other in their appearance and extension.
- Although Panarea is located in the north-eastern sector of the Aeolian arc not only north-east oriented extensional structures can be found but also compressional and transversal structures of different orientation. Most structures prevail an extensional character.
- The neotectonic structures of the Panarea system indicate that the stress field of the volcanic system has undergone a westward rotation.

Mapping campaigns on Panarea Island showed that most structures can be observed within volcanic rocks. Subaerial structures are mostly of large scale, such as the dykes and normal faults along the northern and western shore of Panarea (tens to hundreds of metres in extension). Only few structures could be observed in sedimentary rocks. The most prominent outcrop for tectonically induced structures within sedimentary rocks is located near La Calcara bay where both a lineament structure and silicified degassing pathways were observed. Compared to the large scale dykes and faults, structures in sedimentary rocks extent over several metres at the most.

In contrast to the subaerial portions of Panarea, submarine structures were mostly observed in sedimentary rocks, except for the silicified structures correlated to former discharge pathways which formed by erosional processes in the volcanic host rock. Scales of the submerged structures are often distinctly smaller, ranging between few centimetres to several metres. Only few structures were observed whose extension can be assumed to be of several decametres, such as the silicified dyke near Bottaro islet. Yet, the extension of large-scale structures cannot be stated surely as recent sediment often covers them (cf. La Calcara). As secondary indicators point out a rather large extension of some structures, it is possible that there are single structures which resemble the aerial faults. In addition, proportions of various structures are difficult to be compared to subaerial ones as the visibility is limited in the water and hence, getting an overview of large-scale structures can rarely be ensured. Limits are also set by the water depth, the turbidity of the water, and the amount of light being available.

Hence, the first hypothesis cannot be confirmed. Although there are similar features in the subaerial and submarine feature, the overall appearance and extension differs clearly between both environmental settings. As marine terraces of brown tuffs indicate, today's island of Panarea was submerged for a great part. Consequently, it can be assumed that

tectonically induced structures had developed in the area of today's island, as can be observed in the crater east of the main island nowadays. Due to sea level changes and/or tectonic uplift and the resulting altered environmental settings, the majority of the structures in sedimentary rocks could not be preserved over a time span of several tens of thousands of years.

As the study of the tectonically influenced structures in the Panarea volcanic system show, tracing a line along the sea level does not provide a precise view of the entire area of investigation. Hence, a combination of both submarine and subaerial study sites has delivered a more detailed image of the working area. The possibility to explore the submerged portions of the crater east of Panarea offered more details on structures as well as their surroundings and the environmental settings compared to scanning methods, such as Bathymetry. In addition, indicators could be taken into account which cannot be recognized by scanning methods (e.g. bio-indicators, fluid discharges, discharge features/structures, …). With the help of such additional indicators, a complex network of structures could be prevailed in the submerged portions. This network shows various structures of different orientations ranging mainly between NW-SE to NE-SW. Hence, the second hypothesis can only partly be confirmed. According to literature, the dominating orientation of structures coincides with the NE-SW orientation along which the islands of Panarea and Stromboli are aligned. But it is also said that Panarea displays an intermediate between Stromboli and Vulcano concerning rock composition (e.g. CALANCHI ET AL., 2002). Hence, an influence from the central sector is indicated by this and could be confirmed with the study of structures at smaller scale in the submerged portions. In addition, structures were observed which show distinct orientations that are typical for the western NW-SE oriented sector of the Aeolian arc. However, it cannot be stated which of these documented orientations dominates over the other. Most of the uncovered structures show rather extensional characteristics.

Within the Panarea volcanic system, several indicators were found which point out an altered stress field which influences the system:

1) A variety of structures throughout the investigation area along with their varying orientations prove that there is not just one single preferential orientation along which tectonically induced structures developed.
2) Under the assumption that the preserved lineament structure near La Calcara bay is distinctly older than *Lineament* at Area 26 and that both structures developed under the same environmental settings, their different orientations might be related to an altered stress field.
3) Shear structures observed in the submerged portions of Panarea prevail a sinistral shear sense. This sense of rotation would coincide with a rotation to the west. The covered structure at the submarine portions of La Calcara indicates a rotation to the west as well when assuming that the secondary indicators display precisely the pathways of the fault.

However, all these facts can only be seen as hints to a possible westward rotation as suggested by the third hypothesis. None of the accounting factors are definite proofs for a rotation of the stress field as such observations can also be explained by other processes. The fact that

no indicators for such a rotation could be found on the main island of the Panarea system indicates that this rotation would be quite recent and does not influence the subaerial portions. Therefore, the hypothesis that the neotectonic structures of the Panarea system indicate a westward rotation can neither be neglected nor confirmed. In order to state this more clearly, further research is necessary focusing on this fact and promotive factors. The thesis' author assumes that a changed stress field would not only influence a rather small region, such as the Panarea volcanic system. Consequently, indicators for a rotated stress field would also be observable within the regions of the neighbouring islands Stromboli and Volcano.

6.2 Outlook

In order to gain a more detailed few of the structural setting of the Panarea volcanic system, further investigations would have to be carried out. These investigations should focus on exploring submarine areas which have not yet been concentrated on by scuba divers. To get a better understanding of the overall extent of large-scale structures, such as the dykites in the eastern parts of the crater, an exploration of the north-western regions of the crater could deliver answers to these open questions. In addition, a detailed exploration of supposed structures as well as their surroundings would be of interest to expand the knowledge on the structural setting of the Panarea volcanic system.

Furthermore, it would be of interest to explore the submarine surroundings of Panarea Island itself as there are several locations where the structures are supposed to continue underneath the water surface. It would be of great interest to (partly) uncover supposed structures which cannot be accessed due to the overlying sediment cover. That way more precise data could be derived for these features. To investigate the submarine area between Panarea Island and the eastern crater (up to 120 m bsl) with scuba or tech divers requires a number of logistical problems to be solved in advance, such as the availability of mixed gases and proper equipment at Panarea. Furthermore, the limited exploration time at the expected depths would have to be considered. Preliminary investigations, for example using LIDAR, could hint on areas of interests.

Another unanswered question is if there is a correlation between certain kinds of structures and the lithofacies in which these structures develop. However, this would require a detailed inventory of the submarine lithofacies of the Panarea volcanic system. If such an inventory was developed, promoting or limiting factors for certain structures could be deviated. Such information would be helpful in the risk assessment concerning earthquakes or volcanic outbursts for the Panarea volcanic system.

References

ACOCELLA, V., NERI, M., WALTER, T.R. (2009): Structural features of Panarea volcano in the frame of the Aeolian Arc (Italy): Implications for the 2002–2003 unrest. Journal of Geodynamics, 47, pp. 288-292.

ADAMEK, J., STANULLA, R., POHL, T., KÜRZINGER, V. (2019): Geological and structural mapping of holocene small-scaled secondary subrosion structures at Area 26, Panarea, Italy. In: 5th European Conference on Scientific Diving, Gdansk. Book of abstracts, p. 52.

ADAMEK, J., STANULLA, R., POHL, T. (2020): Large and small scale neotectonic structures in the submarine hydrothermal system of Panarea Island. In: 6th European Conference on Scientific Diving, Freiberg. Book of extended abstracts, in press.

ALBERTI, G. (2013): Making Sense of Contingency Tables in Archaeology: The Aid of Correspondence Analysis to Intra-Site Activity Areas Research. Journal of Data Science, 11, pp. 479-499.

ALIANI, S., BORTOLUZZI, G., CARAMANNA, G., RAFFA, F. (2010): Seawater dynamics and environmental settings after November 2002 gas eruption off Bottaro (Panarea, Aeolian Islands, Mediterranean Sea). Continental Shelf Research, 30, pp. 1338-1348.

ANDALORO, F., ROMEO, T., RENZI, M., GUERRANTI, C., PERRA, G., CONSOLI, P., PERZIA, P., FOCARDI, S.E. (2010): Trace elements levels in aeolian archipelago (Central Mediterranean Sea) following an episode of intense volcanic activity. In: Italiano, F. (eds): 2nd International Workshop on Research in Shallow Marine and Fresh Water Systems, pp. 9–10.

ANZIDEI, M. (2000): Rapid bathymetric surveys in marine volcanic areas: a case study in Panarea area. Physics and Chemistry of the Earth, 25, pp. 77–80.

ANZIDEI, M., ESPOSITO, A., BORTOLUZZI, G., DE GIOSA, F. (2005): The high resolution bathymetric map of the exhalative area of Panarea (Aeolian Islands, Italy). Annals of Geophysics, 48 (6), pp. 899-921.

BARBERI, F., GANDINO, A., GIONCADA, A., LA TORRE, P., SBRANA, A., ZENUCCHINI, C. (1994): The deep structure of the Eolian arc (Filicudi-Panarea-Vulcano sector) in light of gravity, magnetic and volcanological data. Journal of Volcanology and Geothermal Research, 61, pp. 189–206.

BAUER, K., BAUER, D., FÜTTERER, W., KLEUTGES, J. (2009): Flow rate measurements at submarine volcanic gas emissions. In: MERKEL, B., SCHIPEK, M. (eds): 1st International Workshop on Research in Shallow Marine and Fresh Water Systems, pp. 112–117.

BECCALUVA, L., ROSSI, P.L., SERRI, G. (1982): Neogene to recent volcanism of the Southern Tyrrhenian-Sicilian area: Implications for the geodynamic evolution of the Calabrian Arc. Earth Evolution Sciences, 3, pp. 222-238.

BECCALUVA, L., GABBIANELLI, G., LUCCHINI, F., ROSSI, P.L., SAVELLI, C. (1985): Petrology and K/Ar ages of volcanic dredged from the Eolian seamounts: Implications for geodynamic evolution of the Southern Tyhrrenian basin. Earth and Planetary Science Letters, 74, pp. 187-208.

BONACCORSO, A. (2002): Ground deformation of the southern sector of the Aeolian islands volcanic arc from geodetic data. Tectonophysics, 351, pp. 181-192.

CALANCHI, N., CAPACCIONI, B., MARTINI, M., TASSI, F., VALENTINI, L. (1995): Submarine gas-emissions from Panarea Island (Aeolian Archipelago): distribution of inorganic and organic compounds and inferences about source conditions. Acta Vulcanologica, 7 (1), pp. 43-48.

CALANCHI, N., ROMAGNOLI, C., LUCCHINI, F., ROSSI, P.L. (1999): Explanatory notes to the geological map (1:10.000) of Panarea and Basiluzzo islands (Aeolian Arc, Italy). Acta Vulcanologica, 11, pp. 223-243.

CALANCHI, N., PECCERILLO, A., TRANNE, C.A., LUCCHINI, F., ROSSI, P.L., KEMPTON, P., BARBIERI, M., WU, T.W. (2002): Petrology and geochemistry of volcanic rocks from the island of Panarea: implications for mantle evolution beneath the Aeolian island arc (southern Tyrrhenian sea). Journal of Volcanology and Geothermal Research, 115, pp. 367-395.

CALIRO, S., CARACAUSI, A., CHIODINI, M., DITTA, M., ITALIANO, F., LONGO, M., MINIPOLI, C., NUCCIO, P.M., PAONITA, A., RIZZO, A. (2004): Evidence of a recent input of magmatic gases into the quiescent volcanic edifice of Panarea, Aeolian Islands, Italy. Geophysical Research Letters, 31, L07619.

CANZLER, W., BARTH, G., GRAB, T., MERKEL, B. (2013): Geothermal investigations of the submarine caldera of Panarea with respect to energy utilization. 3rd International Workshop: Research in Shallow Marine and Fresh Water Systems, Bremen, February 2013.

CAPACCIONI, B., TASSI, F., VASELLI, O., TEDESCO, D., POREDA, R. (2007): Submarine gas burst at Panarea Island (southern Italy) on 3 November 2002: A magmatic versus hydrothermal episode. Journal of Geophysical Research, 112, B05201.

CARACAUSI, A., DITTA., M., ITALIANO, F., LONGO, M., NUCCIO, P.M., PAONITA, A-. RIZZO, A. (2005): Changes in fluid geochemistry and physico-chemical conditions of geothermal systems caused by magmatic input: The recent abrupt outgassing off the island of Panarea (Aeolian Islands, Italy). Geochimica et Cosmochimica Acta, 69/12, pp. 3045-3059.

CIMARELLI, C., DE RITA, D., DOLFI, D., PROCESI, M. (2008): Coeval strombolian and vulcanian-type explosive eruptions at Panarea (Aeolian Islands, Southern Italy). Journal of Volcanology and Geothermal Research, 177, pp. 797-811.

CAS, R., GIORDANO, G., ESPOSITO, A., BALSAMO, F., LO MASTRO, S. (2011): Hydrothermal Breccia Textures and Processes: Lisca Bianca Islet, Panarea Volcano, Aeolian Islands, Italy. Economic Geology, 106, pp. 437-450.

DAWSON, H. (2015): Deciphering the elements: Cultural meanings of water in an island setting. Accordia Research Papers, pp. 13-26.

DE ASTIS, G., VENTURA, G., VILARDO, G. (2003): Geodynamic significance of the Aeolian volcanism (Southern Tyrrhenian Sea, Italy) in light of structural, seismological, and geochemical data. Tectonics, 22 (4), pp. 14-1 – 14-17.

DEKOV, V.M., KAMENOV, G.D., ABRASHEVA, M.D., CAPACCIONI, B., MUNNIK, F. (2013): Mineralogical and geochemical investigation of seafloor massive sulfides from Panarea Platform (Aeolian Arc, Tyrrhenian Sea). Chemical Geology, 335, pp. 136-148.

DOHERTY, A.L., CANNATELLI, C., RAIA, F., BELKIN, H.E., ALBANESE, S., LIMA, A., DE VIVO, B. (2015): Geochemistry of selected lavas of the Panarea volcanic group, Aeolian Arc, Italy. Miner Petrol, 109, pp. 597-610.

ESPOSITO, A., GIORDANO, G., ANZIDEI, M. (2006): The 2002–2003 submarine gas eruption at Panarea volcano (Aeolian Islands, Italy): Volcanology of the seafloor and implications for the hazard scenario. Marine Geology, 227, pp. 119-134.

ESPOSITO, A., ANZIDEI, M., ATZORI, S., DEVOTI, R., GIORDANO, G., PIETRANTONIO, G. (2010): Modeling ground deformations of Panarea volcano hydrothermal/geothermal system (Aeolian Islands, Italy) from GPS data. Bull Volcanol, 72, pp. 609-621.

ESPOSITO, V., ANDALORO, F., CANESE, S., BORTOLUZZI, G., BO, M., DI BELLA, M., ITALIANO, F., SABATINO, G., BATTAGLIA, P., CONSOLI, P., GIORDANO, P., SPAGNOLI, F., LA CONO, V., YAKIMOV., M.M., SCOTTI, G., ROMEO, T. (2018): Exceptional discovery of a shallow-water hydrothermal site in the SW area of Basiluzzo islet (Aeolian archipelago, South Tyrrhenian Sea): An environment to preserve. PLoS ONE, 13(1), e0190710.

FABRIS, M., BALDI, P., ANZIDEI, M., PESCI, A. (2010): High resolution topographic model of Panarea island by fusion of photogrammetric, lidar and bathymetric digital terrain models. The Photogrammetric Record, 25 (132), pp. 382-401.

FAVALLI, M., KARATSON, D., MAZZUOLI, R., PARESCHI, M.T., VENTURA, G. (2005): Volcanic geomorphology and tectonics of the Aeolian archipelago (Southern Italy) based on integrated DEM data. Bulletin of Volcanology, 68, pp. 157-170.

GABBIANELLI, G., GILLOT, P.Y., LANZAFAME, G., ROMAGNOLI, C., ROSSI, P.L. (1990): Tectonic and Volcanic Evolution of Panarea (Aeolian Islands, Italy). Marine Geology, 92, pp. 313-326.

GAMBERI, F., MARANI, M., SAVELLI, C. (1997): Tectonic, volcanic and hydrothermal features of a submarine portion of the Aeolian arc (Tyrrhenian Sea). Marine Geology, 140, pp. 167-181.

GUGLIANDOLO, C., ITALIANO, F, MAUGERI, T.L. (2006): The submarine hydrothermal system of Panarea (Southern Italy): biogeochemical processes at the thermal fluids-sea bottom interface. Annals of Geophysics, 49, pp. 783-792.

HAMEL, M. (2010): Investigation and modelling of the geochemical processes in the hydrothermal system of Panarea, Italy. Diploma thesis, TU Bergakademie Freiberg, Institute of Geology, Freiberg Online Geology, 25.

HEINICKE, J., ITALIANO, F., MAUGERI, R., MERKEL, B., POHL, T., SCHIPEK, M., BRAUN, T. (2009): Evidence of tectonic control on active arc volcanism: the Panarea-Stromboli tectonic link inferred by submarine hydrothermal vents monitoring (Aeolian arc, Italy). Geophysical Research Letters, 36, L04301.

HILDEBRANDT, M.C. (2013): Charakterisierung von sedimentären Ablagerungen und Präzipitaten des Arbeitsgebietes Black Point nahe der Insel Panarea (Italien). Unpublished Bachelor thesis, TU Bergakademie Freiberg, Institute of Geology.

ITALIANO, F. (2009): Hydrothermal fluids vented at shallow depths at the Aeolian islands: relationships with volcanic and geothermal systems. In: MERKEL, B., SCHIPEK, M. (eds): Research in shallow marine and fresh water systems. 1st international workshop - proceedings. Freiberg, pp 55–60.

ITALIANO, F., NUCCIO, P.M. (1991): Geochemical investigations of submarine volcanic exhalations to the east of Panarea, Aeolian Islands, Italy., Journal of Volcanology and Geothermal Research, 46, pp. 125-141.

KELLER, J. (1967): Alter und Abfolge der vulkanischen Ereignisse auf den Äolischen Inseln. Berichte der Naturforschenden Gesellschaft zu Freiburg. 57, pp. 33-67.

KÜRZINGER, V. (2019): Determination and differentiation of the hydrothermal precipitates of Panarea, Italy. Mineralogical and Geochemical Investigations of the Submarine Hydrothermal System at Panarea Island. Master thesis, University Bremen, Institute of Marine Geosciences, Freiberg Online Geology, 54.

LANZAFAME, G., BOUSQUET, J.C. (1997): The Maltese escarpment and its extension from Mt. Etna to Aeolian Islands (Sicily): Importance and evolution of a lithospheric discontinuity. Acta Vulcanologica, 9, pp. 121–135.

LUCCHI, F., TRAENNE, C.A., CALANCHI, N., ROSSI, P.L. (2006): Late Quaternary deformation history of the volcanic edifice of Panarea (Aeolian Arc). Bulletin of Volcanology, 69 (3), 239-257.

LUCCHI, F., TRANNE, C.A., CALANCHI, N., ROSSI, P.L., KELLER, J. (2007): The stratigraphic role of marine deposits in the geological evolution of the Panarea volcano (Aeolian Islands, Italy). Journal of the Geological Society, London, 164, pp. 983-996.

LUCCHI, F., PECCERILLO, A., KELLER, J., TRANNE, C.A., ROSSI, P.L. (eds)(2013a): The Aeolian Islands Volcanoes. Geological Society, London, Memoirs, 37, pp. 351–395.

LUCCHI, F., TRANNE, C.A., PECCERILLO, A., KELLER, J., ROSSI, P.L. (2013b): Geological history of the Panarea volcanic group (eastern Aeolian archipelago). In: LUCCHI, F., PECCERILLO, A., KELLER, J., TRANNE, C.A., ROSSI, P.L. (eds) (2013): The Aeolian Islands Volcanoes. Geological Society, London, Memoirs, 37, pp. 491–510.

MANETTI, P., PASQUARÉ, G., TIBALDI, A., TZEGAYE, A. (1989): Geologia dell'isola di Alicudi (Arcipelago delle Eolie). Bollettino del Gruppo Nazionale per la Vulcanologia (GNV), 2, pp. 903- 915.

MAUGERI, T.L., LENTINI, V., GUGLIANDOLO, C., ITALIANO, F., COUSIN, S., STACKEBRANDT, E. (2009): Bacterial and archaeal populations at two shallow hydrothermal vents off Panarea Island (Eolian Islands, Italy). Extremophiles, 13, pp. 199-212.

MAUGERI, R., MASTROLIA, A., ITALIANO, F., FAVALI, P. (2010): SMM: A New Submarine Monitoring Module for Real-Time Data Transmission from the Seafloor. In: Italiano, F. (eds): 2nd International Workshop on Research in Shallow Marine and Fresh Water Systems, Milazzo, pp. 46-48.

MAZZUOLI, R., TORTORICI, L., VENTURA, G. (1995): Oblique rifting in Salina, Lipari and Vulcano Islands (Aeolian Islands, Southern Tyrrhenian Sea, Italy). Terra Nova, 7, pp. 444–452.

MEINARDIUS, F. (2016): Chemical investigations of groundwater and submarine hydrothermal fluid exhalations at Panarea, Italy. Master thesis, TU Bergakademie Freiberg, Institute of Geology, Freiberg Online Geology, 48.

MERKEL, B., KUMMER, N.S., PLANER-FRIEDRICH, B., POHL, T., SCHIPEK, M. (2011): Development of a gas sampling technique for determining trace elements in submarine volcanic exhalations. Procedia Earth and Planetary Science, 4, pp. 50-56

NERI, G., CACCAMO, D., COCINA, O., MONTALTO, A. (1991): Shallow earthquake features in the Southern Tyrrhenian region: Geostructural and tectonic implications. Bollettino di Geofisica Teorica ed Applicata, 33, pp. 47–60.

NERI, G., CACCAMO, D., COCINA, O., MONTALTO, A. (1996): Geodynamic implications of earthquake data in the Southern Tyrrhenian Sea. Tectonophysics, 258, pp. 233–249.

NERI, G., ORECCHIO, B., TOTARO, C., FALCONE, G., PRESTI, D. (2009): Subduction beneath southern Italy close to the ending: result from seismic tomography. Seismic Research Letters, 80, pp. 63-70.

ORDOSCH, A. (2016): Scientific Diving field trip Panarea, 2016. Unpublished report, TU Bergakadmie Freiberg.

ORLANDO, A., TUSA, S., GORI, D. (2018): The prehistoric vilages of the Aeolian Archipelago and Milazzo: Astronomy and landscape, preliminary results. Mediterranean Archeology and Archaeometry, Vol. 18 No 4, pp. 219-226.

PECCERILLO, A., DE ASTIS, G., FARAONE, D., FORNI, F., FREZZOTTI, M.L. (2013): Compositional variations of magmas in the Aeolian arc: implications for petrogenesis and geodynamics. In: LUCCHI, F., PECCERILLO, A., KELLER, J., TRANNE, C.A., ROSSI, P.L. (eds) (2013): The Aeolian Islands Volcanoes. Geological Society, London, Memoirs, 37, pp. 491–510.

PECCERILLO, A. (2017): Cenozoic Volcanism in the Tyrrhenian Sea Region. Springer International Publishing, 2nd edition.

PETERS, M, STRAUSS, H., PETERSEN, S., KUMMER, N.A., THOMAZO, C. (2011): Hydrothermalism in the Tyrrhenian Sea: inorganic and microbial sulfur cycling as revealed by geochemical and multiple sulfur isotope data. Chem Geol 280(1–2), pp. 217–231.

PONEPAL, M., BARTH, G., FÜTTERER, W., SCHIPEK, M., MERKEL, B. (2010): Discharge measuring of massive gas emissions at Panarea, Italy. In: Italiano, F. (eds): 2nd International Workshop on Research in Shallow Marine and Fresh Water Systems, Milazzo, pp. 66–70.

PRAUTSCH, A., STANULLA, R., POHL, T., MERKEL, B. (2013): Geochemical- mineralogical investigation of degassing structures caused by recent volcanic hydrothermalism — case study: La Calcara, Isle of Panarea (Italy). In: 3rd International Workshop on Research in Shallow Marine and Fresh Water Systems, Bremen.

ROMAGNOLI, C., CASALBORE, D., BORTOLUZZI, G., BOSMAN, A., CHIOCCI, F.L., D'ORIANO, F., GAMBERI, F., LIGI, M., MARANI, M. (2013): Bathy-morphological setting of the Aeolian Islands. In: LUCCHI, F., PECCERILLO, A., KELLER, J., TRANNE, C.A., ROSSI, P.L. (eds) (2013): The Aeolian Islands Volcanoes. Geological Society, London, Memoirs, 37, pp. 491–510.

ROMANO, R. (1973): Le isolie di Panarea e Basiluzzo. Riv. Miner. Sicil, 25, pp. 1-40.

ROSSI, P.L., CALANCHI, N., GABBANELLI, G., LANZAFAME, G. (1987): Nuovi dati strutturali su Salina e sull'area sottomarina circostante. Bollettino del Gruppo Nazionale per la Vulcanologia (GNV), pp. 599–611.

SANTO, A.P., CLARK, A.H. (1994): Volcanological evolution of Aeolian Arc (Italy): Inferences from $^{40}Ar/^{39}Ar$ ages of Filicudi rocks. Paper presented at IAVCEI Congress. International Association of Volcanology and Chemistry of the Earth's Interior, Ankara.

SCHIPEK, M., MERKEL, B. (2011): Continuous monitoring of dissolved CO2 and H2S: Technical application in the submarine hydrothermal system of Panarea, Italy. Procedia Earth and Planetary Science, 4, pp. 74-79.

SIELAND, R. (2009): Chemical and isotopic investigations of submarine hydrothermal fluid discharges from Panarea, Aeolian Islands, Italy. Diploma thesis, TU Bergakademie Freiberg, Institute of Geology, Freiberg Online Geology, 21.

SOLOVIEV, S.L., KUZIN, I.P., KOVACEV, S.A., FERRI, M., GUERRRA, I., LUONGA, G. (1990): Microearthquakes in the Tyrrhenian Sea as revealed by joint land and seabottom seismograph. Marine Geology, 94, pp. 131–146.

STANULLA, R., GANß, R., ENGEL, J., POHL, T., MERKEL, B. (2016a): Detailed mapping of small-scaled hydrothermal fluid escape structures at Area 26 and La Calcara, Panarea, Italy. 2nd European Conference on Scientific Diving, Kristineberg, Sweden, Mai 2016.

STANULLA, R., BARTH, G., GANß, R., REICH, M., MERKEL, B. (2016b): Development of a mobile airlift pump for scientific divers and its application in sedimentological underwater research. Underwater Technology, 34, 1-5.

STANULLA, R., POHL, T., MÜLLER, C., ENGEL, J., HOYER, M., MERKEL, B. (2017): Structural and mineralogical study of active and inactive hydrothermal fluid discharges in Panarea, Italy. Environmental Earth Science, 76, 404.

STANULLA, R. (2021): Geological and mineralogical investigation of hydrothermal fluid discharge features at the sea bottom of Panarea, Italy. Doctoral Thesis, TU Bergakademie Freiberg, in preparation.

STEINBRÜCKNER, D. (2009): Quantification of submarine degassing of Panarea Volcano in the Aeolian archipelago, Italy. Diploma thesis, TU Bergakademie Freiberg, Institute of Geology, Freiberg Online Geology, 23.

TASSI, F., CAPACCIONI, B., CARAMANNA, G., CINTI, D., MONTEGROSSI, G., PIZZINO, L., QUATTROCCHI, F., VASELLI, O. (2009): Low-pH waters discharging from submarine vents at Panarea Island (Aeolian Islands, southern Italy) after the 2002 gas blast: Origin of hydrothermal fluids and implications for volcanic surveillance. Applied Geochemistry, 24, pp. 246-254.

TASSI, F., CAPACCIONI, B., VASELLI, O. (2014): Compositional spatial zonation and 2005-2013 temporal evolution of the hydrothermal-magmatic fluids from the submarine fumarolic field at Panarea Island (Aeolian Archipelago, southern Italy). Journal of Volcanology and Geothermal Research, 277, pp. 41-50.

TIBALDI, A. (2001): Multiple sector collapses at Stromboli volcano, Italy: How they work. Bulletin of Volcanology, 63, pp. 112–125.

TRUA, T. SERRI, G., MARANI, M.P., ROSSI, P.L., GAMBERI, F., RENZULLI, A. (2004): Mantle domains beneath the southern Tyrrhenian: constraints from recent seafloor sampling and dynamic implications. Per Mineral, 73, pp. 53-73.

VENTURA, G. (1995): Relationships between tectonics and volcanism in the central and eastern sectors of the Aeolian Islands. In: Proceedings of the National Congress, Gruppo Nazionale di Geofisica Terra Solida - Consiglio Nazionale delle Ricerche, Rome, pp. 957–965.

VENTURA, G. (2013): Kinematics of the Aeolian volcanism (Southern Tyrrhenian Sea) from geophysical and geological data. In: LUCCHI, F., PECCERILLO, A., KELLER, J., TRANNE, C.A., ROSSI, P.L. (eds) (2013): The Aeolian Islands Volcanoes. Geological Society, London, Memoirs, 37, pp. 491–510.

VENTURA, G., VILARDO, G. (1999): Seismic-based estimate of hydraulic parameters at Vesuvius volcano. Geophysical Research Letters, 26, pp. 887–890.

VOLPI, V., DEL BEN, A., MARTINI, F., FINETTI, I. (1997): Elaborazione ed Interpretazione della Linea CROP-MARE 2A5 nel Bacino di Gioia (Tirreno Sud-Orientale). Paper presented at the 16th National Congress. Gruppo Nazionale di Geofisica Terra Solida – Consiglio Nazionale delle Ricerche, Rome.

List of figures

Figure 6: Overview of some investigated sites near Panarea Island. A - Sandy plains surrounded by Posidonia fields (arrow 1) at Area 26. Some small hydrothermal fluid vents occur throughout the area (arrow 2). In some cases, these outlets are indicated by whitish bacterial mats, as can be seen at the 3-Bowls structure in the southeast of Area 26 (arrow 3). B – A measuring station by the INGV is installed next to the shallow water smoker Black Point (arrow). The smoker is located in the inner crater of the location Black Point which is covered with light sediment. Biota cover the outskirts of the crater as well as its rims (lower right hand corner). C – Gravel field between large boulders at Bottaro North. Numerous strong hydrothermal vents (e.g. arrow) are located between the boulders, often accompanied by mineral precipitations or bacterial mats. Behind the boulders the slope rises towards the islet of Bottaro. D - Diffuse hydrothermal fluid vents in the southern crater at Bottaro West (outlined by dotted line). The crater is filled with gravel underneath which conglomerates occur. Whitish bacterial mats settle on the gravel (arrow). E - Overview of Cave. The depression is filled with Posidonia leaves covering the sediment on the ground. Around the depression, large boulders can be found as well as some hydrothermal fluid vents. The southern portion of Cave represents a grotto (arrow) in which the discharge of hydrothermal fluids can be observed and the walls are covered with thick bacterial mats. F - Silicified rocks (arrow) in the south of the gravel field at Fumarolic Field. G - Wide sediment field at La Calcara, partly covered with whitish bacterial mats (arrow 1). At some spots, such as Mordor (arrow 2), hydrothermal fluid discharges can be found only a few centimetres underneath the sediment cover. H - Plateau (left hand side) traversed by cracks and fissures next to the scarp wall at Point 21. On the bottom of the scarp wall the FSVG (arrow) is located which is used by the SDC Freiberg to measure gas flow-rates. The construction is positioned at the two strongest hydrothermal fluid vents that could be found throughout the investigated sites of the SDC. (Photography: A, G – R. Stanulla; B, D – L. Schüler; C – M. Kleinschroth; E, H – S. Kluge; F - SDC)..... 22

Figure 7: A – Technical model of an airlift pump with its major elements: mixing chamber for gas injection (1), suction hose (2), riser pipe (3), buoy (4), ejector (5), air reservoir (6), control panel (7), and counterweight (8) (STANULLA ET AL., 2016b). B – Mobile airlift pump in use at 3 Bowls, Area 26 in order to excavate the sediment filled bowl structures. 29
Figure 8: Thin section of a strongly altered dacite-andesite from Point 21. A crust of native sulphur is found on the outer margins of the rock (S). Underneath, single crystals of the dacite-andesite can be recognized, such as Feldspar and Biotite. However, they show signs of severe alteration. Due to this alteration, optical characterization of the rock is difficult. *A* –II-Pol., 2,5x. B – X-Pol., 2,5x. 32

Figure 9: A – Normal fault at Punta Milazzese. The fault cuts through the fan-shaped, jointed volcanic rocks almost perpendicularly. B – Normal faults along the western cliffs of Panarea Island. All of these fault show a NE-SW orientation. Besides the three pictured faults, a fourth one could be identified farther up the cliffs, near the highest peak of Panarea, Punta del Corvo. Due to the steepness of the cliffs along the western flanks of Panarea, the faults could not be investigated in detail. C – Silicified honeycomb structures near La Calcara bay. These structures appear to trace initial pathways of hydrothermal fluids through the surrounding host rocks. While some, nearly upright oriented sections are thicker, the intersecting portions are thinner and more porous. Along the boundary of the dykite material and the dacitic-andesitic host rock, signs of hydrothermal alteration can be recognized. D – Preserved paleo lineament

List of tables

Appendix

Appendix 1 – Sample list Panarea Island

Appendix 2 – Sample list underwater investigation sites

Appendix 3 – Maps

Appendix 4 – Maps of the main underwater investigation sites

Digital Appendix

Appendix 5 – Digital version of the geological map (GIS)

Appendix 6 – Photo documentation